Synthesis of Polyphenylenes with removable side chains - towards an all Polyphenylene material

Abhandlung zur Erlangung des Titels

DOKTOR DER WISSENSCHAFTEN der ETH ZÜRICH

(Dr. sc. ETH Zürich)

vorgelegt von

Samuel Paul Jakob

MSc Chemistry ETH Zürich

geboren am 09.09.1983

Von
Hombrechtikon, ZH

angenommen auf Antrag von

Prof. Dr. A. Dieter Schlüter
Prof. Dr. Paul Smith
Prof. Dr. Holger Frauenrath

2014

Abstract

Polyphenylenes have been subject of research interest because of their materials properties since many years. As high molecular weight pure polyphenylenes are practically insoluble, access to polyphenylenes was limited to their substituted derivatives. Flexible side-chains attached on the rigid polymer backbone induced enough solubility to allow synthesis and processing of high molecular weight polyphenylenes. These side-chains, however, alter and deteriorate the materials properties characteristic for the rigid polymer backbone. The development of a process to make such un-substituted polymer materials available was the subject of the present thesis.
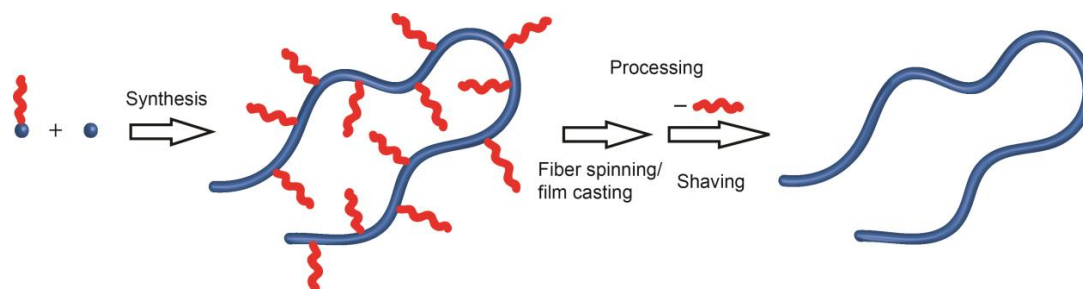

Figure a. Two synthesized monomers were subjected to SPC. The resulting polymer was processed into a desired shape and by a facile post-processing step converted into the target material.

The "shaving" approach was envisioned as follows (Figure a): synthesis of a precursor polymer, decorated with side-chains, which then could be easily removed from the polymer at a desired point, thus resulting in a pure polyphenylene material. The concept was developed bottom up, starting from rationally designed monomer systems, which could be synthesized in multi-gram scale and high purity. Model studies to investigate side-chain cleavage reactions were carried out. Synthesis of the precursor polymers **I** and **II** (Figure b) by Suzuki Polycondensation (SPC) and characterization by NMR-spectroscopy, MALDI-TOF mass spectroscopy and GPC allowed structural analysis and molecular weight determination. The highest molecular weight obtained for an unfractionated polymer sample was M_w = 50 kDa for polymer **I** and M_w= 49 kDa for polymer **II**. Cyclic oligomers could be identified as a major side-product, which could be removed by fractionation, leading to significantly increased molecular weights (M_w = 98 kDa) for polymer **I**. Cleavage reactions in solution (**I**), gel (**I**) and bulk (**I**+**II**) were carried out. Complete cleavage of the side-

chains under various conditions was observed for the transformation of **I**, while a complete transformation of **II** was not observed. Success of the aforementioned transformations was confirmed by solid-state NMR-Spectroscopy, MALDI-TOF mass spectroscopy, ATR-IR spectroscopy and elemental analysis.

In addition, the precursor polymer **I** could be processed into self-supporting fibers. This was done by electrospinning from a 20 wt-% solution of **I** in Chloroform, with a voltage of 7 kV and a spinning distance of 15 cm.
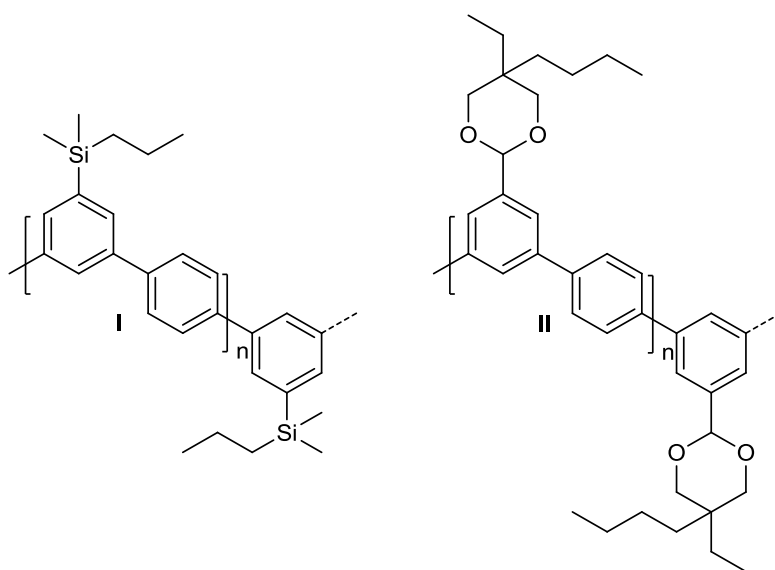
Figure b. Polymer **I** and **II** synthesized during the present thesis carrying two different cleavable side-chains.

Zusammenfassung

Seit einigen Jahren stehen Polyphenylene, aufgrund ihrer Material-eigenschaften, im Interessen von Forschungsarbeiten. Da reine Polyphenylene mit hohem Molekulargewicht praktisch unlöslich sind, ist der Zugang auf deren substituierte Derivate limitiert. Flexible Seitenketten, welche am rigiden Rückgrat angebracht werden, erzeugen genug Löslichkeit um Synthese und Verarbeitung von hochmolekularen Polyphenylenen zu ermöglichen. Diese Seitenketten ändern und verschlechtern jedoch die Materialeigenschaften, welche durch den rigiden Polymerrückgrat erzeugt werden. Die Entwicklung eines Prozesses, welcher die Herstellung solcher Materialien ermöglicht, war das Ziel der vorliegenden Arbeit.
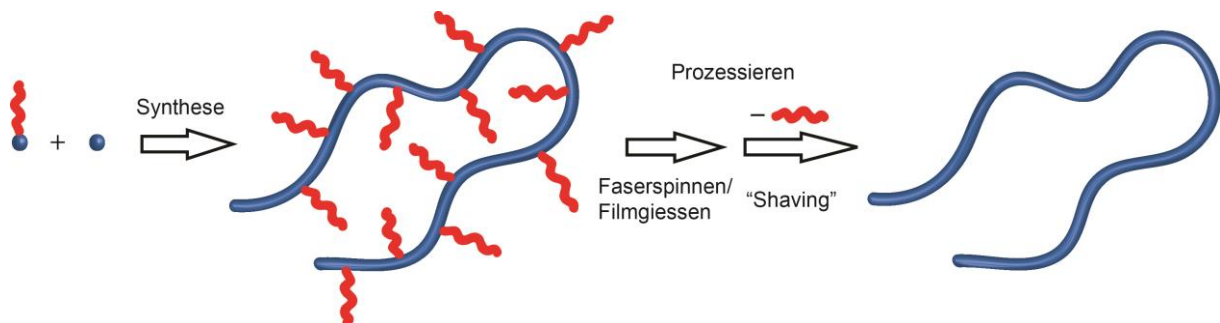

Abbildung a. Zwei synthetisierte Monomere wurden SPC unterzogen. Das resultierende Polymer wurde in eine gewünschte Form verarbeitet und durch eine einfache Nachverarbeitung in das Zielmaterial umgewandelt.

In der Folge wird beschrieben, wie sich der „shaving" Ansatz vorgestellt wurde (Abbildung a): Synthese eines Vorläuferpolymers dekoriert mit Seitenketten, welche an einem gewünschten Punkt einfach vom Polymer entfernt werden können und auf diese Weise in einem reinen Polyphenylene-Material resultieren. Das Konzept wurde von der Basis her entwickelt, ausgehend von der Gestaltung der Monomere, welche im Multi-Gramm Massstab und mit hohem Reinheitsgrad synthesisiert werden konnten. Modell-studien zur Untersuchung von Abspaltungs-Reaktionen der Seitenketten wurden durchgeführt. Die Synthese der Vorläuferpolymere **I** und **II** (Abbildung b) und deren Charakterisierung mit NMR-Spektroskopie, MALDI-TOF Massenspektrometrie und GPC erlaubten strukturelle Analyse und Molekulargewichtsbestimmung. Die höchste Molmasse, welche für eine unfraktionierte Polymerprobe erreicht wurde, war M_w = 50 kDa für Polymer **I** und M_w = 49 kDa für Polymer **II**. Zyklische Oligomere konnten als ein bedeutendes Nebenprodukt identifizert werden. Dieses konnte durch Fraktionierung entfernt werden, was zu einem erheblichen Anstieg der mittleren Molmasse (M_w = 98 kDa)

von Polymer **I** führte. Abspaltungsreaktionen wurden in Lösung (**I**), im Gel (**I**) und im Festkörper (**I+II**) durchgeführt. Komplette Abspaltung der Seitenketten wurde unter verschiedenen Bedingungen für die Umsetzung von **I** beobachtet. Hingegen wurde für die Transformation von **II** keine komplette Abspaltung beobachtet. Der Erfolg der zuvor erwähnten Transformation konnte mit Festkörper NMR-Spektroskopie, MALDI-TOF Massenspektroskopie, ATR-IR Spektroskopie und Elementaranalyse bestätigt werden.

Des Weiteren konnte das Vorläuferpolymer **I** in selbsttragende Fasern gesponnen werden. Dies wurde per Elektrospinnen aus einer 20 gew.-% Lösung von **I** in Chloroform gemacht, die angelegte Spannung betrug 7 kV und die Spinndistanz war 15 cm.
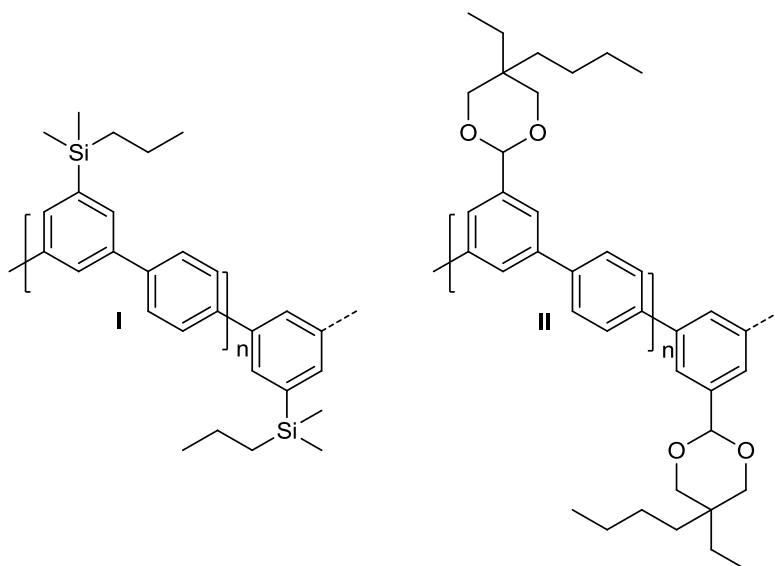

Abbildung b. Polymer **I** und **II**, welche im Verlauf der vorliegenden Arbeit synthetisiert wurden, tragen zwei unterschiedliche, abspaltbare Seitenketten.

Contents

1. Introduction

Polymers are a dominant part of our everyday lives. They are one of the three most wide-spread classes of materials besides metals and ceramics. In 2011 roughly 280 megatons of polymeric materials were produced and sold worldwide. In the European Union an estimate of 1.4 million people are employed by the polymer producing and converting industry.[1] Most polymers are used in the packaging, construction and automotive industries. Virtually every product we use day by day contains a polymer-based component. Probably the main reason for this is the extreme versatility of their materials properties, as well as their low production and processing costs.
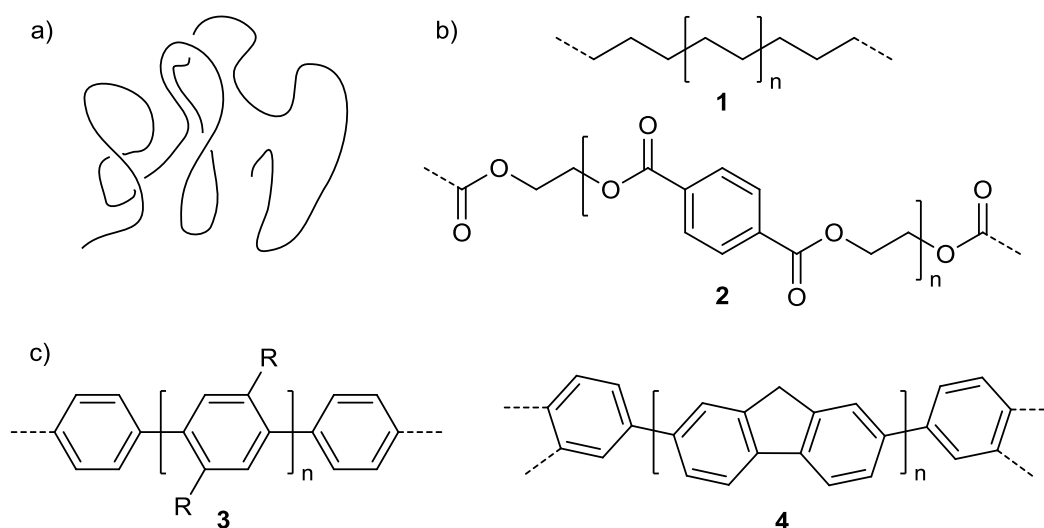
Figure 1. Schematic representation of a coiled polymer chain as they exist in solution and in melt (a) and chemical structures of concrete polymer examples (b,c). b) Two commercially highly relevant polymers: Polyethylene 1 (non-aromatic) and polyethyleneteraphthalate 2 (aromatic). c) Two aromatic polymers of relevance to the present thesis: Poly(para-phenylene) 3 and polyfluorene 4, the base structure of commercialized polyphenylene derivatives.

Simplified, polymers can be envisioned as chain-like molecules consisting of an very large number of links (Figure 1 a). These links (monomers) are connected with each other to form a larger entity. The individual links are referred to as repeat units (RUs) and are denoted by square brackets like shown in Figure 1. It should be noted though that contrary to a woman's necklace where the links are topologically free to change their relative orientation in the case of a polymer the individual links are covalently connected and therefore more limited in their mobility with respect to each other.

Staudinger postulated in 1920 the existence of polymers, which at that time was a major step ahead, considering the fact that most of his contemporaries still believed in the colloidal picture of matter such as leather and cellulose.[2] "Polymerization processes, broadly speaking, are all processes where two or more molecules are united to a product of the same composition, but higher molecular weight."- (H. Staudinger, 1920, translation from German). His more detailed, strict definition of real (polymerizations) and artificial (polycondensations) polymerization processes was slightly revised later. However, the general description of a polymerization process has been fully accepted in the meantime. A unique feature of polymers compared to smaller organic substances is that not all molecules in a given sample have the same molecular weight. This was already noted by Staudinger when investigating natural rubber.[3] Thus, when referring to molecular weight in the context of polymers, one usually refers to a molecular weight distribution. The molecular weight of a polymer is one of the key factors that determine the materials properties of a given polymer sample, the other being its chemical structure. One way to divide polymers is by structural differences, e.g., whether they comprise of saturated units only or are composed of aromatic units. Famous cases for non-aromatic, saturated polymers are polyethylene (PE), polymethylmethacrylate (PMMA), polytetrafluoroethane (PTFE) and various polyamides (PA)s. Important aromatic polymers are, e.g. polyethyleneteraphthalate (PET), the polyparaphenylene family (PPP) and polyaramides (PARA). For this work of particular interest were PPPs. Aromatic polymers are known for their outstanding materials properties and some of them make up for a significant proportion of the yearly production of polymer materials (PET), while others are mainly used in specific niche applications which have extremely high demands on materials performance (e.g. PARAs). Polyphenylene based polymers are, with few exceptions, a poorly investigated family of polymers. The most prominent members thereof are polyfluorenes, which are used in organic, light-emitting diodes (OLEDs) and organic solar cells. Little attention has been brought to the mechanical and thermal properties of polyphenylenes; the present work covers some of these aspects.

2.   Motivation

Aromatic polymers, compared to many non-aromatic ones, are limited in their conformational flexibility. This leads to poor solubility of these materials at high molecular weight in many media because of the unattractiveness to being molecularly dispersed in a solvent. The entropic gain upon dissolution is small.[4],[5] The decreased solubility is further caused by strong chain-to-chain interactions like π-π interactions, which promote close stacking of polymer chains. Thus, not only do the chains not like to stay in solution but also there is an enthalpic attractiveness for them to precipitate out. Non-aromatic polymers on the other hand gain a significant amount of entropy upon dissolution because they then can exercise their entire conformational space. Additionally, the transition into a solid-state packing is associated with less liberation of enthalpy. While low solubility can render synthesis, structure analysis and processing complicated, it can be desirable for certain applications. Polymers of low solubility are expected to have a better long term performance, as most chemical degradation processes are slower in solid materials compared to solutions. Furthermore, insoluble materials are less prone to environmental stresses such as humidity or vapors of organic solvents. Their decreased swelling behavior results in an improved overall performance. The aforementioned characteristics of aromatic polymers not only result in a decreased solubility, but also in increased melting- and glass-transition temperatures. They impose major obstacles for synthesis and processing.

Flexible side chains have been shown to increase solubility of conformationally restricted, unsaturated polymers to a large degree. Thus, synthesizing aromatic polymers with flexible chain decorations looks like an attractive way to address the otherwise severe synthesis and processing complications. Of special interest in this regard is a recent publication by Kandre *et al.*[6] They showed that a poly(*meta-para*-phenylene) with alkyl side-chains can be synthesized by Suzuki-polycondensation (SPC) followed by a fractionation in astoundingly high molar mass of approx. 250 kDa. This material was soluble in chloroform at room temperature! Its structure therefore could be fully analyzed by all tools of organic and macromolecular chemistry. Moreover, the material could be easily processed into durable, fully transparent films. These films were investigated for their mechanical properties and

found to be comparable in their toughness to commercially available polycarbonate. This was a remarkable finding which underlines the importance aromatic polymers may gain supposed they can be synthesized in sufficiently high molar mass. This finding also very convincingly showed the power of the alkyl chain substitution. Nevertheless, while this substitution was so effective in this particular case one may raise the question whether the properties could not have been further enhanced, if the exact same polymer could be made available without the alkyl chain decoration. After all, this decoration basically dilutes the properties of the main chain and is therefore undesired. This is the point at which the present thesis sets in. It will describe a method by which solubilizing groups are used as long as needed and then being removed when the polymer is processed into its final form. It was found that polymer **5** (see Figure 2) has some very interesting mechanical properties (tough and amorphous). The observed properties of **5** were comparable to those of commercial polycarbonate (see Figure 2). This is despite the flexible side-chains which were attached every other phenyl unit.
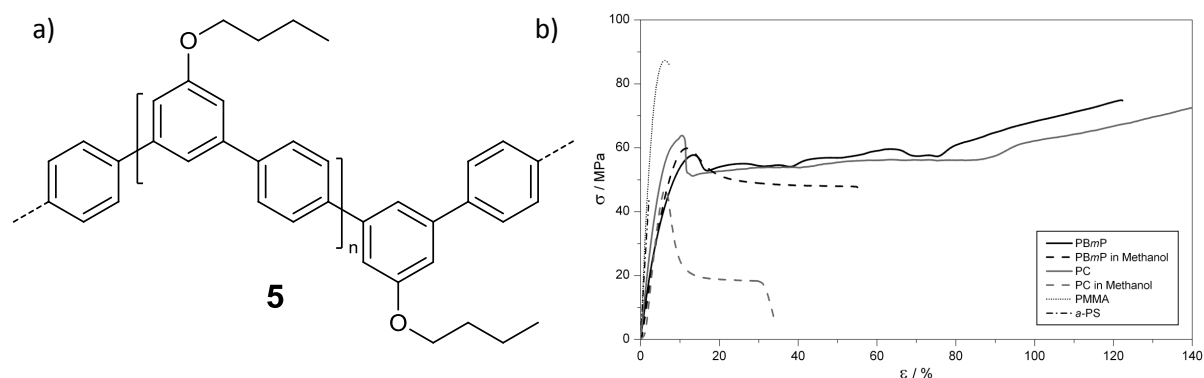
Figure 2. Structure of polymer **5** and stress-strain curves comparing it to other polymers. a) high molecular weight poly(*meta-para*phenylene) referred to by the authors as PB*m*P. b) Stress strain curve of PB*m*P (black) and commercial polycarbonate (PC, grey). Courtesy of "John Wiley and Sons".

While necessary in synthesis and processing the side-chains are often undesirable in a targeted material. Especially in high-end applications where specific materials properties are desired, side-chains are an unwanted feature, since they usually do not contribute to the desired materials properties and therefore deteriorate the overall performance of a product.[7] In other words, the active component, the backbone, is diluted by its decoration with flexible chains. This brought up one of the

key questions leading to the present thesis. What if one could synthesize a polymer similar to **5** without the flexible side-chains?

3. Goals

As described in the introduction the main goal of this thesis is to provide access to an aromatic polymer that initially carries flexible chains so as to improve on its solubility and processability. In the final state on the way to a product, may it be a film or fiber, the polymer must be designed such that the flexible chains can be quantitatively be removed so that the bare and insoluble backbone is obtained (**6**, Figure 3b). This research goal required several steps of action. They are comprised of

1. Design of substituents cleavable off aromatic moieties and test experiments showing the efficiency of such a cleaving process.

2. Synthesis of aromatic monomers applicable to Suzuki polycondensation (SPC) which carry these substituents.

3. Synthesis of a precursor polymer based on the specially designed monomers.

4. Analysis of the intermediate structure with the major tools available to the organic and polymer-chemist.

5. Carry out shaving experiment in order to confirm applicability of the process to a polymer starting material.

6. Confirm success of the protocol with the available solid state analysis techniques.

7. Obtain high molecular weight polymer, either by modifying synthesis conditions until a stock sample of sufficiently high molar mass is obtained or by fractionation of the stock sample.

8. Investigate possible processing methods for the intermediate polymers.

9. Confirm unbrokenness of a bulk structure (e.g. a film) after the shaving process.

10. Investigate effect of the shaving process on the mechanical properties of a bulk structure (e.g. a fiber).
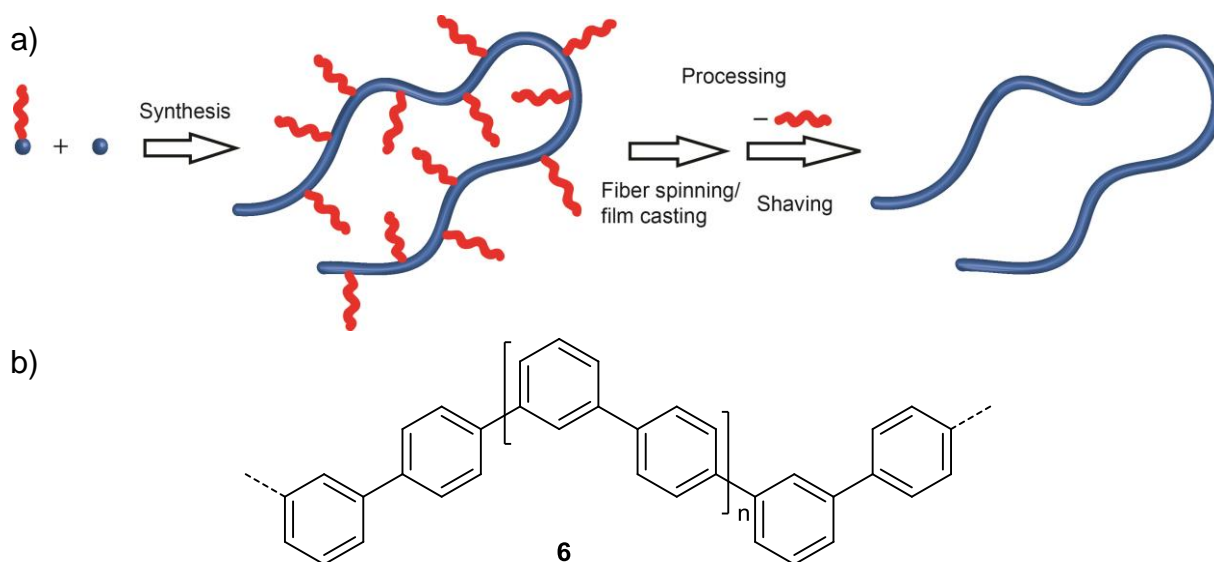
a)

b)

6

Figure 3. a) Synthesis of an aromatic polymer (blue) with flexible side-chains (red), followed by processing during which the chains are removed. The processing steps may be independent or combined. Most side-chains are omitted from the intermediate structure for clarity purposes. b) Chemical structure of the target polymer **6**.

4. Theory

4.1. Suzuki-Miyaura cross-coupling reaction (SMC)

Metal catalyzed cross-couplings are a cornerstone in organic synthesis. The ability to directly form bonds between carbon atoms of all hybridizations has dramatically changed the pathways in the synthesis of small molecules such as drugs or natural products. As an example Johansson *et al.* were able to easily modify a malaria inhibitor to greatly increase its potency by using SMC.[8] This is just one of many examples of what a powerful tool these type of reactions have become, they can be counted as common knowledge for any chemist involved in organic synthesis.[9]

Miyaura and Suzuki first reported a palladium catalyzed cross-coupling of vinyl-boronic acids with various halide compounds in presence of a base during 1979.[10],[11] The protocol was discovered during the development flurry of organometallic coupling reactions in the 1970s. It, however, had some crucial advantages over protocols involving other transition metal species, be it functional group tolerance,[12] avoiding toxic starting materials,[13],[14] or substrate scope.[15] In addition to the aforementioned reasons, the high yields observed in SMC made the method an extremely popular tool. SMC had such a dramatic impact on organic synthesis that Akira Suzuki was among the recipients of the 2010 Nobel Prize in chemistry.

As most transition metal mediated cross couplings, SMC can be divided into three main steps: Oxidative addition, transmetalation and reductive elimination. These three steps are believed to form a catalytic cycle. While the basic steps are generally accepted exact details regarding kinetics and exact transition states are disputed. Two postulated routes are shown in Scheme 1.

$$Pd^{(0)}L_4$$

$$2L \updownarrow -2\,L$$

$$Pd^{(0)}L_2$$

$R^1{-}R^2$

Reductive
elimintation

R^1X

Oxidative
addition

$$\overset{\ominus}{X}B(OH)_3 \qquad R^2{-}\overset{\ominus}{B}(OH)_3$$

$$\underset{L}{\overset{L}{R^1{-}\underset{|}{\overset{|}{Pd}}^{(II)}{-}R^2}} \xleftarrow{\quad by\ Canary \quad} \underset{L}{\overset{L}{R^1{-}\underset{|}{\overset{|}{Pd}}^{(II)}{-}X}}$$

Transmetallation
by Suzuki

R'O-B(OH)$_2$

$$\underset{L}{\overset{L}{R^1{-}\underset{|}{\overset{|}{Pd}}^{(II)}{-}OR'}}$$

NaOR'

R^2-B(OH)$_2$

NaX
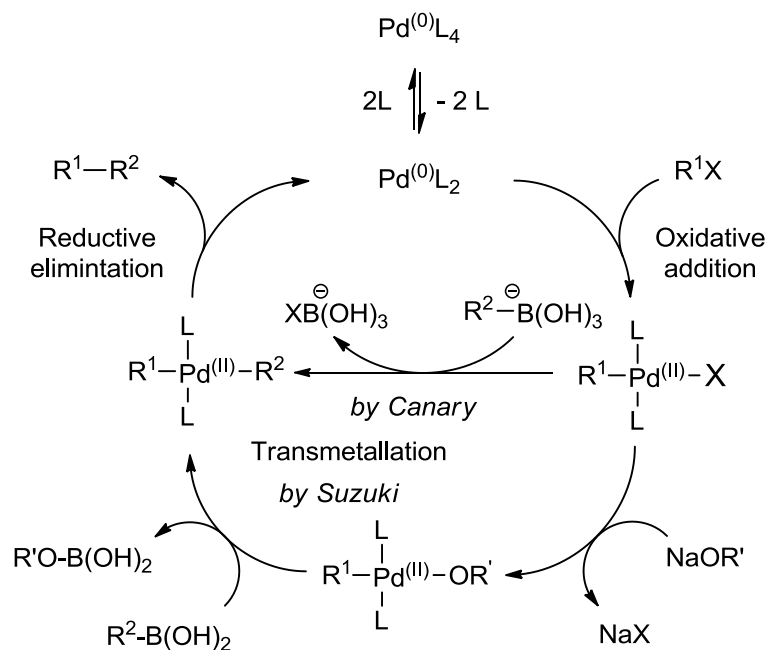
Scheme 1. Two possibilities for a generalized catalytic cycle for SMC.

Despite general notion that the transmetalation is the slowest step in the catalytic cycle,[16] observations by Aliprantis and Canary suggest that this may not be so in all cases[17] and Miyaura *et al.* propose that in fact the oxidative addition is the rate limiting step.[11] Generally disputed are details involving the transmetalation step, where Miyaura and Suzuki propose an oxopalladium(II) complex as transition state and report no direct reaction from palladium bound aryl halides (namely chlorides)[18] Aliprantis *et al.* were unable to observe these species, though they were not able to directly show the exact chemical nature of the boron-species undergoing transmetalation. A study focusing on pH dependency of SMC showed that boronic acid derivatives do not undergo transmetalation at pH values < 8. Quaternary arylborates, however, react readily under the same conditions,[19] proving the necessity for quarternarization of the boronic acid for transmetalation to occur. Contrary to the transmetalation step, the oxidative addition step is well understood and aspects thereof are widely accepted. It is known that electron deficient aromatic units undergo oxidative addition more readily.[20] Of a much more drastic impact, though, is the type of aryl halide (or pseudohalide) involved.[9],[21] The generally observed order of reactivity is I > OTf > Br >> Cl. Omitted from the catalytic cycle in Scheme 1 are *cis/trans* isomerizations. These steps proceed during the SMC reaction, but are difficult to experimentally characterize. However, it is generally assumed that the oxidative addition and the reductive elimination lead to/require *cis-*

isomerisation, respectively. The transmetalation step is assumed to take place in the *trans*-isomer.[22],[23]

4.2. Suzuki-Polycondensation

The application of SMC to polymers was first reported by Rehahn *et al.* in 1989.[24] Applying SMC to bifunctional monomers and therefore allow bidirectional growth by a polycondensation mechanism allowed access to a new family of polymers previously not obtainable. In its roughly 20 years of existence, SPC has led to a multitude of polymeric structures, some of which even made it to industrial application.[25] A few examples are shown in Figure 4.
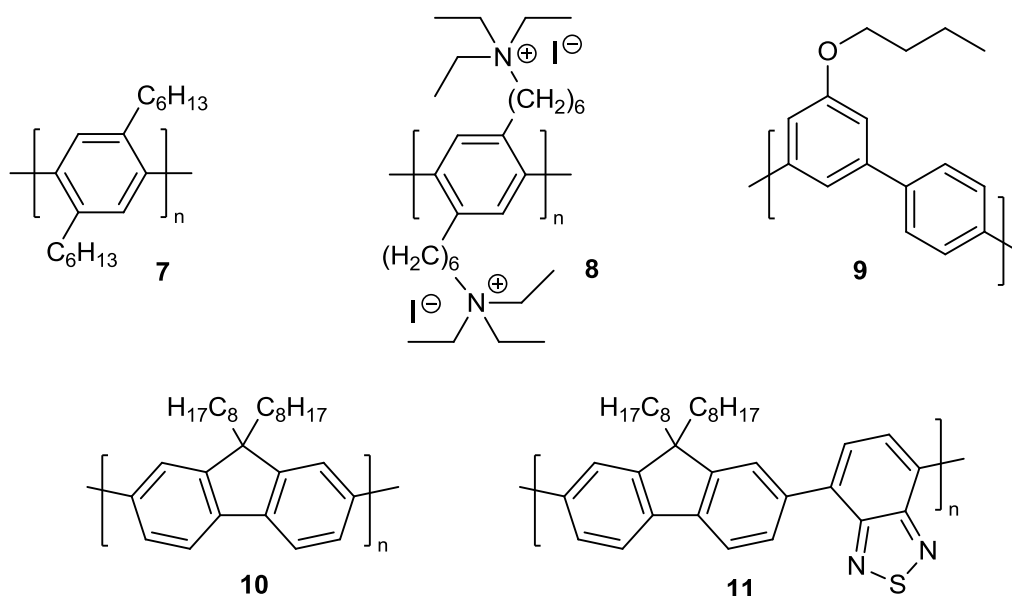
Figure 4. Polymer 7 was the first soluble high molecular weight polyparaphenylene synthesized by Rehahn and Schlüter[24] 8 is a water soluble polyphenylene synthesized by Brodowski et al.[26] 9 is an example of a kinked polyphenylene investigated by Kandre et al.[6] 10 and 11 are polyfluorene type polymers, while 10 is one of the most basic Polyfluorenes, 11 is of commercial importance.

4.2.1.   AA/BB – vs. AB – approach

There are two basic approaches to SPC, the AA/BB- and the AB-approach. In the former two bifunctional aromatic co-monomers are used (Scheme 2). They carry either two halide or two boronic acid functions. Their polymerization leads to polymers in which the two monomers are incorporated in an alternating sequence. In the case of the AB-approach a single bifunctional monomer is used which contains both functionalities at the same time. The resulting polymer is now comprised of only one kind of monomer in its backbone and therefore exhibits directionality.[27] By

design both approaches have their specific advantages and disadvantages. The aforementioned backbone directionality allows controlled head-tail functionalization. In addition, the intrinsic stoichiometry match facilitates the polymerization process (see chapter 6). The price to be paid is the additional synthetic effort required. Usually AB-monomers are obtained by a desymmetrization of a possible AA/BB-type monomer. This not only complicates monomer synthesis but also limits substrate scope. The absence of these synthetic complications is the main advantage of the AA/BB-approach. Moreover, with a small number of monomers, for each functionality, a large library of polymeric structures is available. This feature is of additional value if the structure property relationship of the obtained polymers is of interest. However, the main issue for AA/BB-type SPC remains the requirement for exact 1:1 stoichiometry of the two monomers. This is a requirement to obtain high molecular weight polymer.
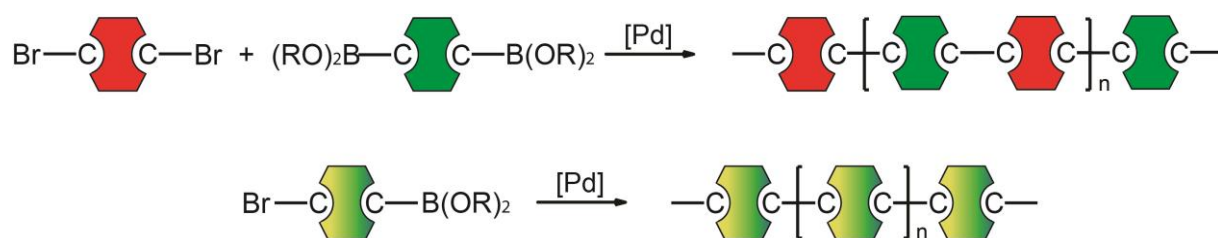
Scheme 2. Illustration of the AA/BB- and the AB-approach for SPC.

This problem is not limited to SPC, but is a general issue in step-growth type polymerization chemistry. According to Carothers' equation high molar mass polymer is only obtained for high conversions (all step-growth type polymerizations) and molar fractions close to 1 (AA/BB-type polycondensations).[28] As can be seen in Figure 5b the degree of polymerization drops rapidly for molar fractions $\neq$ 1. The plot shown assumes conversion $p = 1$. Additionally, as discussed by Carother, for incomplete conversions the degree of polymerization is even lower (Figure 5a).
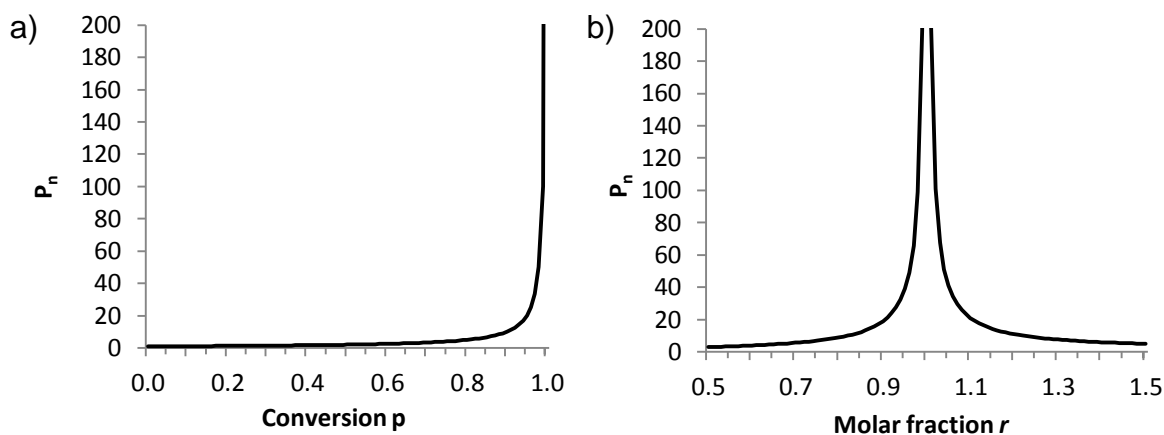
Figure 5. Graphical representation of Carothers equation for a) the effect of conversion on the degree of polymerization (P_n) for ideal reaction stoichiometry and b) the effect of molar fraction r on P_n assuming complete conversion.

Issues arising from mismatched AA/BB stoichiometry are of particular importance when working with small scales or co-monomers of vastly different molecular weight. A good illustration of the problem in hand was given by Bo *et al.* [29] These authors purposely vary the stoichiometry of the two co-monomers to ensure hitting the ideal stoichiometry. This is a measure often taken when monomer impurities are present which cannot be exactly quantified.

4.2.2.   Catalysts – Precursors, concentration and removal

The most wide-spread although not necessarily best catalyst precursor employed in SPC is palladium(0)tetrakistriphenylphosphine (Pd(PPh$_3$)$_4$). While still being a starting point for many optimization studies, it has been replaced by more active complexes such as Pd(P(p-tolyl)$_3$)$_3$[6], Pd(P(o-tolyl)$_3$)$_3$[30] and Pd$_2$(dba)$_3$/SPhos.[27] In all these complexes the metal is in the oxidation state zero. More convenient options are PdCl$_2$(dppf)[31] or Pd(OAc)$_2$/phosphine ligand (e.g. SPhos/P(o-tolyl)$_3$).[32],[30] These catalyst precursors are Pd(II)-species, making them air-stable. However, in order to enter the catalytic cycle they need to undergo reduction before being able to catalyze the cross-coupling reaction. This can be done on purpose by using a solvent capable of reducing Pd(II) to Pd(0)[33] or by adding a suitable reducing agent.[34],[35] If this is not done, reduction may occur by homocoupling of the boronic acid/ester monomers present (Homocoupling is a known side-reaction in SPC which will be discussed below).

Catalyst concentration is a crucial issue in SPC. Most commercial products employing SPC as synthesis method are designed for opto-electrical applications. Leftover metal particles origination from decomposed catalyst have detrimental effects on device performance for example leading to a color shift in OLED. It is therefore desired to reduce catalyst concentrations as much as possible. Usual catalyst concentrations for SPC are in the range of 1-3 mol-% in open literature publications. Kandre and co-workers systematically reduced catalyst loadings in a successful SPC protocol and observed only small molecular weight decrease for catalyst loadings down to 0.03 mol-%.[25]For a case of SMC the applied catalyst loadings went as low as 0.001 mol-% in a conventional reaction setup, [36] in a report by Leadbeater *et al.* the authors use Pd-impurities present in commercially available NaHCO$_3$ as Palladium source and obtain decent yields while using microwave assisted heating.[37]

As previously mentioned reducing the Pd content of SPC products is of crucial importance. Murage and Goodson observed that if palladium is not removed directly after reaction, Pd-clusters are believed to adhere to the formed polymer.[30] The possibility to remove Pd-traces are manifold, (repeated) precipitations being the most straight forward[38] but washing with water,[39] soxhlet extraction,[40],[41] chromatography[29] or scavenger extraction[30] are also feasible options. A very effective and simple case of scavenger extraction is the use of aqueous NaCN to wash the polymer solution during workup. [30],[42] Nielsen *et al.* reported the use of a specially designed Pd-scavenger (**11**).[43] Treating a Pd containing solution with this ligand leads to the formation of complex **12**. It has vastly different solubility properties then most polymers synthesized by SPC. This makes separation of complex **12** and polymer by precipitation possible. Moreover, **12** has strong UV-absorption band in the 800 nm range, which allows a quantification of Pd leftovers by UV/Vis-spectroscopy. An emerging field is the use of solid phase supported ligands which allow simple catalyst removal by filtration after the reaction.[44],[45] Some of these catalysts are of special interest for industry (some of them have been commercialized) as the employment of heterogeneous and reusable catalysts is usually sought after since recycling catalyst greatly improves the cost-benefit ratios of large-scale processes.
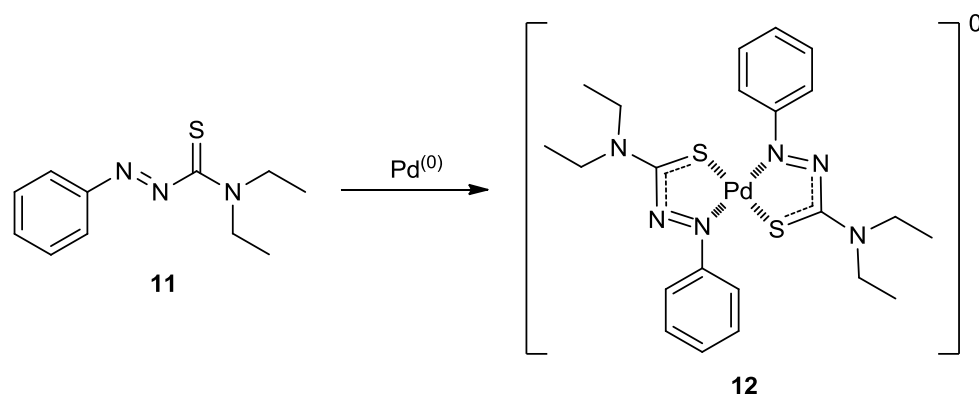
Scheme 3. Formation of a quantifiable Pd$^{(0)}$-complex which can be easily removed from the polymer by precipitation of the latter in MeOH (complex stays in solution).

4.2.3. Side reactions

Side reactions are present in all chemical processes, this is no different for SPC. Subsequently the most important side reactions are introduced. Most of them terminate a chain-end and therefore hinder bidirectional growth. They can also alter the stoichiometric ratio of the two functionalities, which greatly diminishes the possibility to obtain high molecular weight polymer (see 4.2.1).

4.2.3.1. Ligand Scrambling

A well-known side-reaction involving the ligands of the catalyst is generally referred to as ligand scrambling. It's a side-reaction limited to phosphine ligand containing catalyst systems. Since almost exclusively phosphine based catalyst systems are employed in SPC this side-reaction is a common obstacle since its very early history.[46],[47] An example of a ligand scrambling event is given in Scheme 4. Ligand scrambling events are promoted by higher temperatures but not exclusive to them. Agrawal *et al.* also observed ligand Pd-Ar to P-Ar exchange reactions at room temperature.[48] Moreover, deducting from a temperature ramp experiment Herrmann and co-workers reported that ligand scrambling events take place at lower temperatures for electron rich substrates, whereas for electron poor substrates no Pd-Ar to P-Ar migration was observed prior to catalyst decomposition.[47]

It is evident considering structure **13** in Scheme 4 ligand scrambling can lead to phosphor incorporation into the polymer backbone which in consequence induces additional kinks into the polymer backbone or may even lead to a significant degree of branching as observed by Goodson and Novak[49] This, however, is only the case

for hydrophilic solvents and using $Pd(PPh_3)_4$. When using a non-hydrophilic solvent like DCM and using $P(o\text{-tolyl})_3$ as phosphine ligand, ligands scrambling could be suppressed to a degree that no ^{31}P-signals could be observed using NMR-spectroscopy. Schlüter *et al.* carried out a study aiming at the quantification of phosphorus incorporation and showed that the phosphorus incorporation was increasing with increasing molecular weight of the obtained polymer.[50] Besides the commercially available $Pd(PPh_3)_4$ they used $Pd[P(p\text{-tolyl})_3]_3$ as catalyst precursors and toluene/water as reaction solvent. Contrary to Goodsons report Schlüter found evidence for phosphorus incorporation in all products (ranging from 0.75 – 0.05 mol-%). Ligand scrambling is the only relevant side-reaction which does not affect the monomer-stoichiometry in a negative way, as functionalities are not removed, but simply transferred.
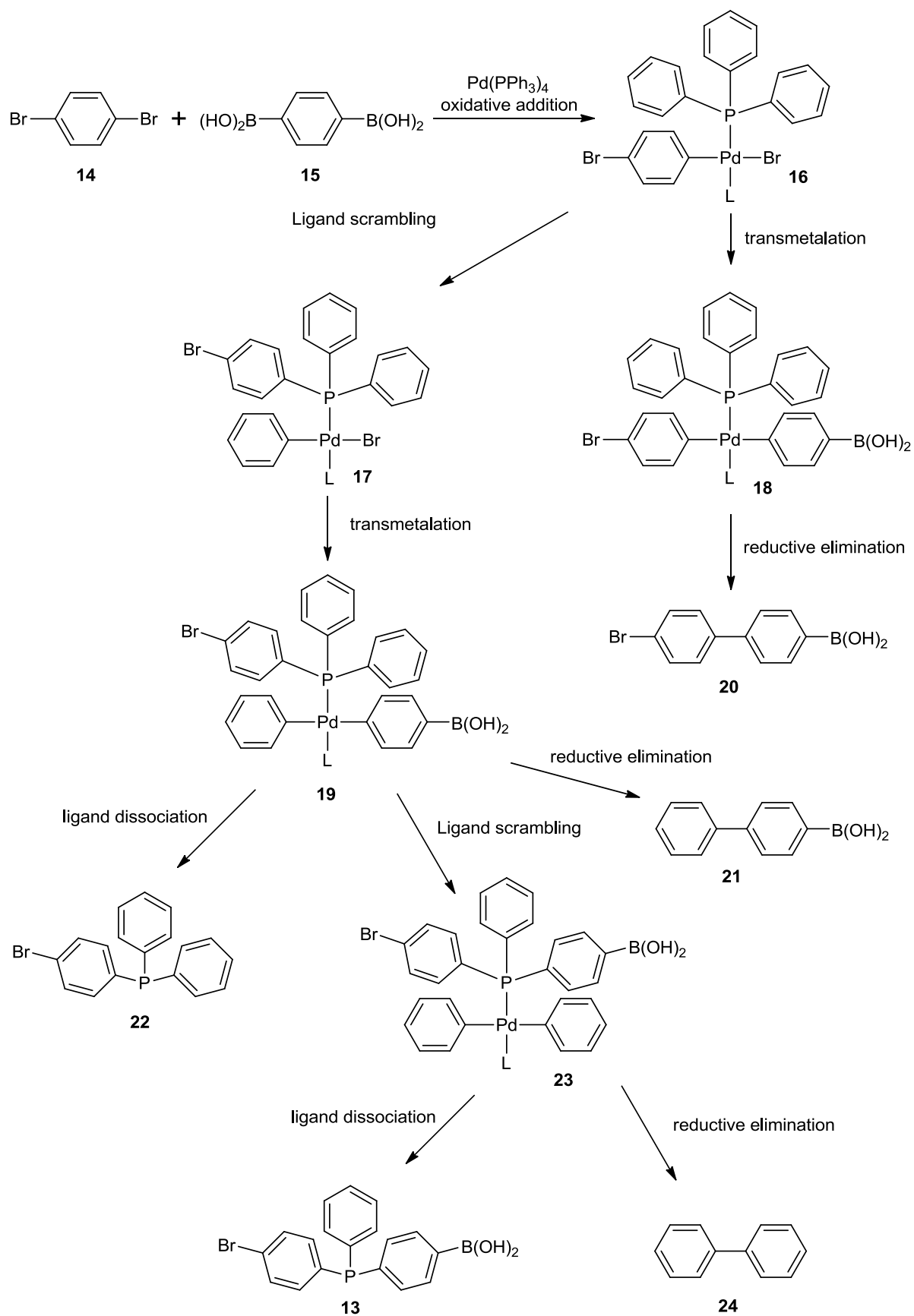
Scheme 4. Example for ligand scrambling processes which take place during SPC reactions.

4.2.3.2. Hydrolytic deboronation

It is generally believed that the hydrolytic deboronation of boronic acids (also known as protodeboronation) is the side reaction which has the most detrimental effect on molecular weights in SPC-products.[30] In the reaction the boronic ester functionality is replaced by a proton. The reaction was discovered, before SPC was developed.[51] In small molecule synthesis (SMC) this problem is usually circumvented by the addition of excess of the boronic acid species.[52] This, however, is not an option for SPC as this would lead to low molecular weight product (see Figure 5b, Chapter 4.2.1). Protodeboronation is facilitated by ortho-substituents as reported by Kuivila and co-workers.[53] These authors also propose three different mechanisms for the hydrolytic deboronation, depending on the pH-value present. The mechanism relevant for SPC is believed to follow an S_E2-pathway (see Scheme 5).
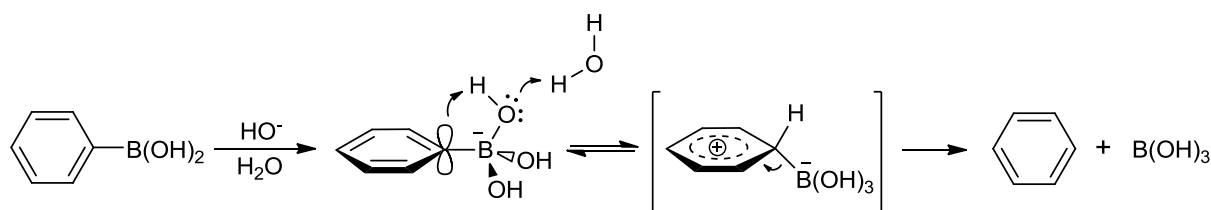
Scheme 5. Proposed mechanism for the hydrolytic deboronation according to Kuivila *et al.*

Electron poor aryl-systems undergo deboronation more rapidly, but the use of weaker bases can suppress the side-reaction.[54] Besides using weak bases for activation of the boronic acid alternative options include decreasing the amount of boronic acid present in the reaction mixture, this can be achieved by slow addition of monomer to the reaction solution[27] or by using a Ar-BF_3 precursor which is hydrolyzed during the reaction.[55]

4.2.3.3. Homocoupling

When two arylboronic acid species are symmetrically coupled by a $Pd^{(II)}$ to form a biaryl this is referred to as homocoupling (Scheme 6). Most commonly in connection with SPC/SMC when a Pd(II)-catalyst precursor is employed, the catalytic active species for SMC is generated by homocoupling.[32] This, however, leads to issues with stoichiometry match or structure imperfection if this reduction is accounted for and a slight excess of boronic acid monomer is used. The exact

mechanism was postulated by Pleixats and co-workers.[56] A double transmetalation is followed by reductive elimination, releasing the biaryl species. Homocoupling does not proceed in oxygen free atmosphere. It should therefore be a minor issue in properly prepared SPC. Electron donating substituents on the aryl unit are beneficial for homocoupling.
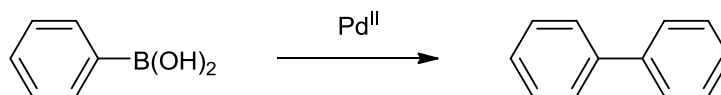
Scheme 6. General description of the homocoupling reaction.

4.2.3.4. Dehalogenation

The last noteworthy side-reaction is the dehalogenation of aryl halides. The aryl boronic esters commonly employed in Suzuki-coupling reactions are readily hydrolyzed under the basic reaction conditions. The generated alcohols can, by β-hydride elimination, lead to palladium-hydride complexes. These hydrides consecutively lead to Ar-H side-products (Scheme 7).[18] This can easily be avoided by using tertiary alcohols for boronic acid esterification (e.g. pinacol).
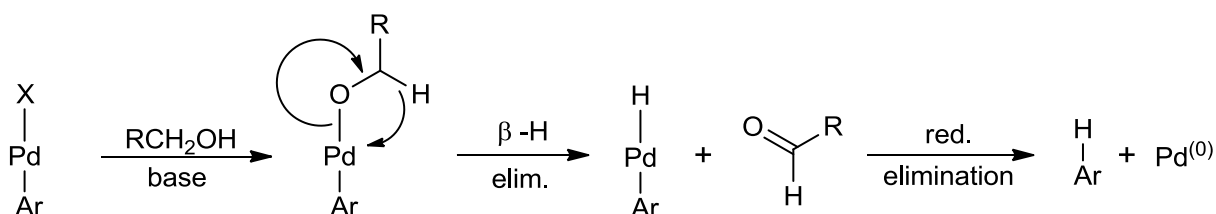
Scheme 7. After addition of a deprotonated alcohol, hydride elimination and reductive elimination the dehalogenated substrate is released.

4.3. All polyphenylene materials – a polymer chemists dream

Aromatic polymers are used in various different applications in our everyday life whether to contain our daily beverage (PET), as high performance lubricants (Polyether)[57] or as high stability fibers in safety equipment or sport gear (polyaramides e.g. Kevlar^{TM}). All these materials have in common that the phenylene units comprised in the polymer backbone are not directly adjoining each other but connected via linker groups including esters, aramides and the like. These groups influence the overall polymer properties through increased flexibility and processability (eg. Polyethers) or increased chain-to-chain interactions

(Polyaramides). However, they are believed to decrease the thermal, oxidative or photochemical stability of the resulting polymer. The original motivation for the synthesis of polyphenylenes was the expectation that they would be the best candidate of all linear polyaromatics with regard to overall stability.[58]

Most syntheses of polyphenylene based structures in fact targeted PPP. Kovacic *et al.* were among the first to report a synthesis of an all phenylene based material.[59] According to their report the reaction of benzene with $FeCl_3$ yielded an insoluble black material which was "difficult to ignite". Their obtained product most likely was a structurally ill-defined oligomer. Additional attempts using Ullman coupling[60] and the Wurtz-Fittig-reaction[61] were published. However, the relatively harsh reaction conditions lead to branching. The Kumada-coupling conditions employed by Yamamoto *et al.*[62] were a further step ahead towards true PPP.

The first report of a PPP synthesized by SPC was published in 1989 by Rehahn *et al.*[24] Using flexible alkyl side-chains to increase solubility, it was possible to obtain a soluble PPP derivative of 6000 to 8000 g mol^{-1}. Since then SPC has become one of the most widespread tools to synthesize polyphenylene based materials, not only in academia but also in industry.[25]

Kinked polyphenylenes have received only little attention compared to their straight PPP counterparts. The first report of PMPs was included in the report of Yamamoto *et al.* towards PPPs.[62] The authors obtained PMP as white powder and carried out a fractionation by Soxhlet extraction. Both fractions showed relatively high melting points 190-200 °C for low molecular weight (soluble) fraction and 280-295 °C for high molecular weight (insoluble) fraction. No quantitative molecular weight determination was possible for the obtained polymers. Musfeldt *et al.* reported the synthesis of kinked polyphenylenes (**6**, **25** – **28**) with varying length of straight segments between kinks (Figure 6) and the effect on opto-electrical properties of the resulting materials.[63] The materials were synthesized by Stille-polycondensation and composed of soluble and insoluble parts. The molecular weight of the soluble fraction was reported to be 1000-1500 Da.
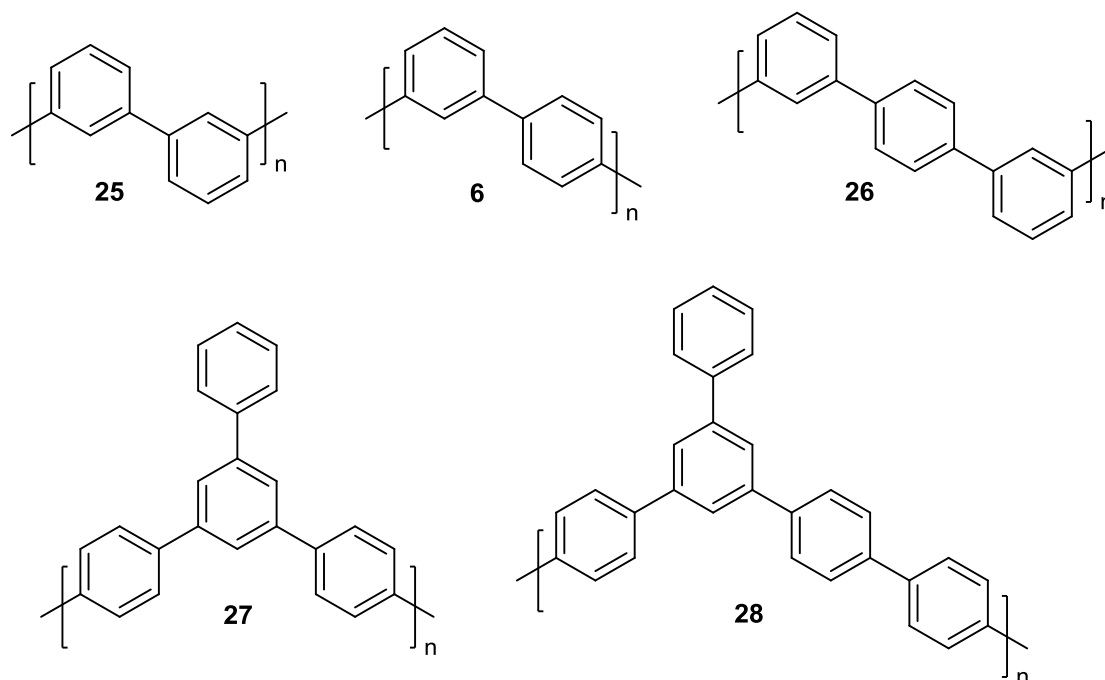
Figure 6.Kinked polyphenylenes synthesized by Musfeldt *et al.* The phenyl side-groups of polymers **27** and **28** were introduced to enhance solubility.

A case of a PMP of slightly higher molecular weight (9700 Da) was published by Reddinger and co-workers.[64] The Ni-catalyzed homo-coupling of the dichloride monomer **29** afforded the desired polymer **30** which possessed remarkable thermal stability (Scheme 8).

Scheme 8. Synthesis of PMP **30** by Ni-catalyzed homocoupling. BPY: 2,2'-Bipyridine.

Kandre *et al.* reported the synthesis of a high molecular weight kinked polyphenylene (Scheme 9).[6] Polymer **5** was prepared by SPC with M_w = 83 kDa on a multi-gram scale. Fractionation of **5** by repeated precipitation gave a polymer with M_w = 255 kDa which could be processed into transparent films. The material properties exhibited by this polymer were remarkable. As Figure 2b indicates, they are comparable to those of commercial polycarbonate under regular conditions. If subjected to chemical stress (exposure to MeOH), the mechanical properties of **5** suffered far less than those of polycarbonate.
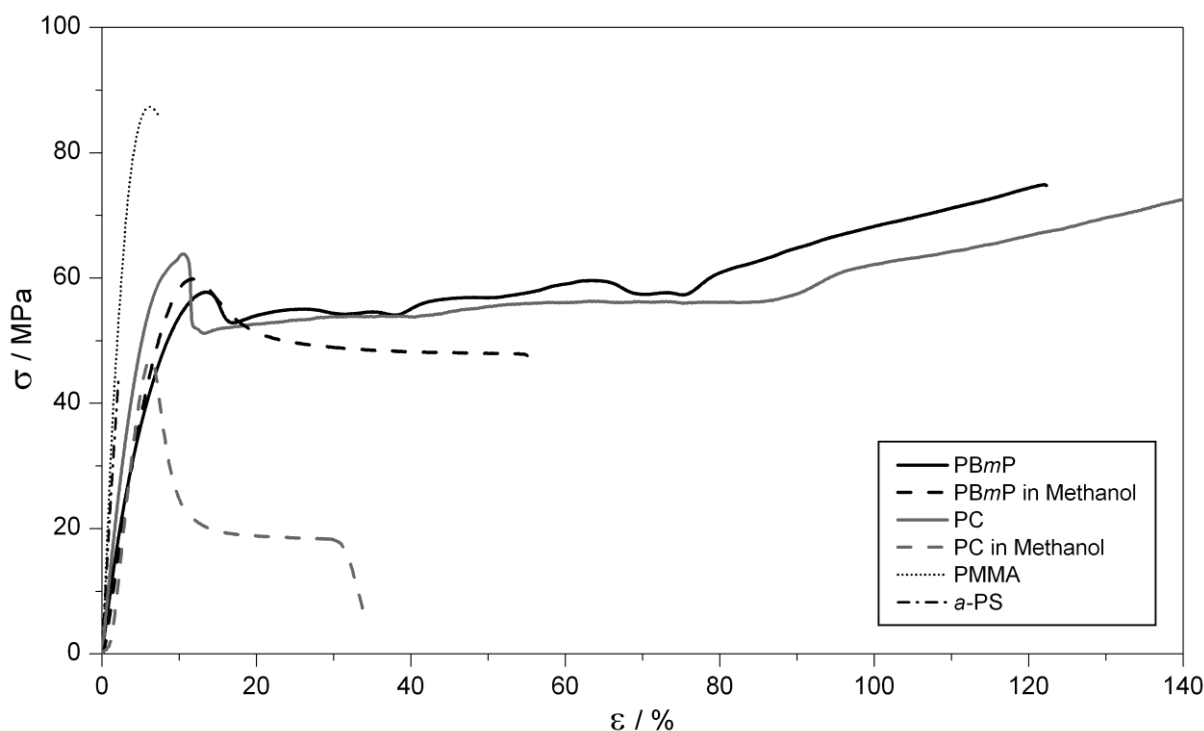
Figure 2b. Stress strain curve of Polymer **5** (PB*m*P) as reference served atactic polystyrene (M_w: 350 kDa), poly(methylmethacrylate) (M_w: 250 kDa) and a commercial polycarbonate (Makrolon LQ-2847, Bayer). Courtesy of "John Wiley and Sons".
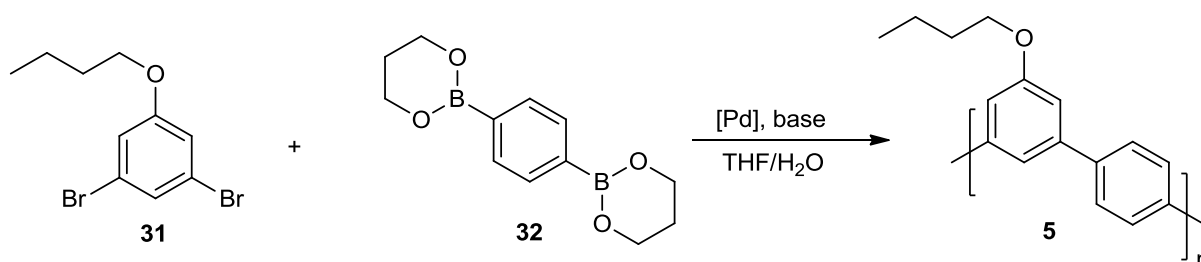
Scheme 9. Example for a Poly(*m,p*-phenylene) (Pb*m*P) synthesized by Kandre *et al.*

4.3.1.   Side-chains and their removal

The first reports of side-groups used to enhance solubility of polyphenylenes was done by Claesson and Kern.[65] They used methyl groups to enhance solubility of a polyparaphenylene synthesized by Ullmann coupling. The principle to attach longer side-chains to rigid polymers was since employed numerously.[66],[67] Jones and Kovacic induced solubility to PPP by alkylation of insoluble material, rendering the material soluble again.[68] Rehahn *et al.* then applied the concept of using flexible chains to synthesize the first polyphenylenes by SPC.[24] This remained a common feature for all polyphenylene based polymers which were synthesized by the SPC protocol. Another study by Rehahn *et al.* could show that beyond a certain threshold

the length of the side-chain does not lead to higher degrees of polymerization. In addition, the authors showed that not only the length of the side-chain is relevant but also the density with which they are placed at the backbone.[69] Increased numbers of longer side-chains as expected showed a higher solubility of the resulting polymer. However, these side-chains have a tremendous effect on the overall materials property. When thinking about the opto-electrical properties of PPP bulky side chains lead to an out-of plane rotation of the phenyl units with respect to each other which consequently leads to a blue shift[70]. Moreover, interesting mechanical properties of a rigid polymer backbone are diluted by the flexible side-chains.[7]

Because of the high potential for desirable material properties of polymers with rigid backbones, different attempts to circumvent obstacles in synthesis and processing have been made. The two main approaches are the transformable precursor and the "hairy" precursor approach. The former uses a precursor polymer with slight alterations in the backbone, which is after polymerization and processing converted to the target material. The latter utilizes the concept of mitigating solubility by including side-chains which are designed in a way that their cleavage from the polymer backbone after processing is facile and quantitative.

4.3.1.1. Transformable precursor

The most widespread use of this method is the xanthate process also called viscose process used in the production of regenerated cellulose.[71] The same basic concept was used in the synthesis of polyacetylene[72] and poly(vinylphenylene)[73] respectively. In the case of polyphenylenes concrete cases for this approach were employed by Ballard *et al.*[58] and more recently by Batson and Swager[74] (see Scheme 10). In the former case FRP polymerization is used to obtain the precursors (**34 a,b,c**). As a consequence not exclusive 1,4-connectivity is given but rather a mixture of 1,4- and 1,2-connectivity.[75] In the latter, the obtained PPP **37** still carries substituents. The main advantage of the transformable precursor approach, are the high molecular weights of precursor polymer, which can be obtained. However, monomers and obtainable polymers are structurally limited. Additionally, incomplete conversion to the target polymer leads to defects being incorporated into the polymer backbone.

R = *t*-Bu, Ph, OMe

33 a,b,c

34 a,b,c

35

R' = C$_{16}$H$_{33}$ **36**

37
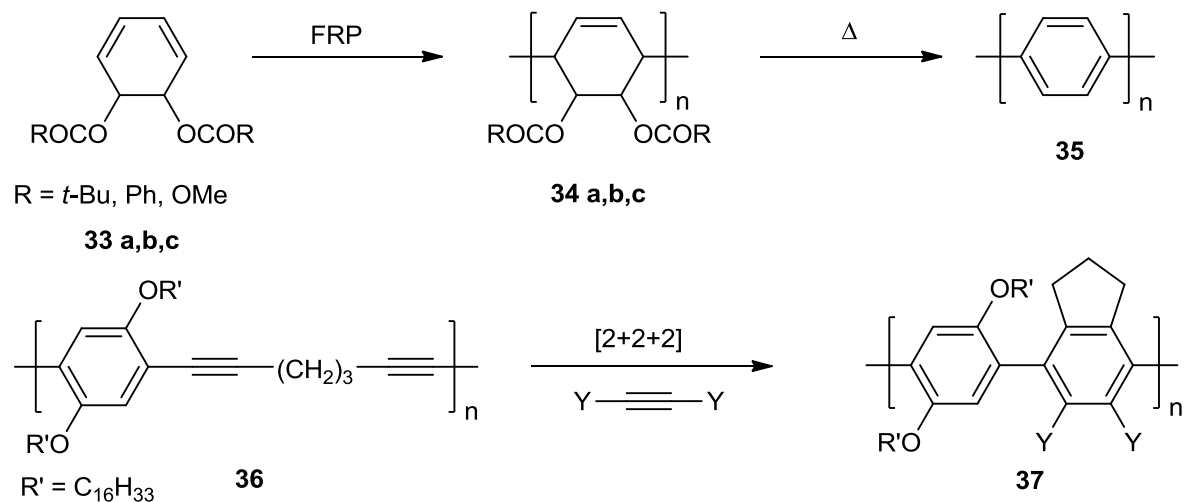
Scheme 10. a) Ballards route to polyphenylene by a soluble precursor. b) Polyphenylene synthesized by Swager and co-workers by a precursor approach.

4.3.1.2. Precursor with cleavable side-chains

An alternative approach to rigid backbone polymers carrying no side-chains is the concept of removable side-chains. This concept is thoroughly investigated in the present work. It has already been applied to polyamides.[76] Long alkyl chains were linked to the backbone with an ester moiety as linking group. Saponification was used to remove the side-chain after processing of the precursor polymer **38** (see Scheme 11). A complete removal of the linking unit was not carried out.
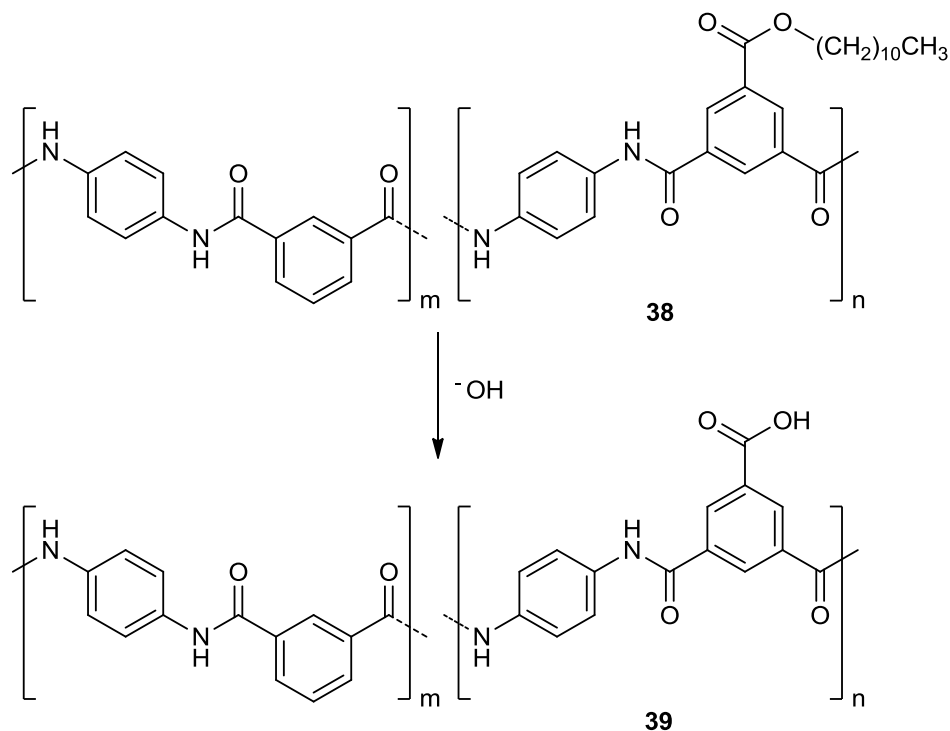
Scheme 11. Polyamides with removable side-chains by He *et al.*[76]

This concept was new to polyphenylenes[42] and was investigated as part of the present work. In concrete terms, a silicon alkyl based side-chain was used, which was cleaved by proto-ipso substitution. The same concept was later applied to polythiophenes.[77] Liu *et al.* previously reported a similar study for polythiophenes.[78] However, these authors used a thermal process to cleave the side-chains of the polythiophene backbone, as in the study investigating the concept for polyamides, the linking group could not be removed from the polymer backbone. In this particular case this led to desirable properties of the polymer and no further attempts to remove the linking group were done.
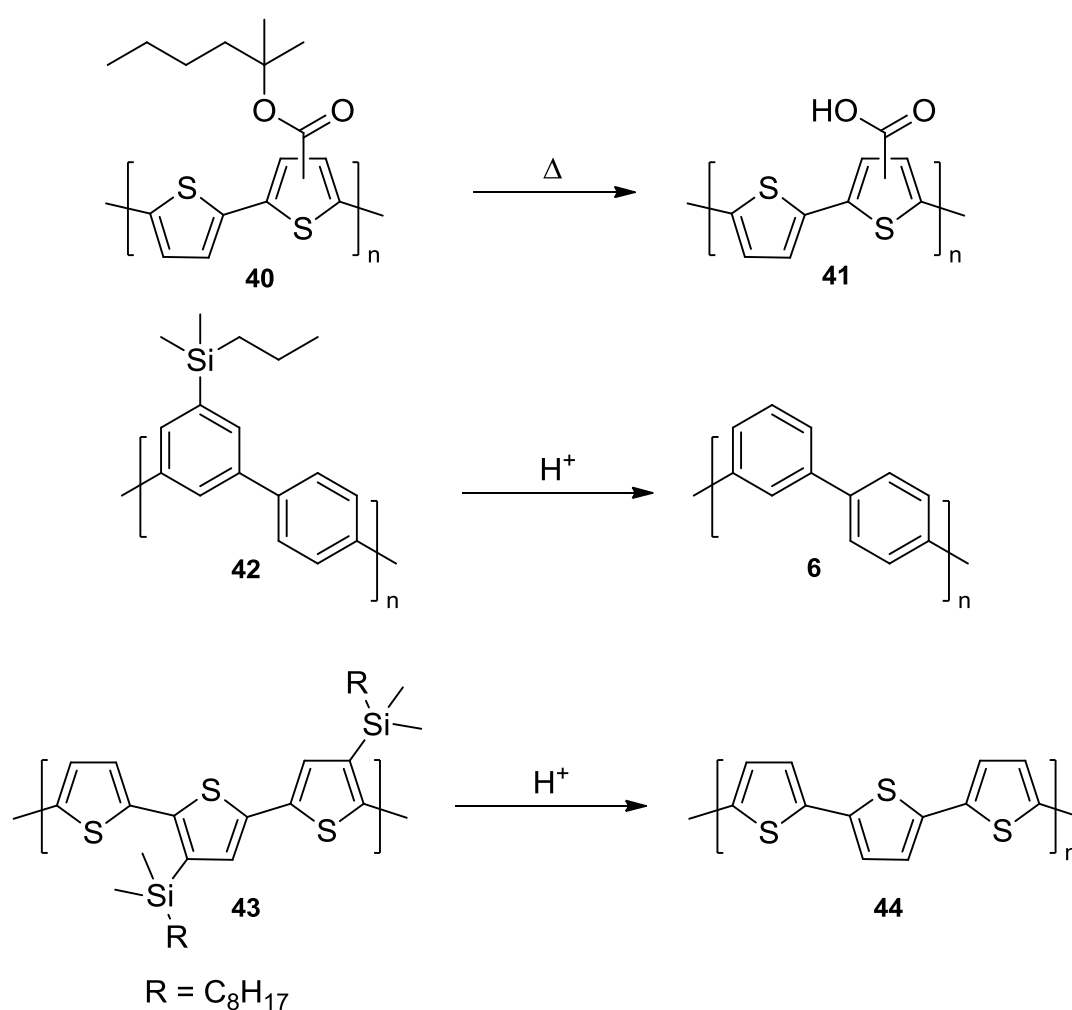
Scheme 12. Removal of side-chains of polythiophenes[77],[78] and polyphenylenes [42] by heat or acid treatment.

4.4. Suzuki-polycondensation by microwave heating

4.4.1. General

In recent years an alternative heating method has started to establish itself in chemical laboratories. Ever since people started using microwave ovens to reheat their leftover meals, it's been a desirable tool for laboratory use because of its ability to quickly heat reaction solutions. Whereas in the early days of microwave ovens in chemistry labs, sometimes even regular kitchen microwave ovens were being used, the present microwave ovens used in chemistry labs bear little resemblance to their domestic counterparts. Magnetic stirring, accurate heating rate, microwave power and temperature control enable exact tuning of reaction parameters. The possibility to work under inert atmosphere conditions broadens the scope of possible reactions. Pressure sensors as well as explosion protected reaction cavities increase working-safety.

The first reports of organic reactions in microwave ovens were made by Gedye *et al.*[79] and Giguere *et al.*[80] in 1986. Both used regular domestic microwaves to carry out basic organic reactions like esterification's, S_N2-reactions, ene-reactions or cope-rearrangements. First reports of Suzuki-Miyaura-crosscoupling in microwave reactors followed in 1996 by Larhed *et al.*[81] The main advantage observed in the studies mentioned above were not necessarily product yield but rather the significantly reduced reaction times at comparable levels of conversion.

4.4.2. Microwave heated polymerizations

As in small molecule synthesis the amount of research dedicated to using microwave heating over conventional heating has been increasing drastically in recent years. Different polymerizations methods such as FRPs, CRPs (mainly RAFT), ROPs and polycondensations were investigated with regard to their performance under microwave heating.[82],[83] Because of the demand for high conversions in polycondensations, the drastically reduced reaction times observed in microwave-heated reactions are of high interest.

Despite considerable research efforts, it is still unclear whether there really is a non-thermal microwave effect which leads to an enhancement of rate of polymerization. Because of the autoclave conditions common for microwave reactors,

very often the observed increase in reaction rate is in good agreement with Arrhenius' law which predicts an increased reaction speed by a factor of roughly 2 for a reaction temperature increase of 10 K.[82] A concrete case showing no non-thermal microwave effects on reaction speed for a RAFT polymerization was published by Paulus *et al.* in 2009.[84] However, in the same year, Roy *et al.* reported considerable rate enhancement for another microwave heated RAFT polymerization compared to conventional heating.[85] In a careful comparative study by Kwak *et al.* only minimal differences in rate of polymerization for FRP was observed.[86] The authors claim that differences in reaction rate can be attributed to insufficient temperature control. More polar monomers were not found to have an enhanced reaction rate compared to their non-polar counterparts in co-polymerization experiments. The main advantage of microwave ovens therefore seems to be the quick and controlled heating at the beginning of a chemical reaction as well as the access to non-conventional reaction conditions with regard to temperature and pressure. These features have made microwave ovens popular tools in otherwise time-consuming processes like reaction condition screening.

4.4.3.   Microwave assisted SPC

The first case of a SPC carried out in a microwave was reported by Nehls *et al.* in 2004.[87] In the synthesis of a ladder-type polymer by a precursor route (see Figure 7) the authors obtained the respective precursor polymer **45** in reasonable molecular weight (M_n: 14.2 kDa, PDI: 1.8, P_n: ~15) and short reaction times (12 min). In a later publication the same research group reported improved molecular weights (M_n: 29.9 k, PDI: 2.3) using a non-aqueous heterogeneous system (THF, powdered KOH), the same system was used to polymerize sterically hindered substrates.[88] In a more recent report, Zhang and co-workers report the microwave-assisted synthesis of Poly(9,9-dihexylfluorene)s by SPC.[31] In their study, the effects of microwave power and reaction temperature are investigated in addition to the conventional reaction parameters like solvent and catalyst species. Within a 14 min reaction time under ideal conditions ($PdCl_2$(dppf), THF/H_2O, 130 °C, 150 W) polymer **46** with a M_w: 40 kDa and a PDI: 1.96 was obtained. However, it should be noted that microwave assisted polymerization has its very own pitfalls. Zhang *et al.* observed the formation of insoluble gel particles if reactions conditions were too harsh as in exceeding a certain reaction time, reaction temperature or microwave power. They attributed this

gel formation to cross-linking which takes places under harsher conditions.[89] The proposed cross-linking mechanism is shown in Figure 8.
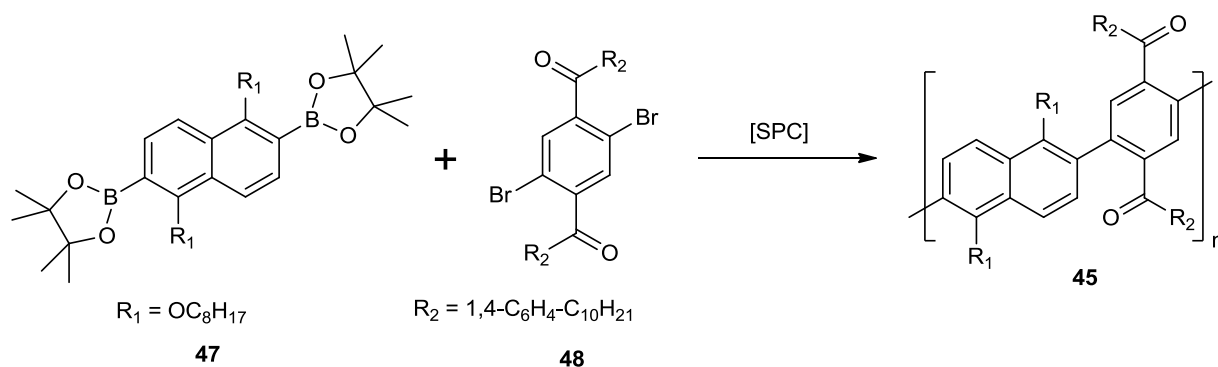
Figure 7. **47** and **48** were coupled by microwave assisted SPC to form precursor polymer **45**.
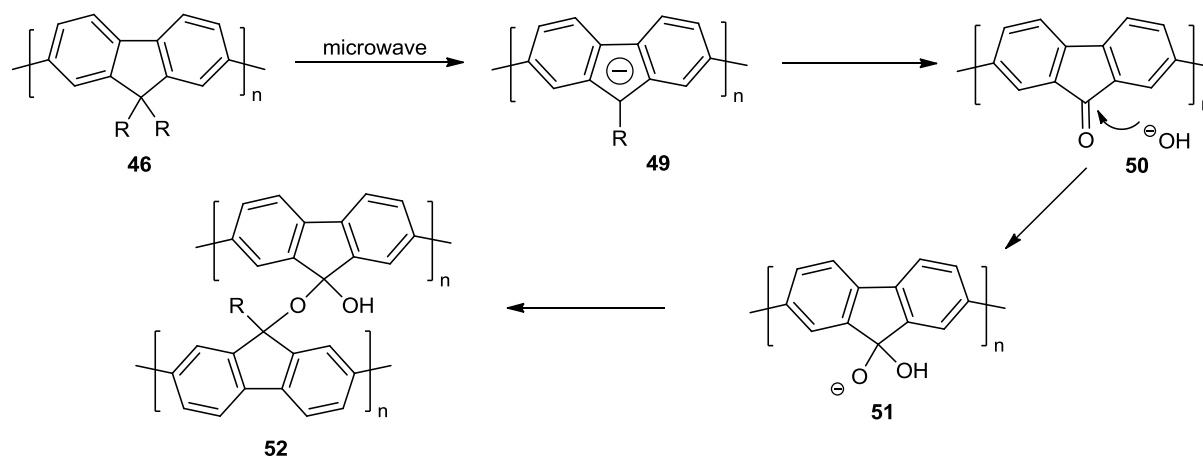
Figure 8. Possible cross-linking mechanism taking place during microwave assisted SPC.

4.5. Electrospinning

Electrospinning is a versatile technique for fiber-formation of a broad variety of polymers. Their thickness ranges from a few nm up to tens of µm. This diversity has lead to electrospun fibers being used for different application purposes. For example can electrospun polymer mats of nanofibers be used as nanoporous filtration devices, while compartmentalized fibers are used in medical applications such as controlled drug delivery. [90]
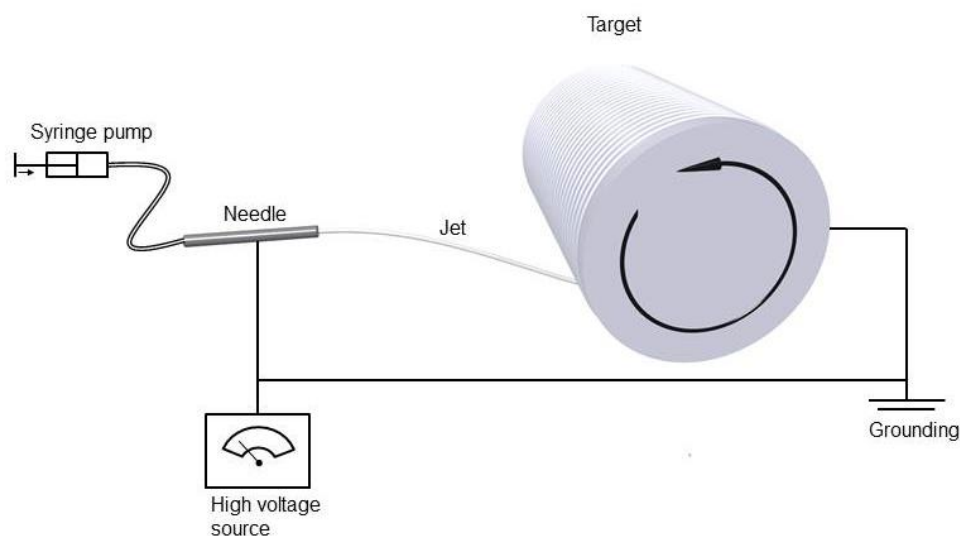
Scheme 13. Sketch of an electrospinning setup. A polymer solution is pumped slowly through a flat tipped needle with high voltage applied. The electric field leads to the formation of a fine jet towards a grounded, rotating cylinder which serves as target.

During the electrospinning process a polymer solution in a polar solvent is pumped through a flat tipped needle which is connected to a high voltage source. The electrically charged solution is deformed at the tip of the needle. If the applied voltage exceeds a critical voltage, a jet erupts from the droplet, which is accelerated by the electric field towards a grounded target (Scheme 13).

The choice of target has a significant effect on the shape of the obtained fibers. A simple metal plate leads to a random mesh of fibers, while a rapidly rotating cylinder leads to relatively nicely aligned fibers. As the jet is accelerated to high speeds, the cylinder itself needs to be rotated at high rpm values. Even then some misaligned fibers may be present. A common drawback of these collectors is the limitation in fiber length. The fibers need to be cut off the cylinder, which constrains the maximum fiber length at the circumference of the cylinder. A possibility to obtain fibers of higher length is the employment of a grounded water bath as target. An additional advantage is that the target can serve as coagulation bath for slow evaporating solvents.[91]

In general obtaining fibers from electrospinning is relatively simple given a polymer solution with a sufficient amount of chain entanglements. There are, however, a few processes characteristic to electospinning which have to be considered. One of these processes is called bending. It originates from an

accumulation of like charges. The resulting coulombic repulsion induces a looping motion of the jet in the horizontal plane. The diameter of these loops increases with distance from the nozzle, leading to a stretching of the jet and the apparent spinning distance. This consequently results in reduced fiber thickness.[90] Generally DC-type high voltage sources are employed in electrospinning. Kessick and co-workers showed that using an AC-type voltage source greatly reduces bending, which leads to thicker fibers obtained during the process.[92] An undesirable but frequently-encountered feature of electrospun fibers is the formation of beads in the fiber. This effect is accounted to surface tension along the jet and is more pronounced for solutions of lower concentration. Fong *et al.* were able to directly correlate the formation of beads in electrospun fibers with the viscosity of the spinning solution.[93] A third phenomenon encountered in electrospinning is called spraying. Spraying occurs when the polymer chains do not have a sufficient amount of entanglements to form a stable jet. The main reasons for spraying are low molecular weight of the polymer sample, excessive dilution of the spinning solution or the use of a solvent which possesses too good dissolution properties for the polymer in question.[94] Usually of highest interest during the fiber spinning process is the fiber diameter. A multitude of studies investigate the effect of spinning parameters on fiber size. The parameters showing the strongest effects on fiber dimensions are viscosity, nozzle diameter, feed rate and spinning distance. Except for the latter, fiber thickness increases with increasing values of these parameters. As previously mentioned, increasing the spinning distance leads to increased stretching of the jet and reduced fiber thickness. [95]

5.   Monomer Synthesis

5.1.   Diboronic esters

Two diboronic acid esters were synthesized for the present work. Both were synthesized starting from the same commercially available starting material phenyl-1,4-diboronic acid (**15**). Using 1,3 – Propanediol and Pinacol as dialcohol species refluxing in toluene at a Dean-Stark-apparatus by means of a condensation reaction the respective diboronic esters were obtained (see Figure 9). Both monomers could be synthesized in large scales (22/55 g) and good yields (73/86 %).
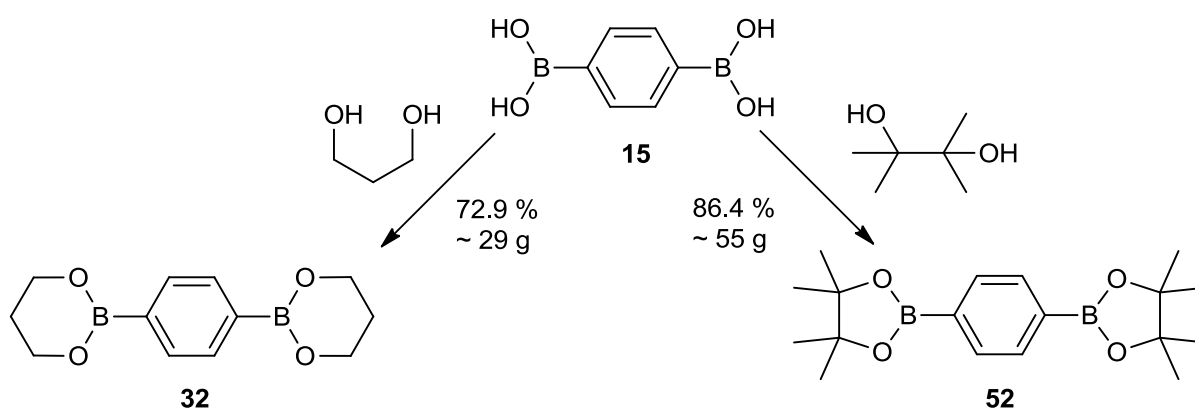
Figure 9. Synthesis scheme for the boronic ester monomers 32 and 52.

5.2.   Dibromide Monomers

As previously mentioned the big advantage of the AA/BB approach to SPC chosen for the present work is the large flexibility in monomer design. A number of monomers bearing different side-chains were synthesized or their synthesis was attempted and deemed unfeasible for the present work. A synthesis-overview for the monomers subjected to SPC is shown in Figure 10, whereas the synthesis for a monomer not subjected to SPC conditions is given in Figure 14.

5.2.1.   'Kinked' monomers

Figure 10. Synthesis overview for monomers subjected to SPC conditions.

The synthesis of the most basic dibromide monomer **53** was carried out by a mono-lithiation of 1,3,5-tribomobenzene (**54**), the monolithiated species build was quenched by the respective silylchloride to form **53**. Because of the high demands regarding purity for AA/BB type SPC-monomers a column chromatography to remove
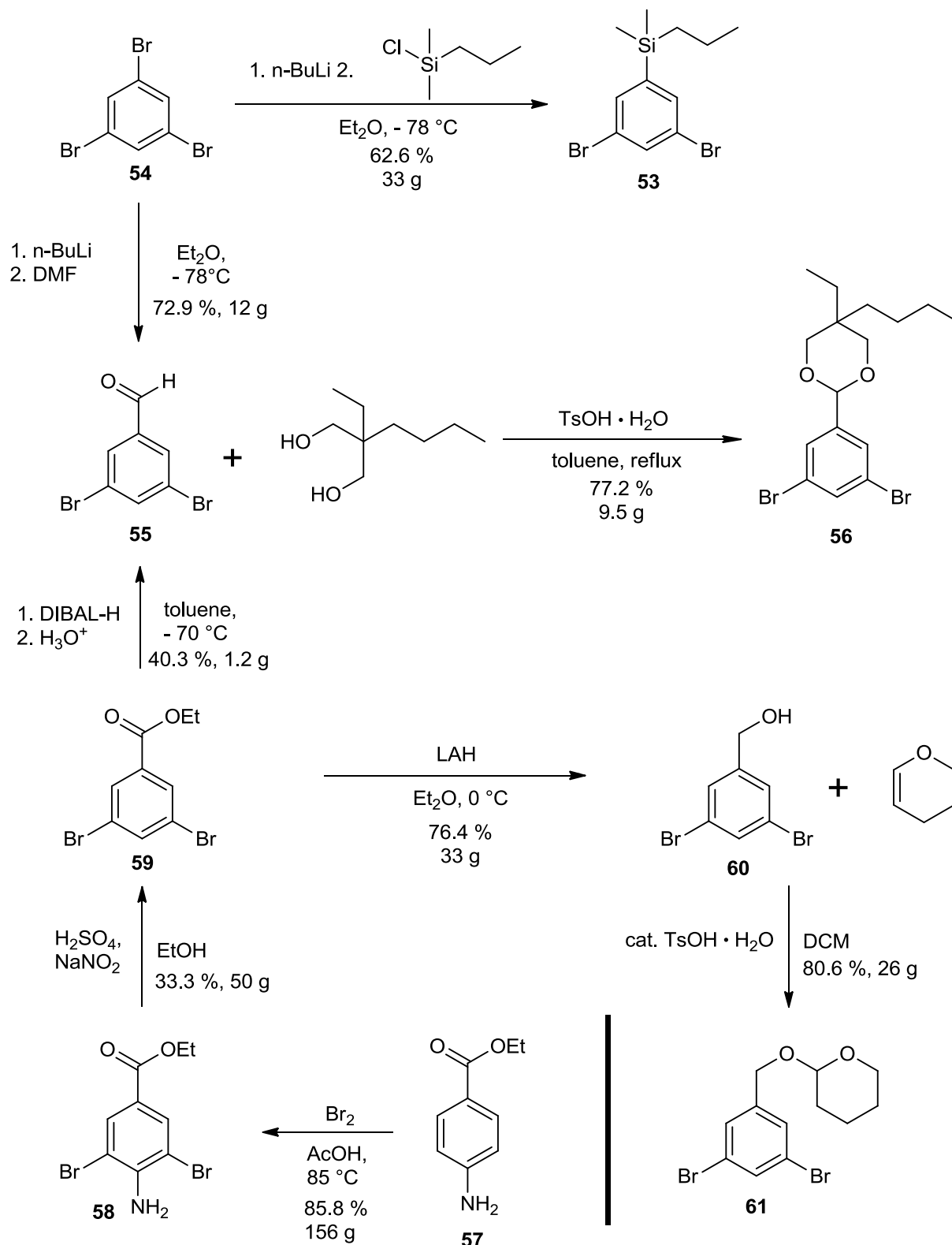
major impurities and a fractionated vacuum distillation to remove excess starting material and obtain pure monomer as colorless oil was needed. After complete purification the monomer could be obtained in good yields (63 %) and large quantities (33 g). The ^{1}H-NMR spectrum (Figure 11) of **53** shows the high degree of purity. Commonly the ^{13}C-satelite peaks are used as an internal standard to determine the purity of a sample.[25]
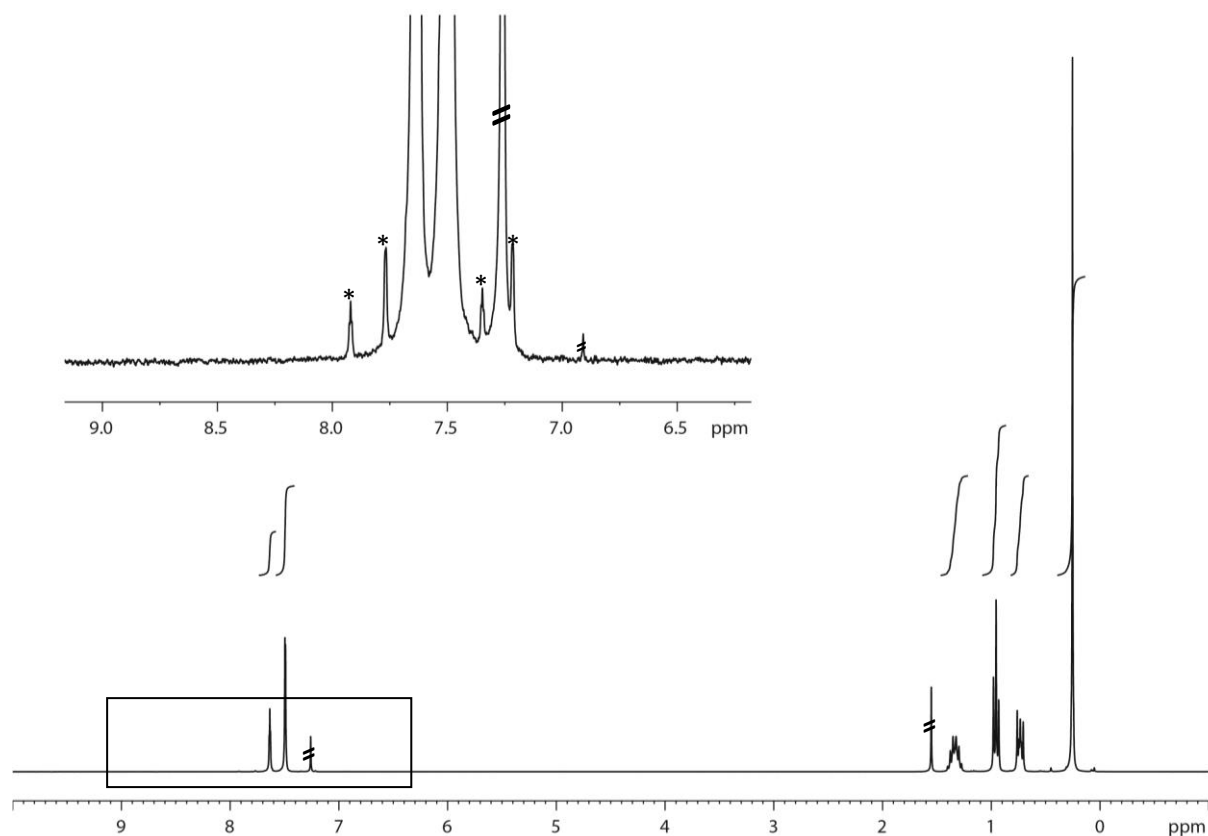
Figure 11. ^{1}H-NMR spectrum of **53** measured in CHCl$_3$ at r.t. Peaks denoted by * are ^{13}C-satelite peaks of the monomer, dashed through peaks are signals belonging to the NMR-solvent (CHCl$_3$, its ^{13}C-satellites and H$_2$O)

From the same starting material **54**, using the same reaction type but a different electrophile (DMF), 3,5 – dibromobenzaldehyde (**55**) a precursor for monomer **56** was obtained.[96] The final step in the synthesis of **56** was a straightforward acid catalyzed acetal formation.[97] An alternative route to obtain **55** started with **57** the dibromination yielded dibromide **58**. Subsequent deamination by diazonium salt formation yielded **59**.[98] Selective reduction of the ethylester with DIBAL-H to the aldehyde yielded **55**.[99] However, it should be noted that problems with the selectivity of the reduction rendered this pathway less feasible than the formerly mentioned one. A small amount of over-reduced product **60** and starting material **59** required

repeated recrystallization to a degree that the yields were not anymore on a satisfactory level (< 50 %).

Figure 12. ^{1}H-NMR spectrum of **56** measured in DMSO-d$_6$ at r.t. Signals denoted by * correspond to ^{13}C-satellite signals, dashed through signals originate from the NMR solvent. The signal marked with a dagger can be accounted to starting material **54**.

The synthesis of monomer **61** followed the same synthetic route until intermediate **59**. Complete reduction to the benzylic alcohol **60** with LAH and subsequent acid catalyzed acetal-formation with DHP yielded the desired monomer **61**. Contrary to the previously mentioned monomers **53** and **56**, for **61** column chromatography resulted in sufficient material-purity, likewise to the aforementioned cases synthesis on large scale (26 g) was possible.
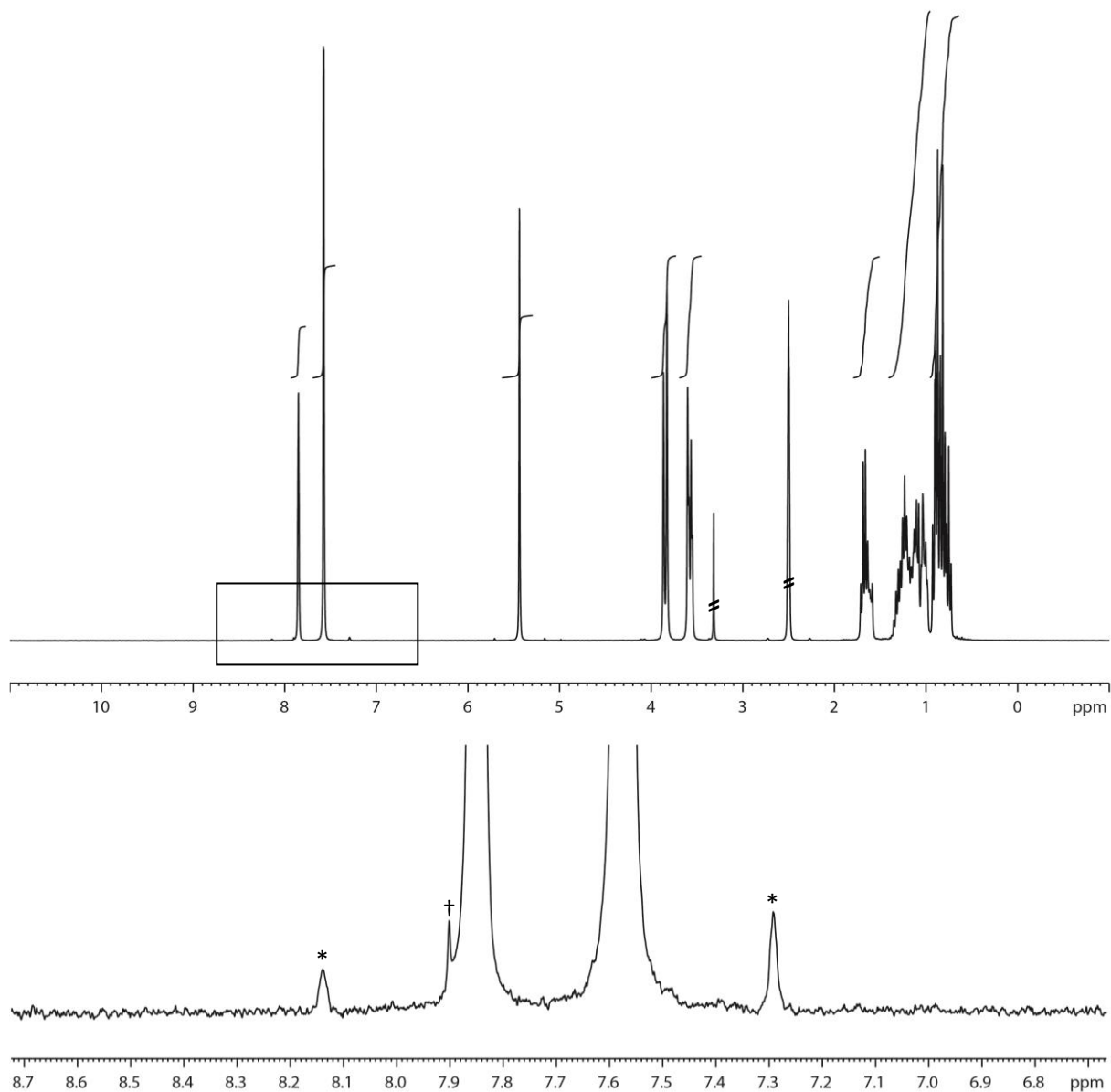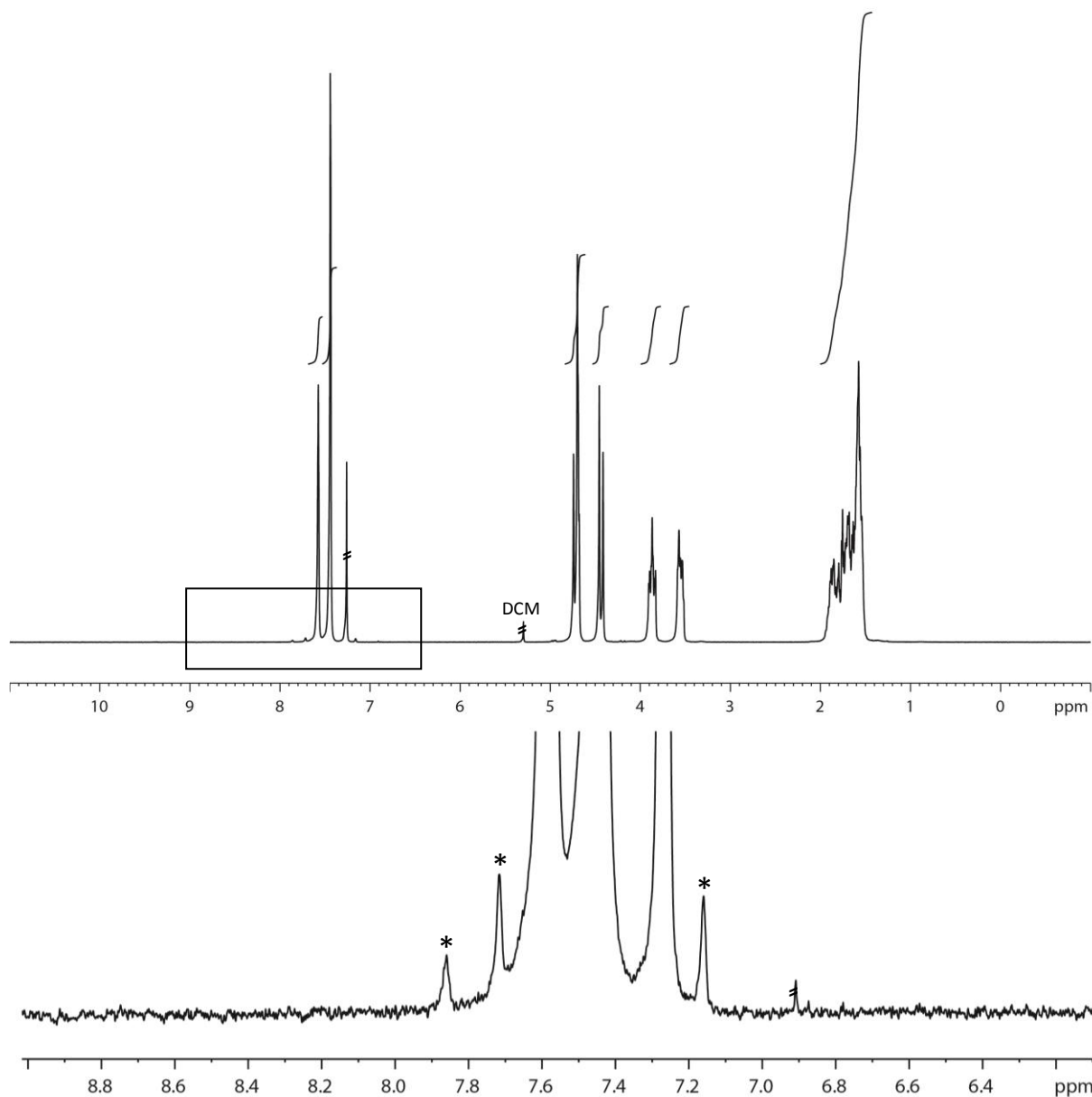
Figure 13. ^{1}H-NMR spectrum of **61** measured in CDCl$_3$ at r.t. Signals denoted by *
are ^{13}C-satellite signals, dashed through signals originate from NMR solvent and a
small solvent impurity (DCM).

In addition, another kinked monomer **62** was synthesized (Figure 14). From 2,5-
Dibromo-4-nitroaniline (**63**) by deamination via diazonium-salt formation 3,5-Dibromo-
nitrobenzene (**64**) was formed. Subsequent reduction of the nitro-group afforded 3,5-
Dibromoaniline (**65**). Protection of the amine group with boc-anhydride yielded the
desired monomer **62** which could be recrystallized from hexane. Contrary to the
previously mentioned monomers, compound **62** was never subjected to SPC
conditions, the reason for this is the yield for the last synthesis step was too poor
(24.4 %) to make large scale synthesis of the monomer feasible.
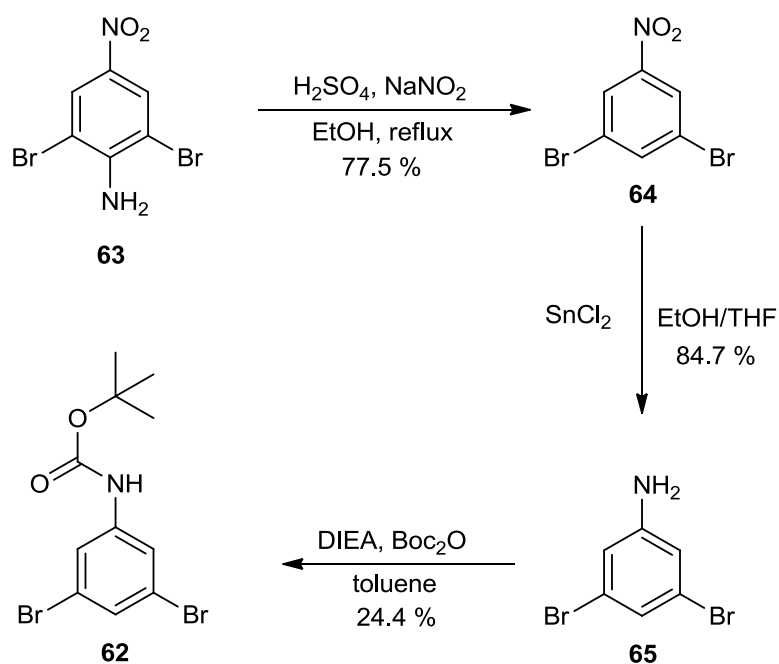
Figure 14. Synthesis of **62** starting from **63**.

5.2.2. Straight monomers

In an attempt to expand the presented concept from P*mp*Ps to PPPs straight monomers were also targeted. These monomers were designed in a way that substituents in ortho-position to the reactive sites were avoided. The reason for this measure was the desire to exclude negative effects on the oxidative addition step in the cross-coupling and consequently the polycondensation rate.[100],[101] This goal, however, came at the price of multiple functionalities which had to be converted in a consecutive manner. These synthetic complications lead to low yields or no obtained product at all. The attempts to linear monomers are summarized in Figure 15 and Figure 16.

The synthesis of possible monomers leading to linear polymer was performed according to literature procedures.[102] Starting from the commercially available **66** by an Ullmann-coupling with solid copper in hot DMF the bifunctional monomer-precursor **67** was obtained in good yields on large scales (70 %, 12 g), subsequent reduction of the nitro groups with solid tin and HCl in EtOH afforded **68** in very good yields (95 %). The functional group conversion by Sandmeyer reaction to obtain the Diiodide-compound **69** only resulted in poor yields (7.2-13 %). Consequently the

synthesis of compound **70** was not driven to completion as the monomer synthesis would have been unfeasible for the present work. An alternative monomer followed the same route to the dianiline compound **68**, subsequent protection of the amine groups with boc-anhydride yielded the desired monomer **71** in moderate yields (48 %).
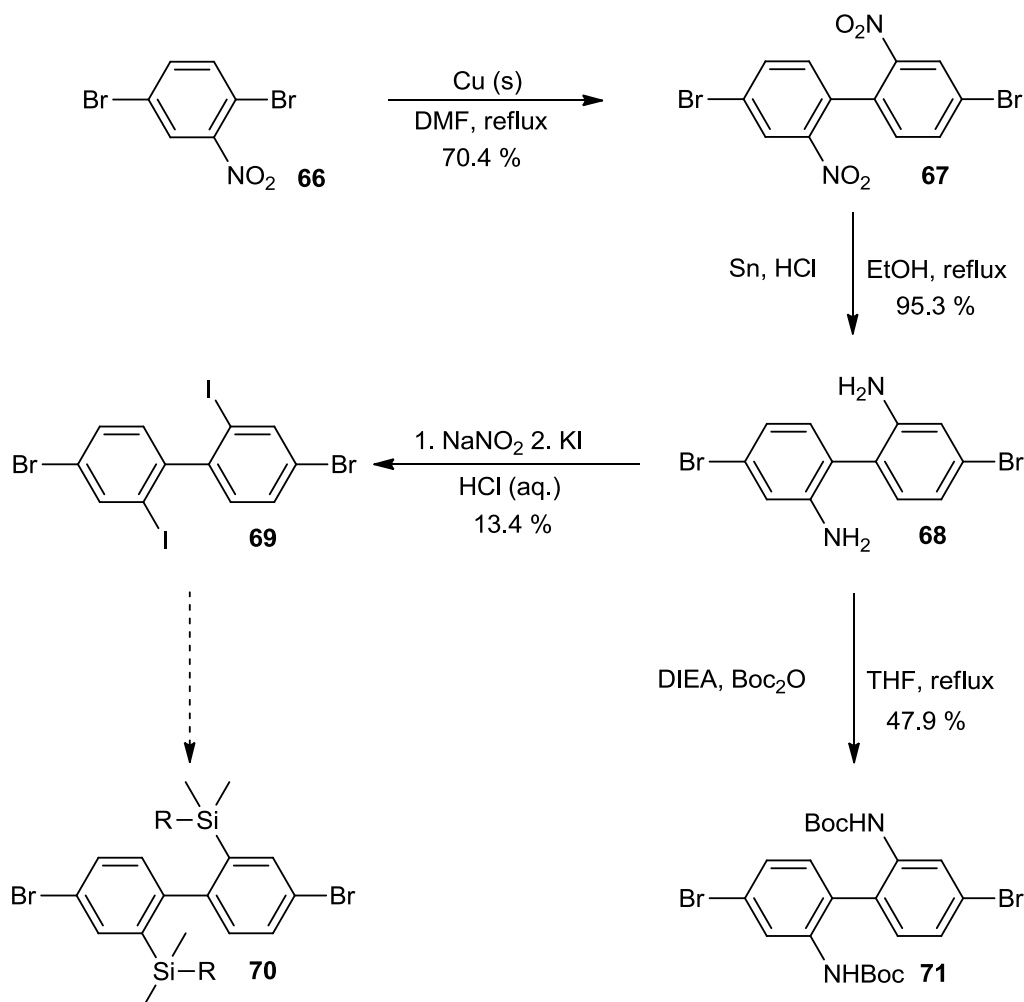
Figure 15. Synthesis scheme for monomer **70** and **71**. The route for monomer **70** was not completed because of low yields for compound **69**.

The synthesis of another monomer containing siliconalkyl side-groups was attempted (see Figure 16). But for the same reason as its closely related bifunctional analogue (low overall yields) the synthesis was deemed unfeasible.

4,4'-Dibromo-1,1'-biphenyl (**72**) was nitrated with nitric acid in acetic acid at 100 °C according to a literature known procedure in good yield.[103] **73** was subsequently reduced using solid tin and HCl in EtOH. This previously employed condition gave **74** in very good yields.[104] In analogy to a literature known procedure the aminogroup of

74 was converted by a Sandmeyer reaction with KI to give **75**, although in poor yields.[105]

Figure 16. Synthesis of possible monomer **76**. **76** was not obtained in sufficient purity and **75** only in poor yields.

6.   Polymer Synthesis

For the present thesis three poly(meta-paraphenylene)s bearing different side-chains were synthesized (Figure 17). Each system was synthesized bearing a specific goal in mind. Polymer 42, which will be referred to as the Si-system, was synthesized in order to explo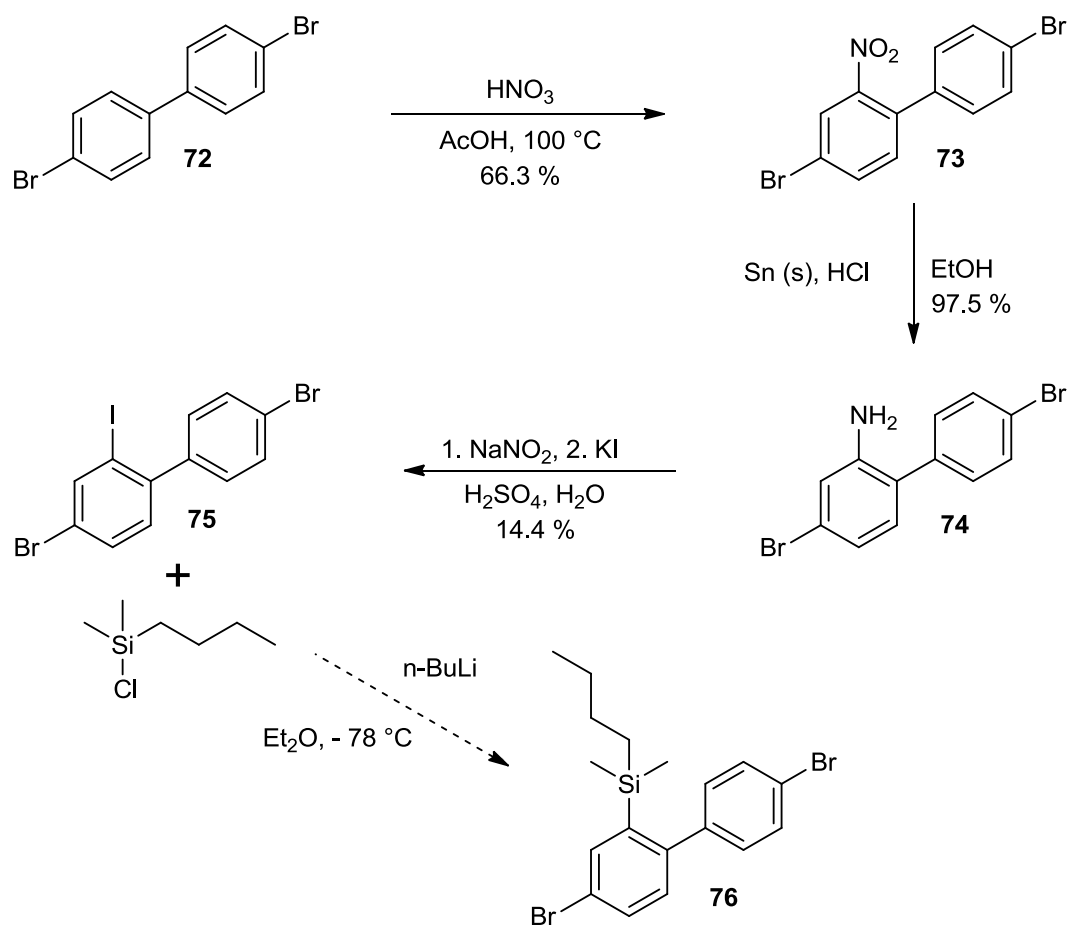re the possibility to use a simple chemical reaction to obtain the target polymer 6. The synthesis of 77 (BnzOTHP-system) was a side-project targeted at end-group analysis in order to get better insight over side-reactions during polymerization. The last polymer 78 (O,O-acetal-system) was envisioned to be an alternative precursor for target polymer 6. However, conversion to 6 should not be carried out by a chemical reaction, but rather by thermal treatment. Polymer 78 should be heated to a temperature which leads to decomposition of the side-chain but is still low enough to leave the polymer backbone undamaged. Following the three different systems are discussed individually.
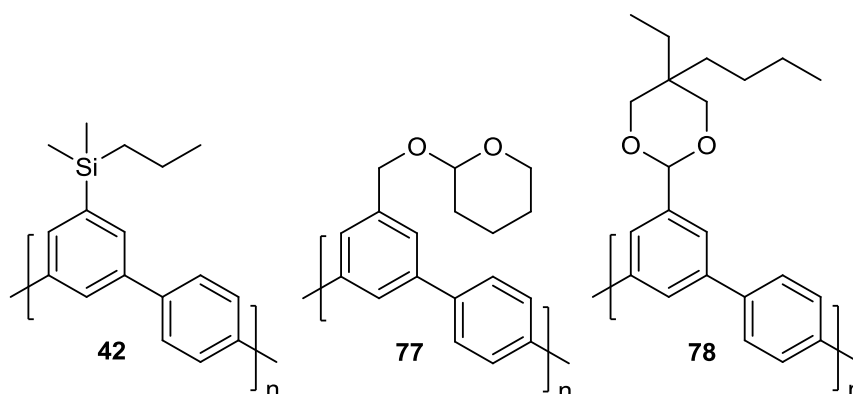
Figure 17. Chemical structure of polymers **42**, **77** and **78** which were synthesized in the present project.

A few technical hurdles are universally applicable to all synthesized polymers. As mentioned earlier an exact 1:1 stoichiometry of the two co-monomers is a crucial element. To exclude low reaction conversion related to stoichiometry mismatch several approaches were taken. A) weighing directly into the reaction vessel, B) using smaller vessels specifically for weighing purposes and transfer in solution with the reaction solvent (repeated rinsing to ensure the transfer is as complete as possible) or C) Preparation of a monomer stock solution. All techniques have some advantages and disadvantages; in the case of A) the most limiting factor is that for technical reasons only certain reaction scales are applicable, the reason being that the combined weight of reaction vessel and monomer quickly exceeds the maximum

load of high precision balances. The largest disadvantage of B) is the human error that comes into the equation during transfer from weighing vessel to reaction vessel even tiniest splashes of monomer solution can lead to a significant mismatch in stoichiometry. C) should be the method of choice when it comes to screening of reaction conditions. The caveat here is that monomer stability in solution can be an issue and needs to be individually evaluated. In the present work for most cases option B) was employed, exceptions to this were studies involving microwave assisted SPC for which C) was chosen. A) was rarely used for the aforementioned reason.

The conditions used by Kandre in his very successful synthesis of a kinked polyphenylene were chosen as a starting point for SPC (see Figure 18).[6] Optimization studies were not the primary goal of the present thesis and therefore not carried out in detail, if at all.
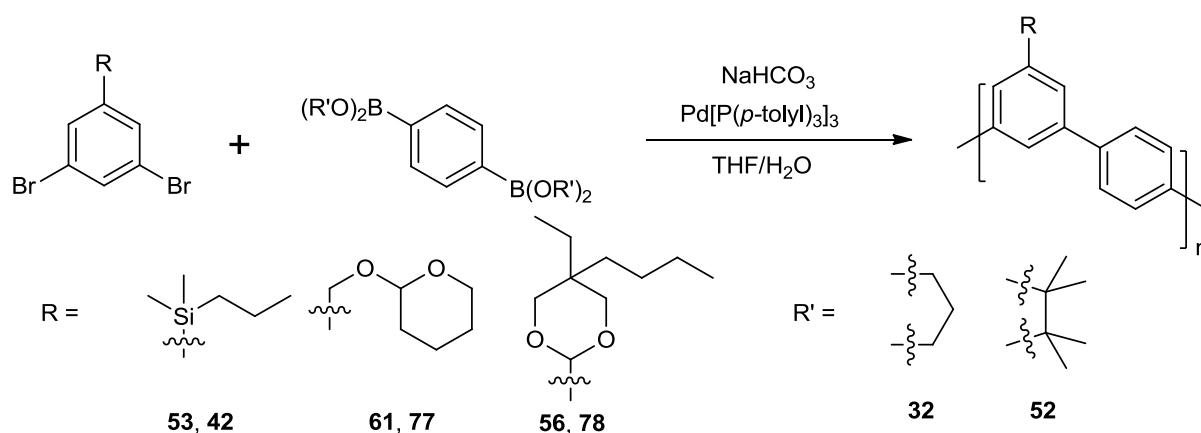
Figure 18. Overview of the synthesis towards polymers **42**, **77** and **78**. The conditions employed were the starting point for polymerizations in the present thesis.

6.1. Synthesis of precursor polymer 42

Polymer **42** could be synthesized reproducibly in high yields using the given reaction conditions. If yields were below 90 % this was a strong indication of flawed reaction or work-up conditions, such as uncontrolled fractionation. The precursor polymer was analyzed by the common organic synthesis tools. ^{1}H-NMR and ^{13}C-NMR proof the structural integrity of the precursor material (Figure 19,Figure 20). Small signals next to the strong Si-CH$_3$ signal could be accounted to end-groups. This was confirmed by NMR analysis of fractionated samples (see Figure 21). With decreasing molecular weight the intensity of the signals in question increased with respect to the main signal.
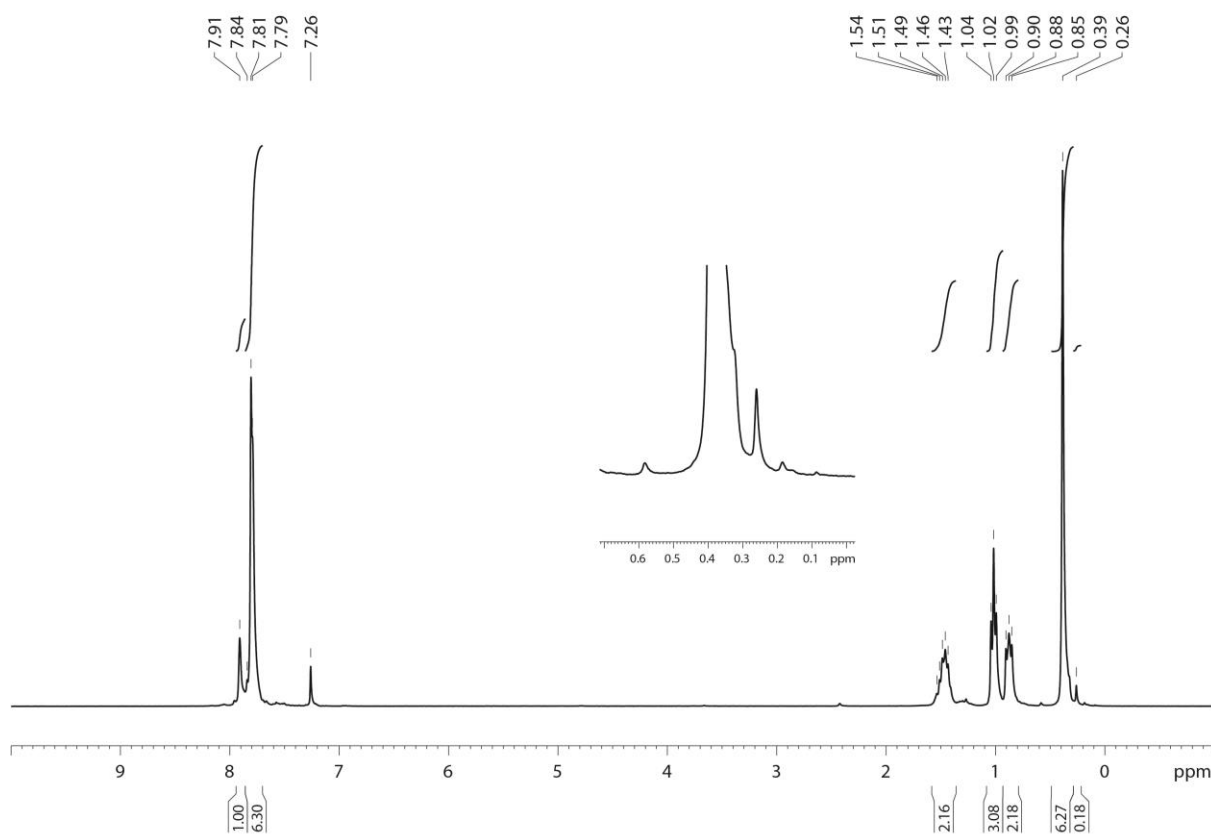
Figure 19. ^{1}H-NMR spectrum of polymer **42** in CHCl$_3$ at r.t.
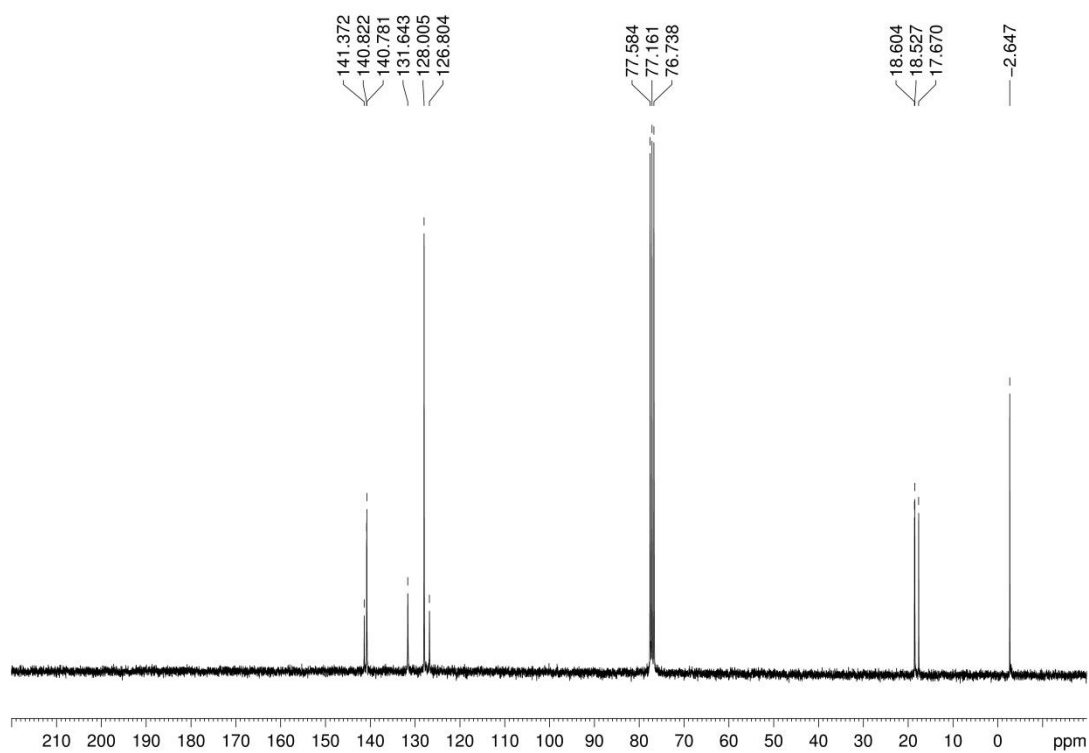
Figure 20. ^{13}C-NMR spectrum of polymer **42** in CDCl$_3$ at r.t.
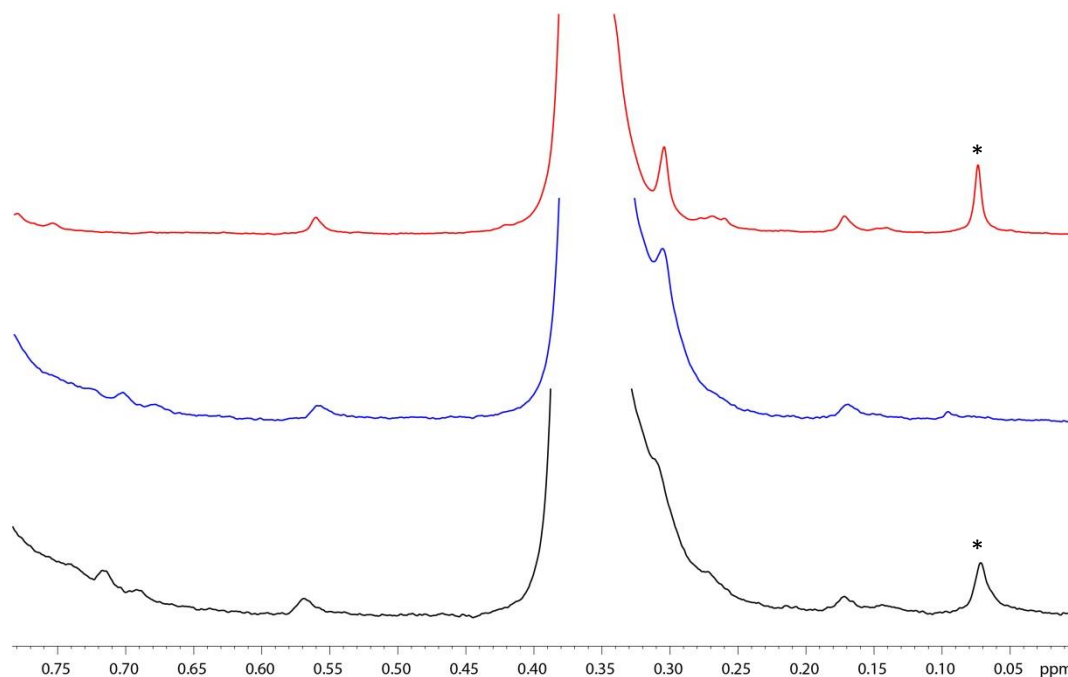
Figure 21. Sections of ^{1}H-NMR spectra of three fractions of polymer **42** recorded in CDCl$_3$ at r.t. Molecular weight of the fractions increases from top (red) to bottom (black). The peaks marked with * are silicon-grease impurities.

6.1.1.   MALDI-TOF MS analysis

For detailed end-group analysis of particular interest was the MALDI-TOF mass spectrum (Figure 22 a&b). The stepwise insertion of the two monomer units can be seen clearly, giving strong evidence for a step-growth type polymerization mechanism. This was of particular interest since very recently for a similarly kinked monomer different observations were made.[27] A similar mechanism could be envisioned, if in a first step all monomers dimerize pairwise and the thus formed AB-type monomer undergoes further polymerization. This, however, is not observed. Unfortunately unambiguous end-group assignment could not be carried out for polymer **42**, the reason being fragmentation processes taking place during ionization. The, by-design, labile nature of the Si-based side-chain becomes an obstacle in analysis.
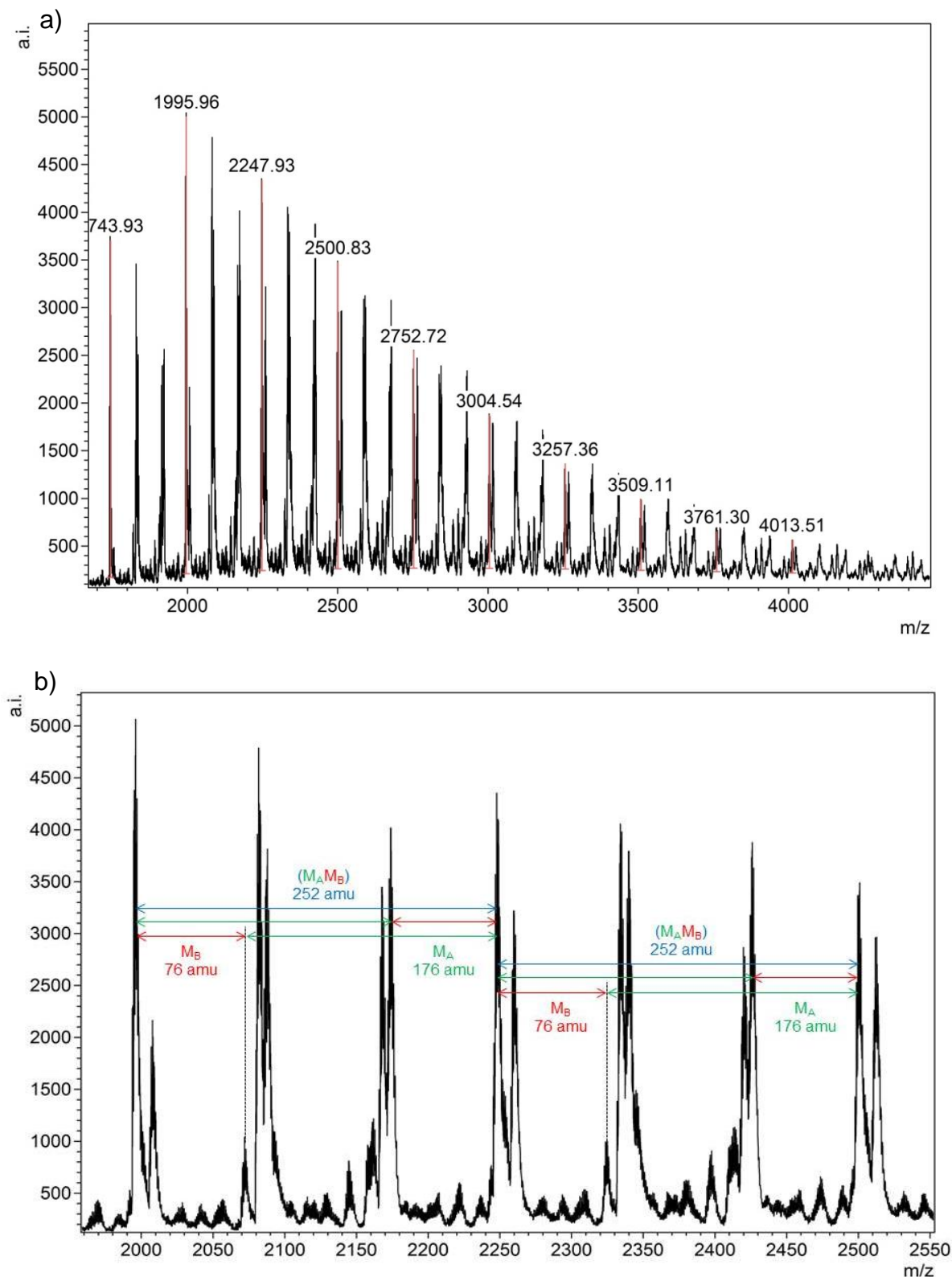
Figure 22. a) MALDI-TOF mass spectrum of polymer **42**, showing a large number of signal series. The nature of these different signals are either different end-groups or fragmentation of the side-chains during the ionization process. b) Section of the MALDI-TOF mass spectrum of polymer **42**, spanning the m/z-range of two repeat units. M_A (green) corresponds the mass of the phenyl unit carrying the side-chain, while M_B (red) represents the unsubstituted phenyl unit of the polymer.
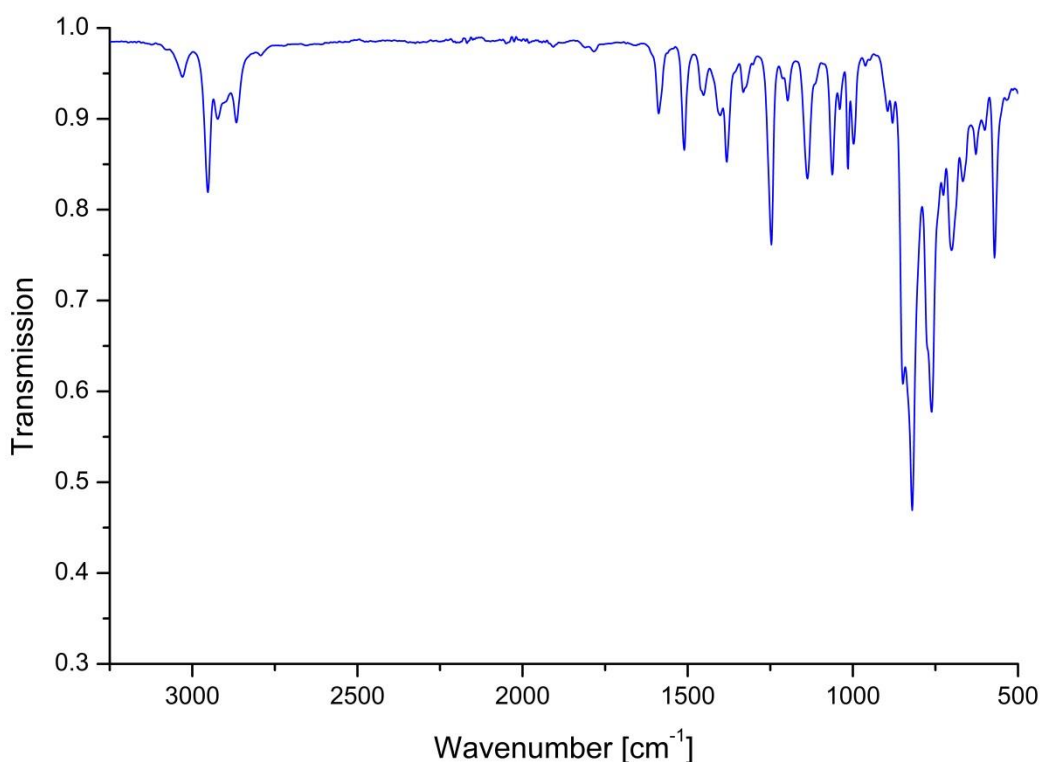
Figure 23. ATR-IR spectrum of polymer **42**.

ATR-IR spectroscopy showed the main characteristics to be expected (see Table 1). The C-H stretching bands at 3030 (aromatic) and 2951-2864 cm^{-1} were of particular importance as they are a clear indication for the presence or absence of the side-groups (further detailed in **7.1.1**). Moreover, the bands observed are summarized in Table 1.

Table 1. Summary of the IR-signals observed for polymer **42**.

Signal [cm^{-1}]	Assignment
1587, 1512	Aromatic st (C-C, C=C)
1455, 1383	CH3 δ (as, sy)
1247	Si-CH3 δ (sy)
1136, 1061, 1014, 992	C-H δ in plane
822, 762	Si-(CH3)2 framework vibrations

The main advantage of the current approach, however, is the possibility to carry out molecular weight determination by GPC. This allows an estimation of the mass for the target polymer. A typical GPC curve for SPC leading to **42** is shown in Figure 24.
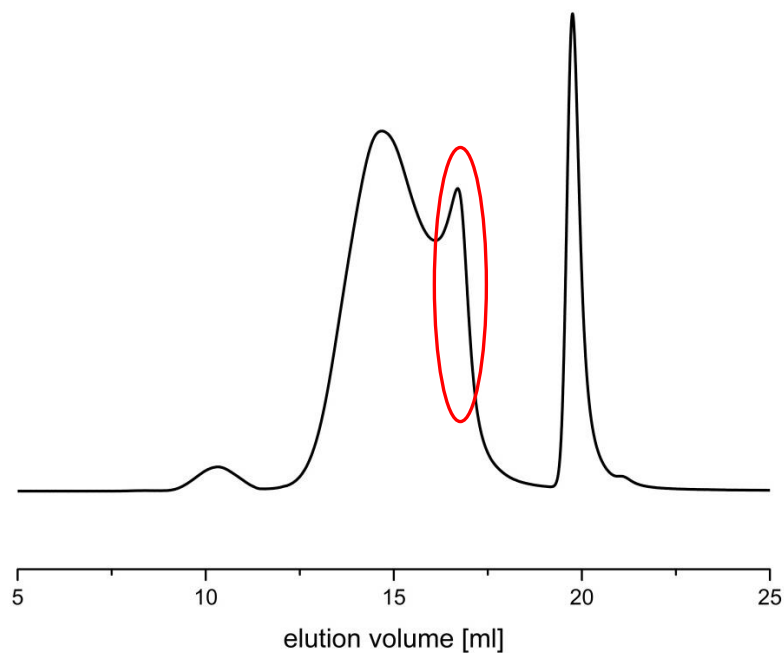
Figure 24. Exemplary GPC elution curve of polymer **42**. The red elypsoid emphasizes the low molecular weight cyclic oligomers.

Most interesting is the bimodal molecular weight distribution. The lower molecular weight peak was attributed to oligomeric, cyclic material. The presence of these kinds of oligomers was shown after further reaction of the precursor (see 7.1.1). These cyclic oligomers are not minor impurities and have a significant effect on average molecular weight. In particular, number average molecular weight (M_n) is very low for all samples obtained as shown in Table 2. The formation of cycles can be suppressed by using increased concentrations during polymer synthesis (see Figure 25). For the present system the use of increased concentrations is limited by the solubility of polymer **42** in the reaction solvent (THF). As for the general reaction condition a gel-like precipitation was observed at later reaction stages (>48 h).

Table 2. Summary of molecular weights and yields obtained for SPC of **53** and **32/52**. For the entry marked with an asterisk, it is reasonable to assume that during the precipitation step of the work-up a significant amount of low molecular weight species was lost.

Entry	Monomers & Batch	Mn [kDa]	Mw [kDa]	PDI	Polymer obtained [g]	Yield [%]
1	**32** & **53** A	4.0	9.3	2.3	2.66	88.1
2	**32** & **53** A	5.0	48.4	9.7	2.24	99.6
3	**32** & **53** B	6.5	14.9	2.3	3.75	98.6
4	**32** & **53** B	8.2	49.7	6.1	5.08	96.6
5*	**52** & **53** B	9.9	93.8	9.5	2.73	83.0
6	**52** & **53** C	5.6	32.9	5.9	4.99	93.5
7	**52** & **53** C	3.9	26.6	6.8	1.06	94.5
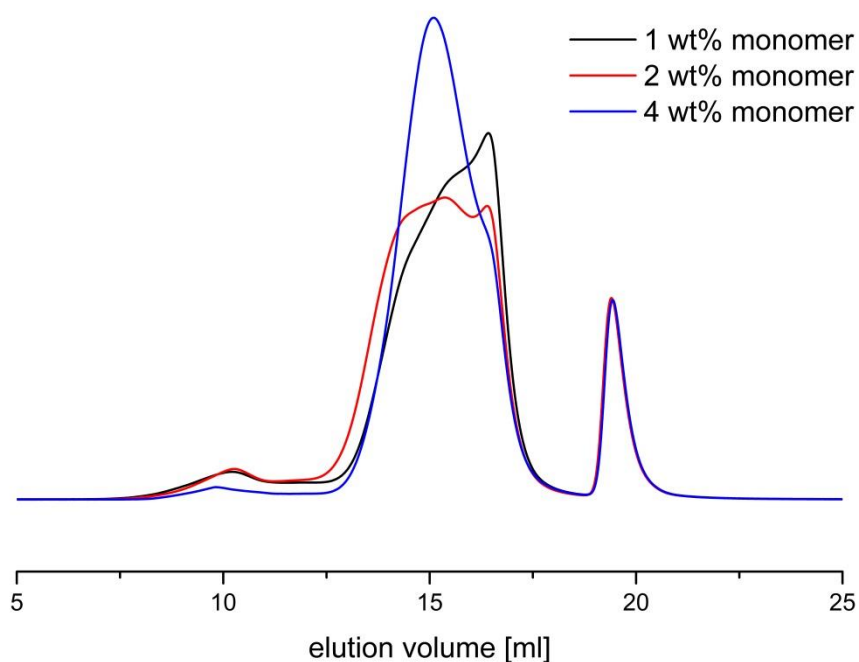
Figure 25. GPC elution curves of polymer **42** synthesized in three different concentrations.

The reduction in cyclic oligomers is evident. They seem to be the major product in the case of the lowest concentration investigated, but barely visible for the highest concentration. For the medium and highest concentration, a precipitation during synthesis was observed. This necessitated the use of relatively low concentrations

during polymer synthesis, leading to a significant degree of cyclic oligomers present in the product. As these low molecular weight species would significantly deteriorate the mechanical properties of a polymer material, their removal was paramount.

6.1.2.   Fractionation of polymer 42

Polymer **42** was fractionated by three different methods: top down precipitation fractionation,[106] fractionation by open GPC and fractionation by precipitation with a selective solvent. The results are illustrated in Figure 26. The top down precipitation fractionation method employed $CHCl_3$ as solvent and MeOH as non-solvent, fractions accounting for 10 % of total sample mass were obtained. Fractionation by open GPC was carried out with toluene as eluent. In the precipitation with selective solvents toluene was used as solvent and EtOH as non-solvent in a ratio of 1:1.

Figure 26. GPC elution curves illustrating two fractionation techniques on a sample of polymer **42**. a) top down precipitation fractionation, black: desired sample, red: stock sample. b) Fractionation by open GPC, comparison of the three obtained fractions (high: black, medium: blue, low: magenta).

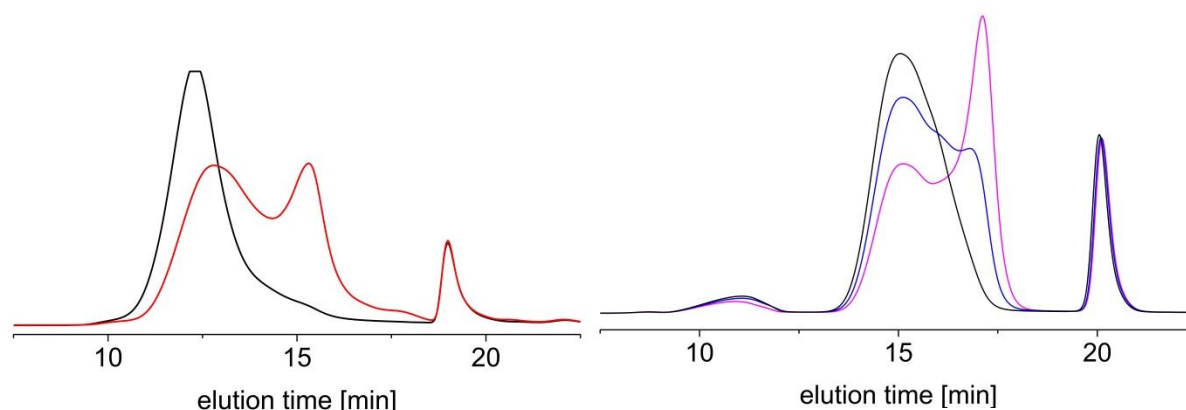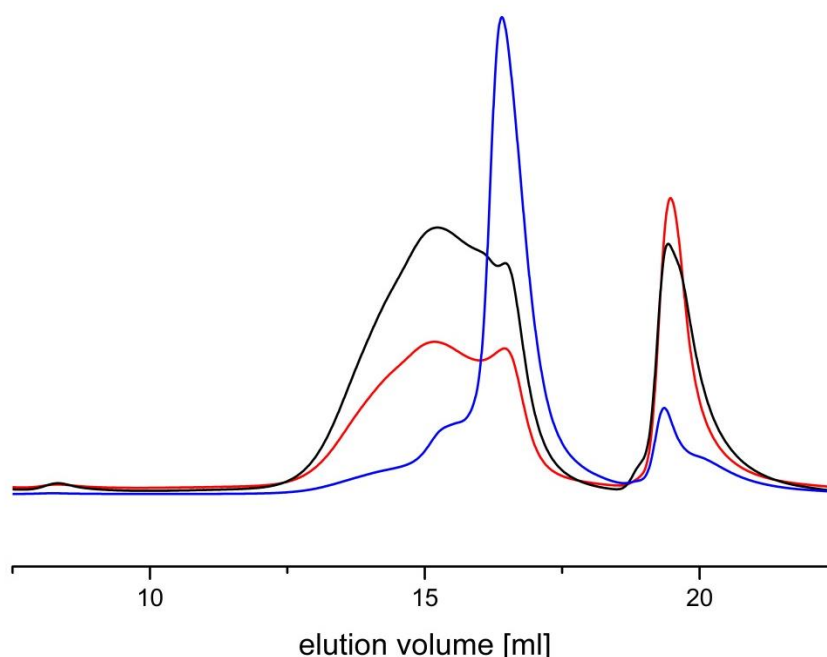Figure 27. GPC elution curve of a precipitation fractionation with selective solvents of polymer **42**. In red the stock sample, in black the gel phase after two precipitations, in blue the sol phase of the first precipitation. Intensity differences are due to varying concentrations of polymer **42** in the GPC samples.

The top-down precipitation fractionation and fractionation by GPC gave samples of high molecular weight with small (top down precipitation) to negligible (GPC) low molecular weight species. However, in these methods, the obtained high quality fractions account for a low percentage of overall sample mass (10% and 30 % respectively). This is nicely illustrated by the GPC elution curve of the medium molecular weight fraction in the GPC-method, which still contains a large amount of high molecular weight material. This is the main advantage of the selective solvent which allowed removal of low molecular weight material with minimal loss of high molecular weight polymer.

6.1.3.   Variation of solvents

A common feature for almost all SPC reactions carried out with the Si-system was the observation of a precipitate at late reaction stages. This led to the assumption that THF might not be the ideal solvent for this system, as molecular weight was not limited by reaction conversion but rather by solubility of product in the reaction solvent. The results of the solvent variation studies are summarized in Table 3. The extremely low molecular weight material of **42** obtained after SPC in

toluene/water is believed to be a matter of phase-transfer kinetics. This is supported by the observation of increased reaction speed when adding increasing amounts of THF to the solvent mixture (see Figure 28). THF can be viewed as a phase transfer catalyst. Contrary to a report by Bo *et al*,[107] polymer **42** obtained from SPC in THF/toluene/water mixtures was of lower molecular weight than the one obtained from SPC in THF/water.

Table 3. Results of the solvent variation study, showing the highest molecular weights of polymer **42** could be obtained using THF as solvent. All reactions were carried out with water as co-solvent.

Entry	Org. Solvent	M_p [kDa]	M_w [kDa]
1	Dioxane	16.1	20.4
2	Toluene	0.45	0.50
3	THF	26.0	33.0
4	Toluene/THF (1/1)	12.9	13.3
5	Toluene/THF (1/2)	8.8	22.0
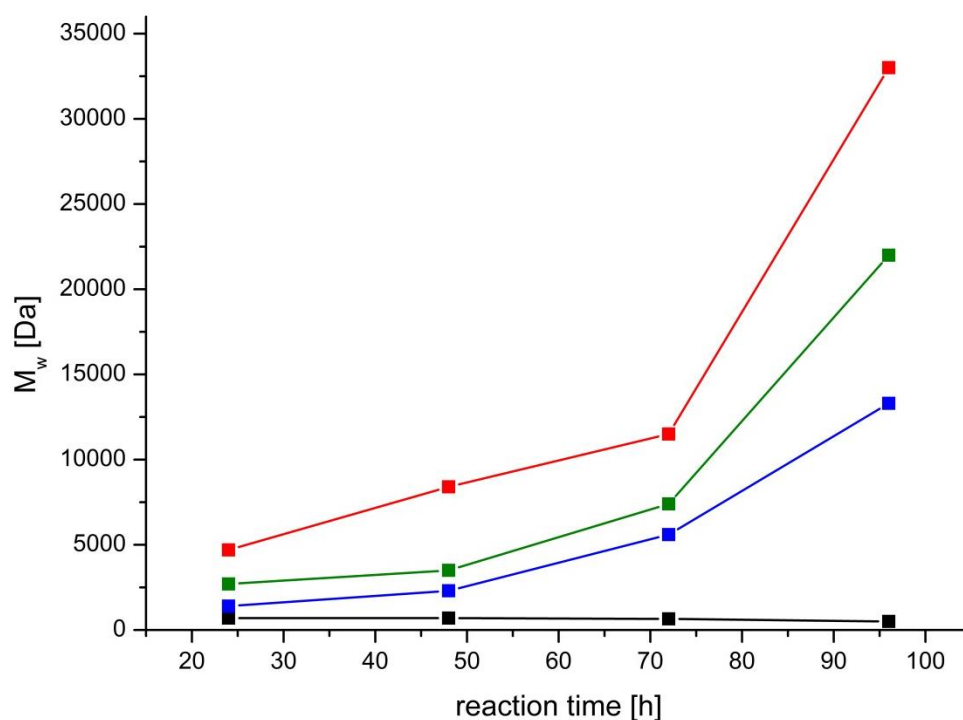
Figure 28. Molecular weight vs. reaction time for four different SPC conditions (Table 3, entry 2-5). Entry 2: black, entry 3: red, entry 4: blue, entry 5: green.

6.2. Synthesis of polymer 77

The synthesis of **77** was carried out as a side-project with the main intention to get more information about the end-groups situation of polymer obtained after SPC. As for polymer **42** a clear determination of the end-groups was not possible (see chapter 6.1.1). The side-group was altered in a way to facilitate ionization and be sufficiently stable so fragmentation is avoided. In a report by Hohl *et al.* a THP-protected benzylic alcohol was shown to have excellent ionization properties.[27] Subjecting monomers **61** and **32** to the SPC conditions used for the Si-system lead to polymer **77**. Premature precipitation of a white powder was a sign for the low solubility of **77** in the reaction solvent. This was underlined by reaction monitoring by GPC which showed a halt in polymer growth after 16 hours (Figure 29).
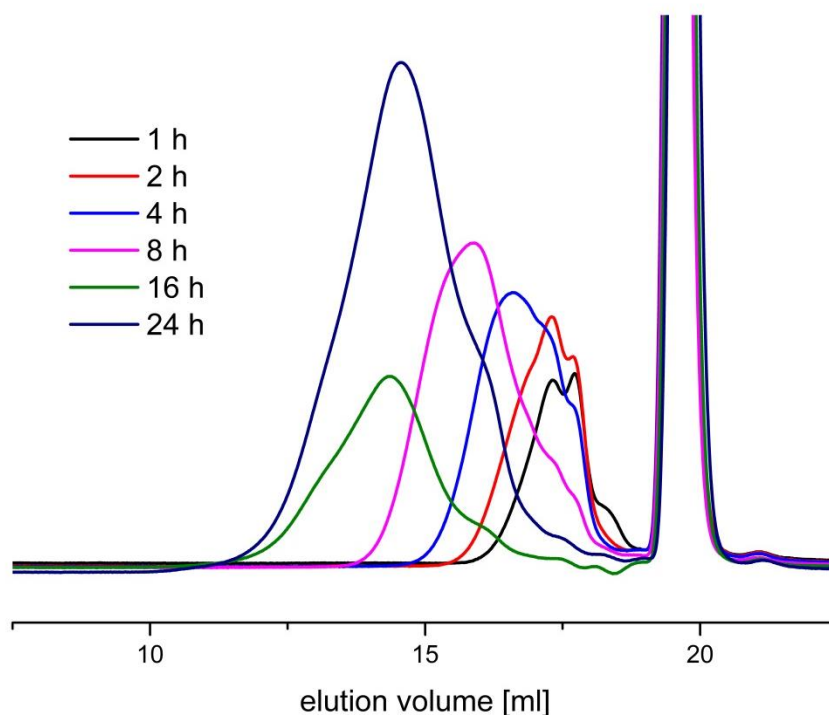
Figure 29. Superimposed GPC elution curves of polymer **77**. Samples of the same volume were taken out of the reaction solution, diluted and freeze dried, before subjecting them to GPC analysis.

6.2.1. End group analysis by MALDI-TOF MS

The MALDI-TOF mass spectrum of **77** showed a major series and several minor ones (Figure 30 a). The former was observed as sodium adduct, whilst the latter were observed as sodium adduct in some cases and as neat molecule ions in others. The fact that the cyclic series is so dominant does not necessarily have to

indicate that these species are predominant in the sample composition but rather that these oligomers "fly" better during MALDI-TOF analysis. As a consequence it is possible that the detection of less dominant species is suppressed. A more detailed analysis of the minor series (Figure 30 b) gives useful information about side-reactions present. Most noteworthy is the absence of free boronic acid end-groups in any of the series. Only one series with a boronic ester end-group was observed. This finding indicates that deboronation reactions are one of the major obstacles to high molecular weight. Ligand scrambling accounts for a multitude of observed series, both expected termini are observed and no clear distinction with respect to which intermediate is more prone to ligand scrambling is possible. Although the early precipitation of **77** may adulterate the observations given by MALDI-TOF mass analysis. To get a more conclusive idea of the end-group situation and detrimental side-reactions early precipitation should be avoided.
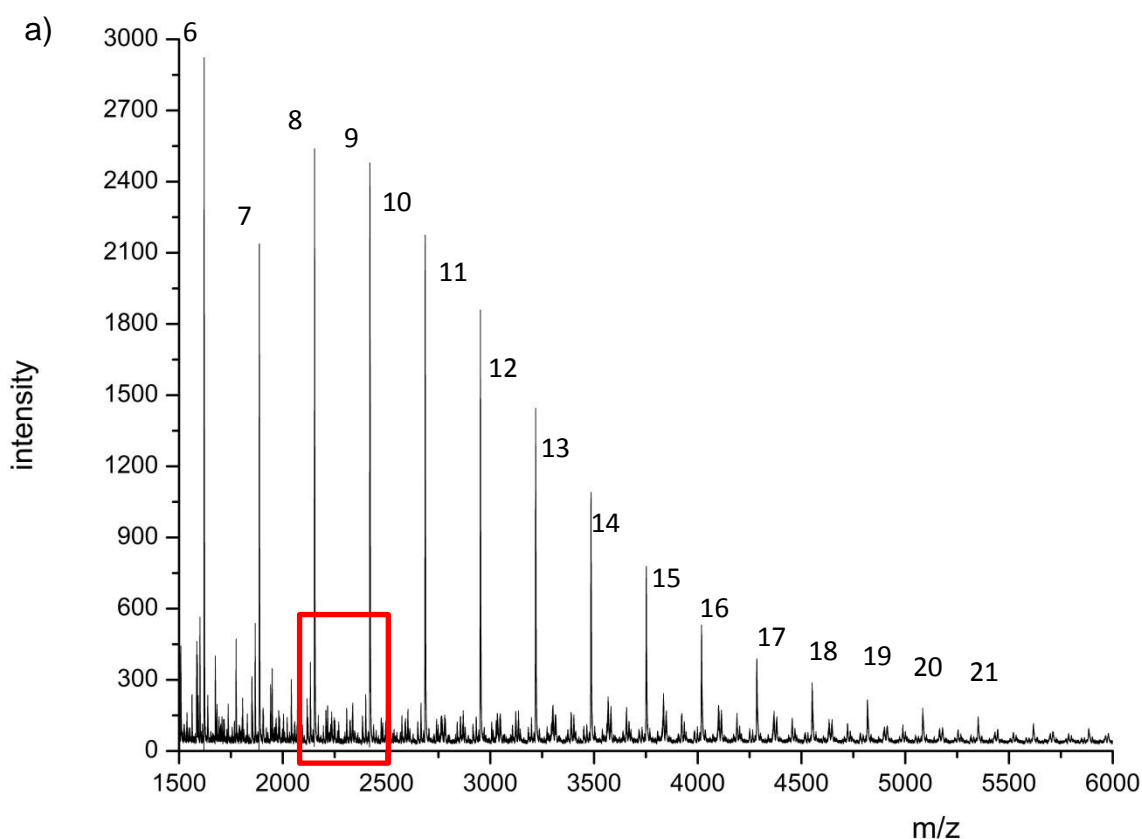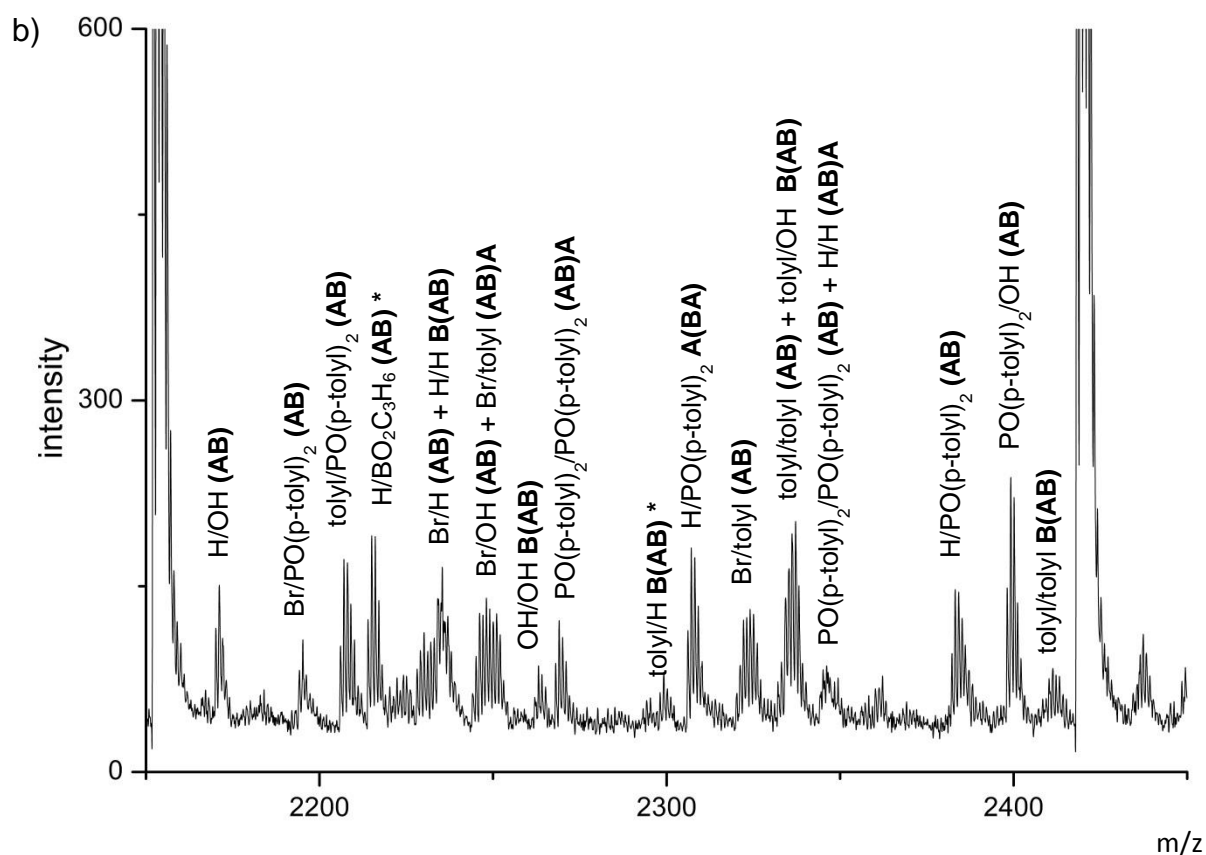
Figure 30. a) MALDI-TOF mass spectrum of **77**. The main series corresponds to [cycle + Na]$^+$ the number next to the signals corresponds to the number of r.u. comprised in the cycle. b) Section of a MALDI-TOF spectrum of **77**, giving an overview over the observed end-groups. All unmarked series are present as sodium adducts [M+Na]$^+$ while the one marked with an asterisk is the [M]$^+$ species.

6.3. Synthesis of precursor polymer 78

Monomer **56** was designed in a way to incorporate the acetal structure responsible for the improved ionization properties, while containing flexible chains to mitigate solubility. It was subjected to the same SPC conditions as the previously mentioned monomers **53** and **61**. The obtained molecular weights are summarized in Table 4.

Table 4. Molecular weights obtained for selected polymerizations of **56** and **32/52** leading to polymer **78**.

Entry	Monomers	Mn [kDa]	Mw [kDa]	PDI	Mass obtained [g]	Yield [%]
1	**56** & **32**	8.1	39.5	4.9	1.03	86.5
2	**56** & **52**	10.2	36.0	3.5	4.12	98.1
3	**56** & **52**	9.0	48.9	5.4	3.60	90.2

A goal of the synthesis of **78** was to investigate the effect of using a pinacol protected diboronic acid instead of a propan-1,3-diol protected one. Unfortunately, only qualitative conclusion can be drawn. To avoid suppression of the signals of interest by signals originating from cyclic oligomers, the investigated sample was fractionated prior to analysis. The drastic reduction in cyclic species compared to unfractionated samples is nicely visible in the GPC elution curve shown in Figure 31. End group analysis by MALDI-TOF mass spectrometry revealed an increased amount of series carrying boronic acid or boronic ester end-groups compared to the case of polymer **77**. In addition, the number of proton endgroups at the bromine terminus, resulting from protodebromination by β-elimination are greatly diminished (see Figure 32). This is a strong sign that using a pinacol protected boronic acid largely enables suppression of the proto-debromination side-reaction (see 4.2.3.4). The major signal, however, could not be univocally assigned, since the possible end-group patterns which are composed of two commonly observed end-groups cannot be distinguished by MALDI-TOF spectrometry.
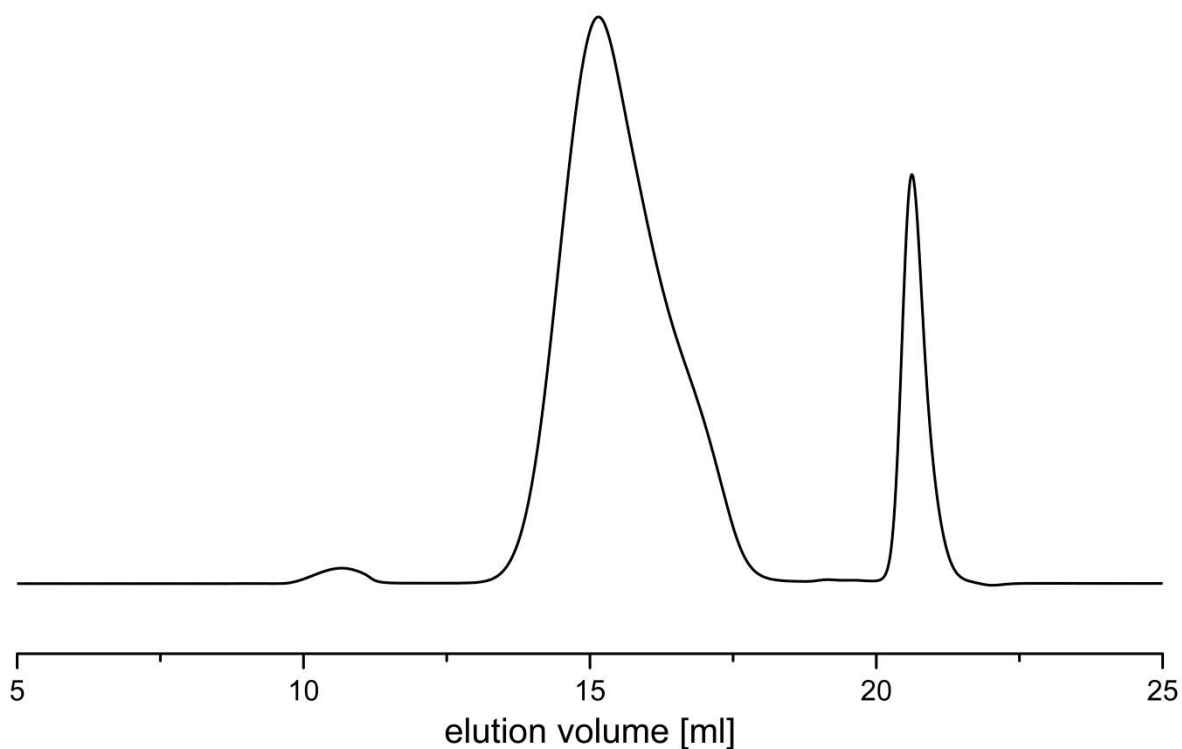

Figure 31. GPC elution curve of a fractionated sample of polymer **78**. The same sample was analyzed by MALDI-TOF spectrometry (see Figure 32).
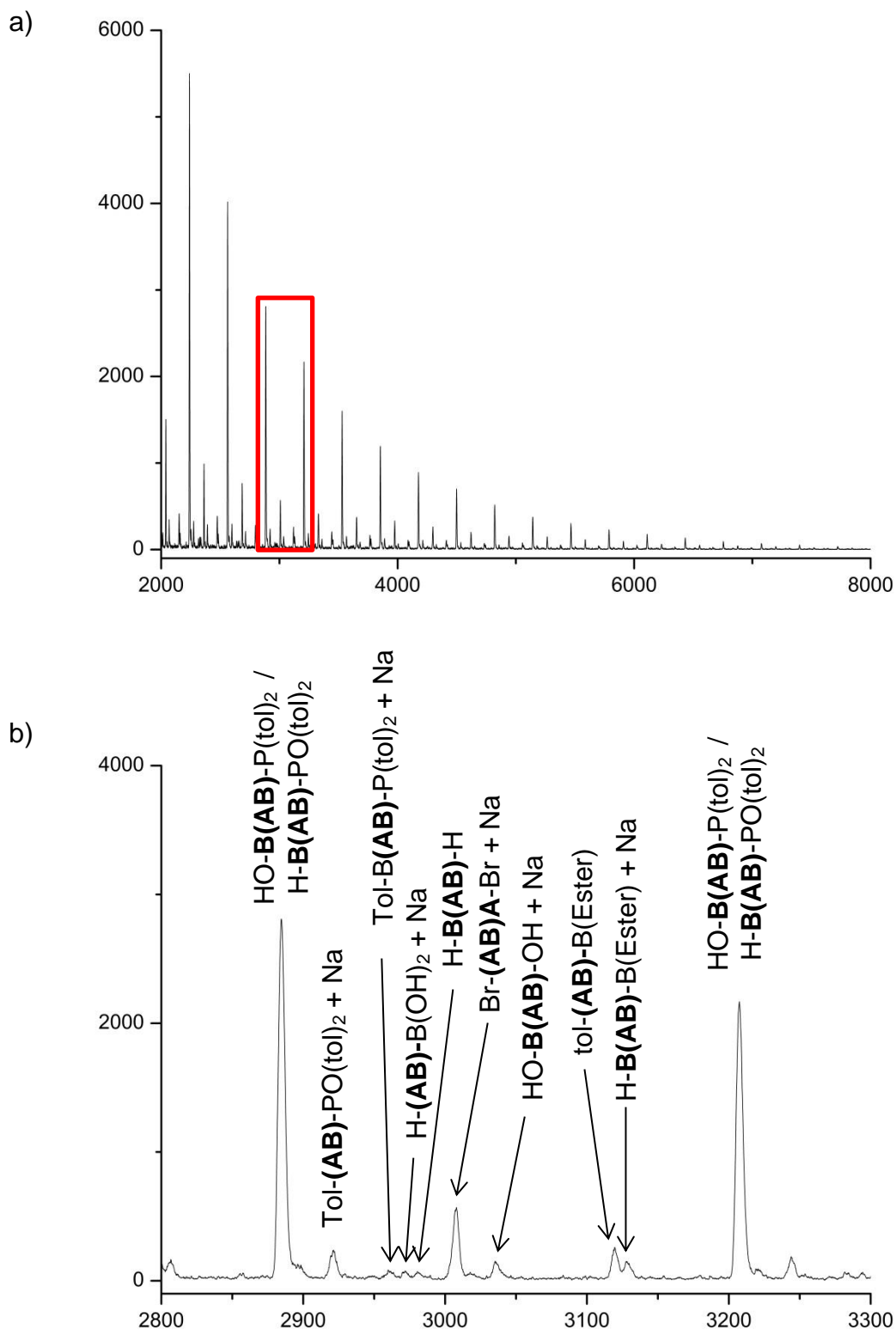
Figure 32. a) Full MALDI-TOF mass spectrum of **78**. b) Enlarged section of a) some series of the type [M+Na]⁺ and [M]⁺ could be observed, contrary to previous cases for similar polymers no cyclic species were observed.

6.4.   **Microwave assisted polymerization**

As the molecular weights obtained by conventional reaction techniques were believed to be too low for processing into robust self-standing structures. One of the main obstacles identified was the relatively poor solubility of **42** in the reaction solvent THF. Previous attempts to obtain polymer **42** with increased molecular weight by changing solvents or using solvent mixtures failed (see 6.1.3). Microwave reactors have been previously used for SPC.[25, 87] Microwave reactors designed for the use in chemistry labs allow the use of increased pressure. In consequence, increased reaction temperatures are possible which should lead to an increased solubility of X in the reaction mixture. The following aspects were investigated: effect of temperature, reduction in reaction time, age of catalyst precursor. All experiments were carried out from the same monomer stock solution to avoid discrepancies associated with monomers stoichiometry. The resulting molecular weights are summarized in Table 5.

Table 5. Molecular weight of polymer **42** obtained by microwave assisted SPC of **53** and **52**. Entry 1 serves as reference and was obtained by conventional heating methods. Entries indicated by asterisk suffered uncontrolled fractionation during the workup process.

| Entry	Reaction time [h]	Reaction temperature [h]	Catalyst batch	Catalys age	M_n [kDa]	M_w [kDa]
1	96	72	-	Fresh	3.9	26.6
2*	90	72	-	Fresh	8.0	25.3
3*	90	100	-	Fresh	10.8	42.7
4*	16	120	-	Fresh	20.0	77.0
5	90	120	-	Fresh	4.9	29.6
6	48	120	-	Fresh	4.8	27.6
7	24	120	-	Fresh	4.2	27.8
8	12	120	-	Fresh	4.3	32.6
9	48	120	A	Fresh	4.0	30.0
10	48	120	A	2 days	4.3	35.7
11	48	120	A	7 days	5.5	27.8
12	48	120	B	Fresh	4.2	11.3
13	48	120	B	2 days	4.3	24.6
14	48	120	B	7 days	4.5	22.4

As the results indicate the molecular weight of obtained polymer was largely unaffected by changes in reaction time and catalyst age. One of the main drawbacks of microwave assisted SPC is the lack of online reaction control. While simple observation by eye-sight might seem a rudimentary technique it gives valuable information about state of the catalyst. Early decomposition of the catalyst precursor would give valuable information with regard to possible mistakes that happened during the reaction setup. It is therefore possible that certain discrepancies in Table 5 are due to random errors like leaks in the degasing vessel or oxygen contamination occurring during transfer to the microwave oven. All reaction mixtures contained a solid black mass once the reaction was finished. At first this solid was removed by filtration (see entry 2-4 in Table 5). This, while being interesting to obtain high molecular weights without the additional effort of a fractionation, is an uncontrolled process and leads to falsified results.

7.   Side chain removal

The removal of side chains as introduced in 4.3.1.2 was commonly referred to as 'shaving' in the present work. Shaving attempts were performed for polymers **42** and **78** respectively and are treated separately because of their differing nature.

7.1.   Shaving of polymer 42

Shaving of **42** is performed by the addition of a strong acid to a polymer solution. *Ipso*-substitution of aryl-silanes by electrophile is a well-known textbook reaction.[108] In the present study TfOH was employed as proton source.
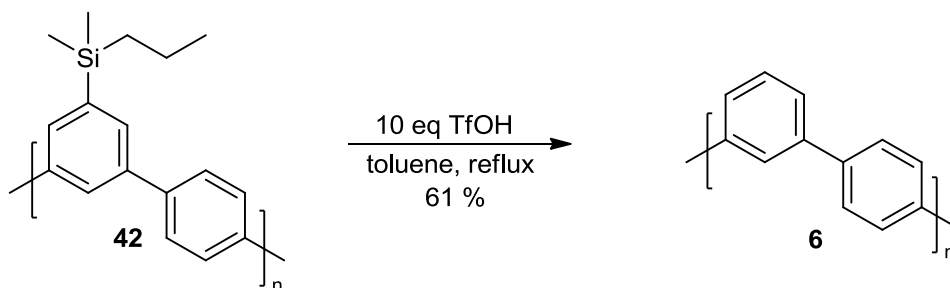
Scheme 14. Shaving of polymer **42** dissolved in toluene by addition of TfOH.

7.1.1. Shaving in solution

At first the shaving reaction was performed in a refluxing toluene solution. Upon addition of the acid a white powder precipitated within a few seconds, to ensure reaction completion stirring and heating was continued for 24 hours. Quenching of the reaction was performed by addition of triethylamine. The whole mixture was subjected to soxhlet extraction with isopropanol, hexane and diethylether. The relatively low yield (61 %) can be attributed to powder residues which are sticking to the glass wall or extraction thimble which cannot be removed without compromising the purity of the sample. Analysis methods are limited to solid state methods. These include solid state NMR-spectroscopy (^{1}H, ^{13}C, ^{29}Si, ^{19}F) (Figure 33 - Figure 36), ATR-IR-spectroscopy (Figure 37), MALDI-TOF mass spectrometry (Figure 38) and elemental analysis (Table 6).

Figure 33. ^{1}H-MAS NMR spectrum of polymer **42** (blue, top) and polymer **6** (black, bottom) measured at 21 kHz spinning frequency.

Figure 34. ^{13}C-CPMAS NMR spectrum of polymer **42** (blue, top) and polymer **6** (black, bottom) measured at 8 kHz spinning frequency. Main signals are marked with arrows, remaining signals are spinning side-bands.
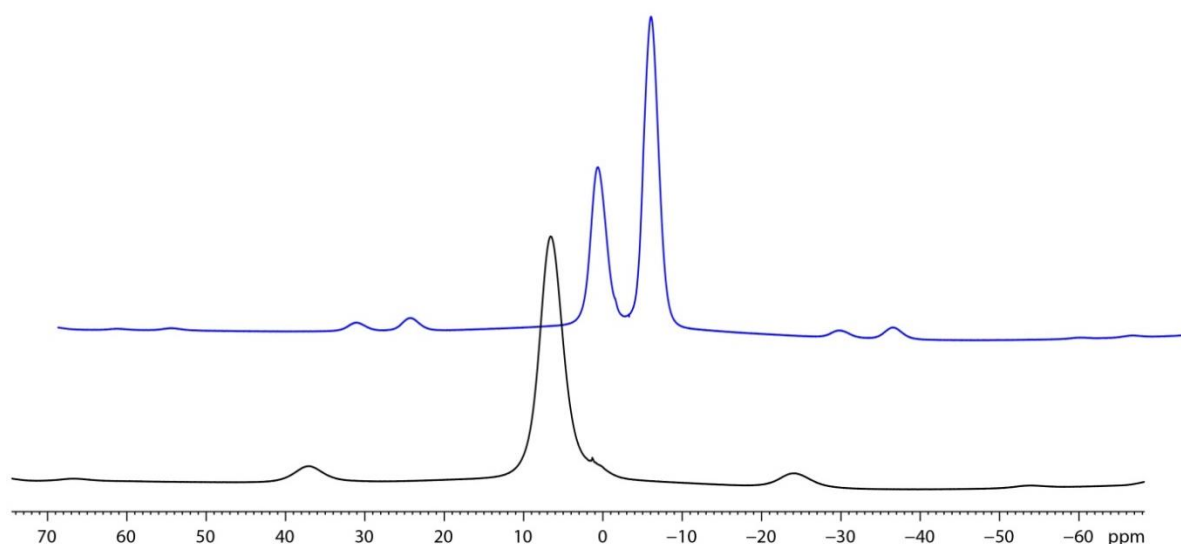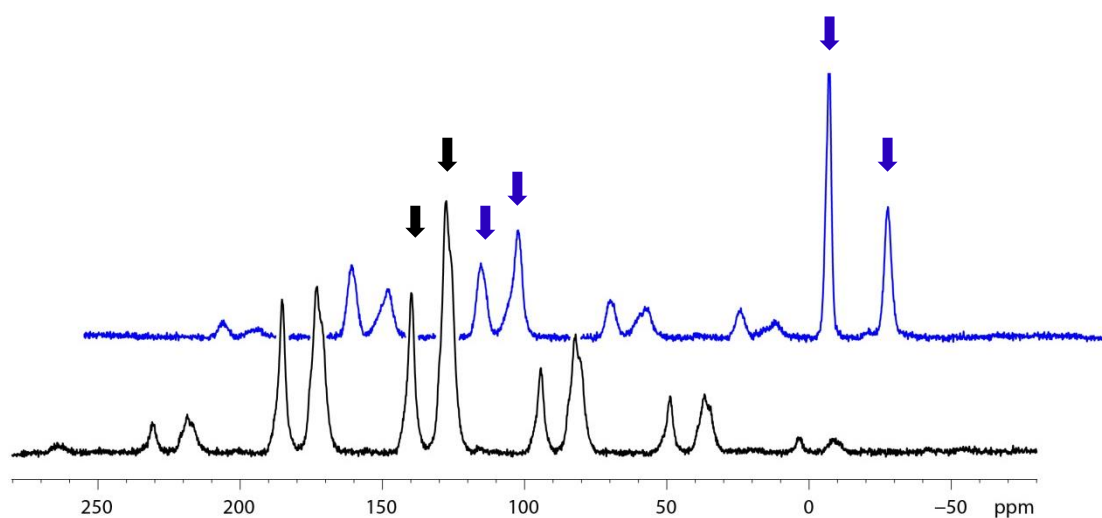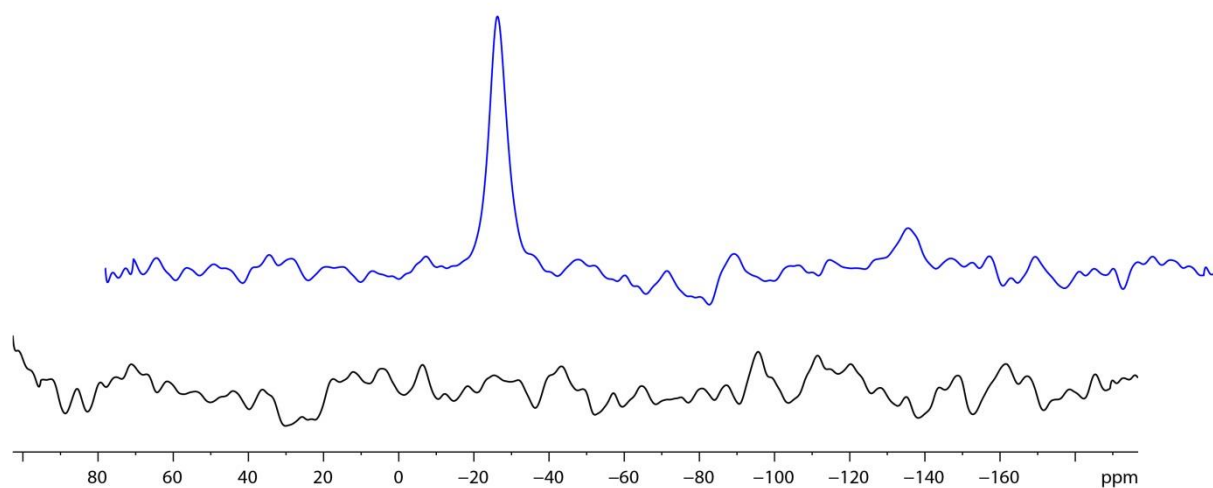

Figure 35. ^{29}Si-MAS NMR spectrum of polymer **42** (blue, top) and polymer **6** (black, bottom) measured at 5 kHz spinning frequency.
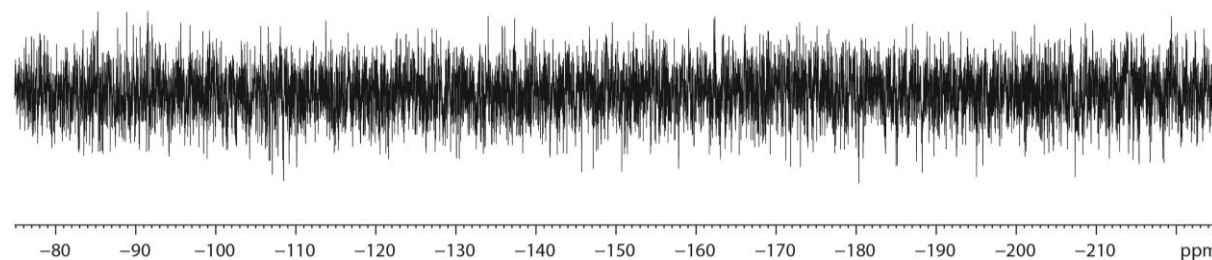
Figure 36. ^{19}F-MAS NMR spectrum of polymer **6**, spinning frequency was 21 kHz.

As the spectra in Figure 33, Figure 34 and Figure 35 show signals related to the side-chain (Silicon and alkyl signals) largely disappear, only in the ^{1}H-NMR spectrum a small residual signal of alkyl protons is visible. A fluorine NMR (Figure 36) was recorded to ensure no reagent was bound to the polymer during the shaving process. Moreover, ATR-IR spectra of polymer **42** and **6** were measured (Figure 37). When comparing the blue (**42**) to the black (**6**) curve a few major features are observable. Firstly the aliphatic C-H stretching vibrations below 3000 cm^{-1} are not observable anymore in polymer **6** contrary to the precursor polymer **42**. In addition, the characteristics Si-CH$_3$ symmetric deformation vibration at 1247 cm^{-1} disappears in addition a strong band at 819 cm^{-1} is not observable after the shaving a band which could be assigned to a Si-CH$_3$ vibrational mode.[109]
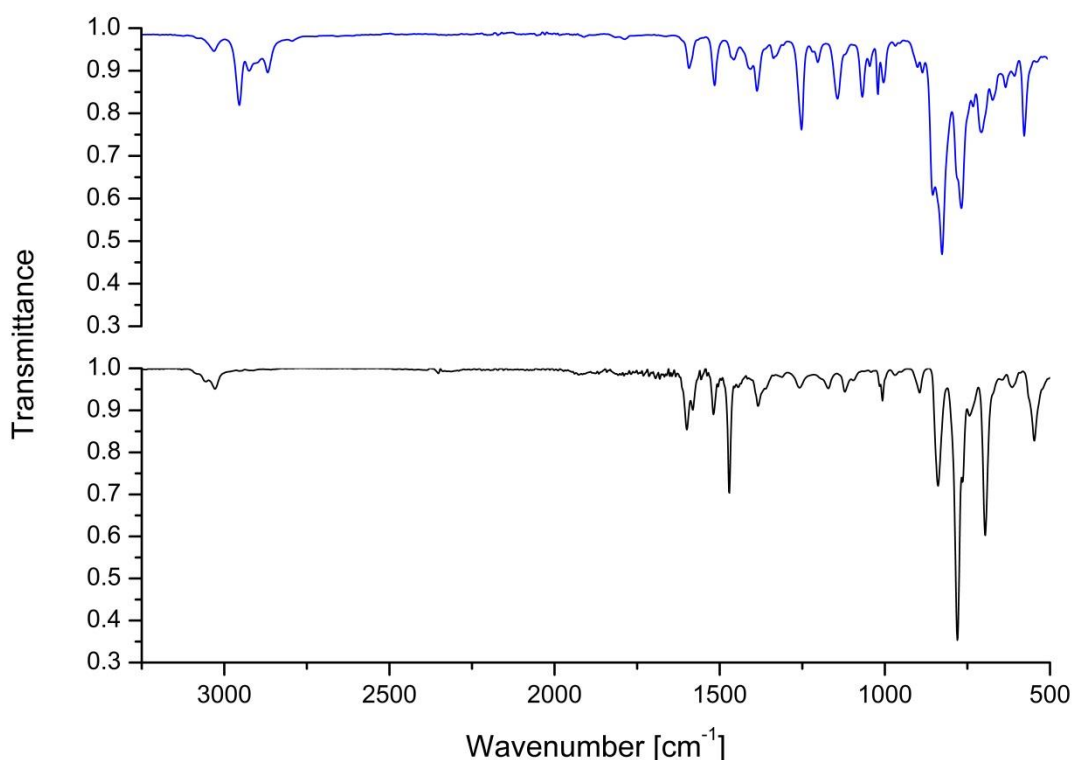
Figure 37. IR-Spectra of polymer **6** (black) and polymer **42** (blue).

MALDI-TOF mass spectrometry analysis for polymer **6** was more conclusive than for its precursor (see 6.1.1). Contrary to the large amount of mass series observed in MALDI-TOF analysis of the precursor only one series is clearly visible in the case of polymer **6**. When assuming the Dibromide monomer is referred to as monomer A and the diboronic ester monomer as monomer B, a key feature of the MALDI-TOF spectrum shown in Figure 38 can be explained as follows. As indicated

by observations from literature and made in the present work (6.2) AA/BB-type SPCs follow a strict step-growth mechanism.[50] This would lead to an expected spectrum containing $(AB)_n$, $(AB)_nA$ and $B(AB)_n$ type structures of whatever end-groups observed. However, the mass spectrum of polymer **6** only shows one series of masses all with AB mass intervals (Δm = 152.06). This is a strong evidence for the formation of cyclic product. The absolute masses observed correspond to the masses expected for $[(AB)_n]^+$ (n = 7-16).
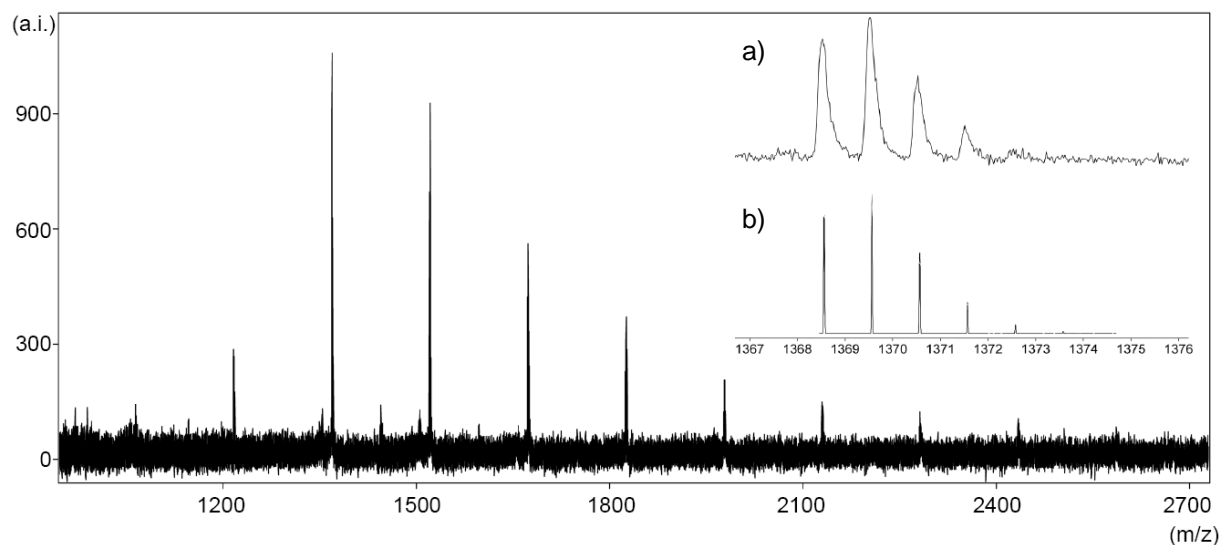
Figure 38. MALDI-TOF mass spectrum of polymer **6**, a) magnification of a signal showing its isotope pattern. b) simulated isotope pattern for the expected signal.

Furthermore elemental analysis showed that indeed the material in question has the chemical composition of an all aromatic compound.

Table 6. Elemental analysis for acid treated polymer **6**, the values for the expected content are deduced from target polymer **6**.

Element	Found content [%]	Expected content [%]
C	93.58	94.70
H	5.40	5.30

7.1.2. Shaving in gel

The desire to apply the thus discovered concept to a bulk structure like a polymer film or a fiber asked for slight adjustments. If no solvent is employed most likely only the periphery of the bulk structure would be affected by the shaving process, leading to core-shell differentiated bulk structures, which was undesirable. Thus a solvent needs to be used to swell the macroscopic structure into a gel like

object in order to make its interior accessible to the employed reagent. For this, however, toluene would not be feasible, because of its dissolution properties of the precursor polymer. Therefore different solvents were employed to investigate the scope of the present concept. Cyclohexanone, 1,4-dioxane and *p*-xylene were chosen for further investigations mainly because of their ability to possess sufficient interaction with the precursor polymer in order to form a swollen object while not possessing the ability to dissolve higher molecular weight material of polymer **42**. In a first step a gel particle was subjected to shaving conditions. The results thereof are illustrated in Figure 39 -Figure 41. Shaving in cyclohexanone was unsuccessful, even at high temperature (Figure 39). The reaction in 1,4-dioxane is slow (10 days reaction time) and requires slightly elevated temperature (50 °C) to achieve a satisfactory degree of conversion. An interesting aspect can be taken from Figure 40. Even at prolonged reaction times, a reduction of the aliphatic signals can be observed. This is a clear sign that using the present methodology the core-shell problem can be properly addressed. The most rapid conversion was found using 1,4-xylene as swelling agent (Figure 41).
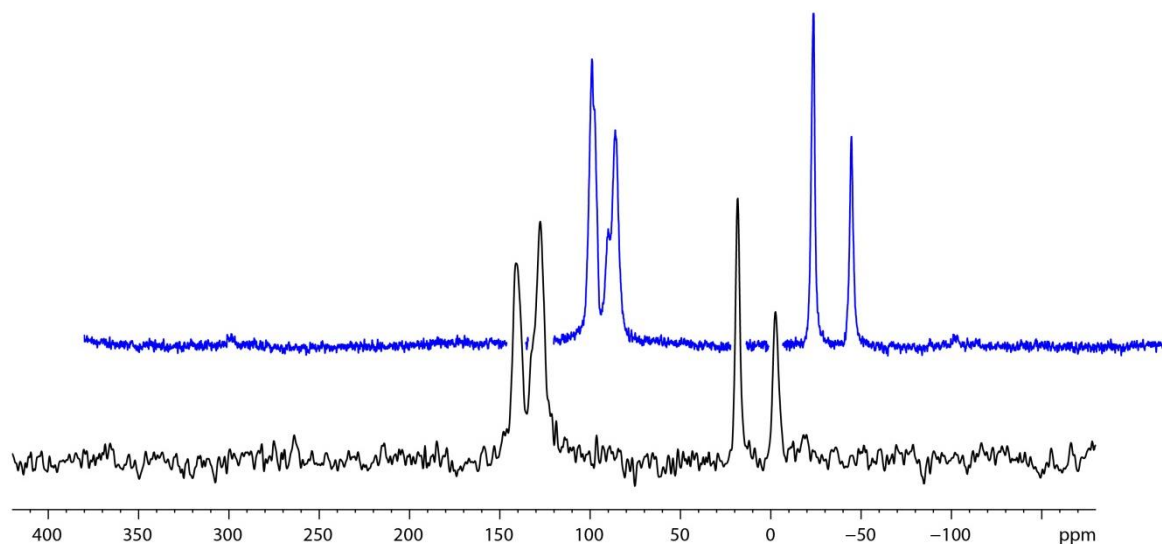
Figure 39. ^{13}C-CP MAS NMR spectra of polymer **42** (top, blue) and the product of TfOH treatment in cyclohexanone (black, bottom) at 110 °C for 24 h.

Figure 40. ^{13}C-CP MAS NMR spectra illustrating the course of the shaving reaction at room temperature (if not noted otherwise) of polymer **42** (top, blue) to polymer **6** in 1,4-dioxane. Reaction time: 21 h (green), 3 days (magenta), 10 days (red), 10 days and 50°C (black, bottom.
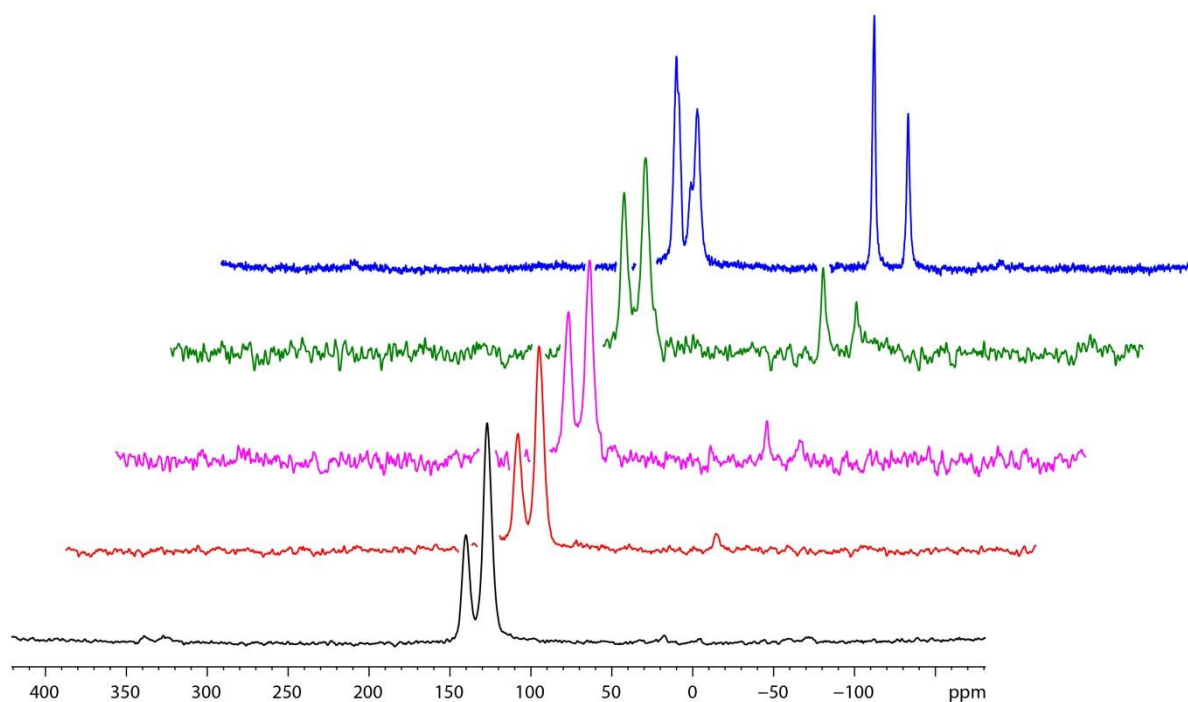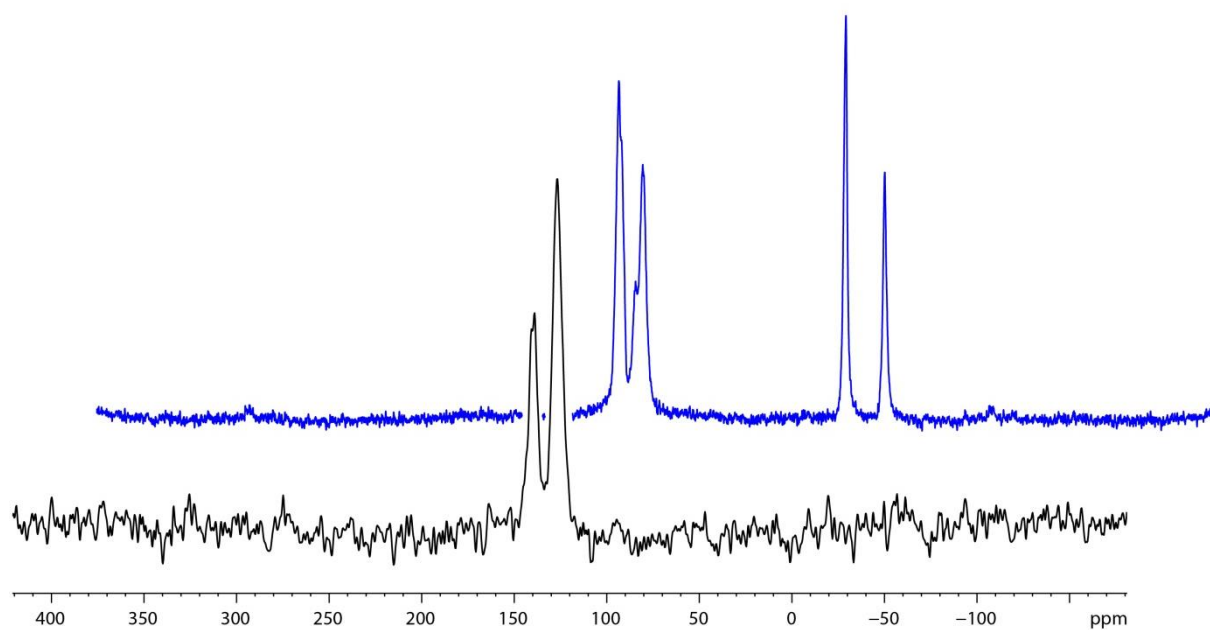

Figure 41. ^{13}C-CP MAS NMR spectra of polymer **42** (top, blue) and **6** after TfOH treatment in 1,4-xylene (black, bottom).

7.1.3. Shaving of macroscopic objects

Since during the shaving process a substantial amount of mass is lost, maintaining the macroscopic structure of a bulk object is important. If the shaving process would lead to a large number of cracks in the film, the protocol would have to be adjusted. A pressed film (~ 230 µm thickness) was first swollen and thereafter subjected to acid treatment. If the film was swollen in 1,4-dioxane, only small pieces could be recovered. Contrary to this, swelling in 1,4-xylene allowed recovery of the acid treated film in one piece. ^{13}C-CP MAS NMR-spectroscopy showed that shaving is proceeding with a large degree of conversion within three days (Figure 42).
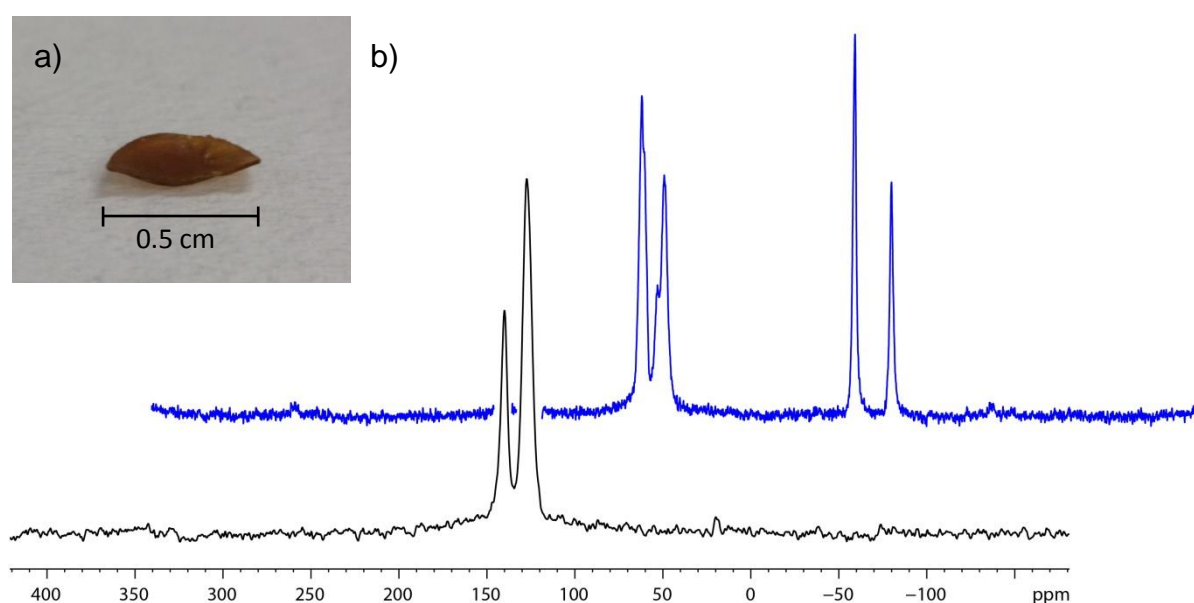
Figure 42. a) Photograph of the shaved film, broken in half (object size:~0.5 cm). b) ^{13}C-CP MAS NMR spectra of a compressed film of polymer **42** (top, blue) and the product of TfOH treatment after swelling the film in 1,4-xylene (black, bottom).

The film is recovered in one piece but there are two noteworthy points. Firstly the color of the film turns brown after acid treatment; this is an issue that might demand alterations to the system. Color changes might be a result of degradation products not being able to escape from the bulk structure. The film is expected to collapse from its gel state during treatment, entrapping degradation products. An alternative explanation could be that the strong acid undergoes undesired reactions with the endgroups. Secondly, the film is not recovered flat as before treatment, but is deformed during treatment (bending). This is a possible obstacle when thinking about applications as a change in morphology from the processing shape is not desirable.

However, the latter issue might arise from inhomogeneous acid deposition, an issue that could be resolved by engineering proper reaction conditions.

7.1.4. Powder X-ray diffraction analysis

The effect of shaving on the crystallinity of the film was investigated by X-ray diffraction (XRD).The powder diffraction patterns can be seen in Figure 43. A superposition of the integration of the two diffraction patterns is shown in Figure 44.
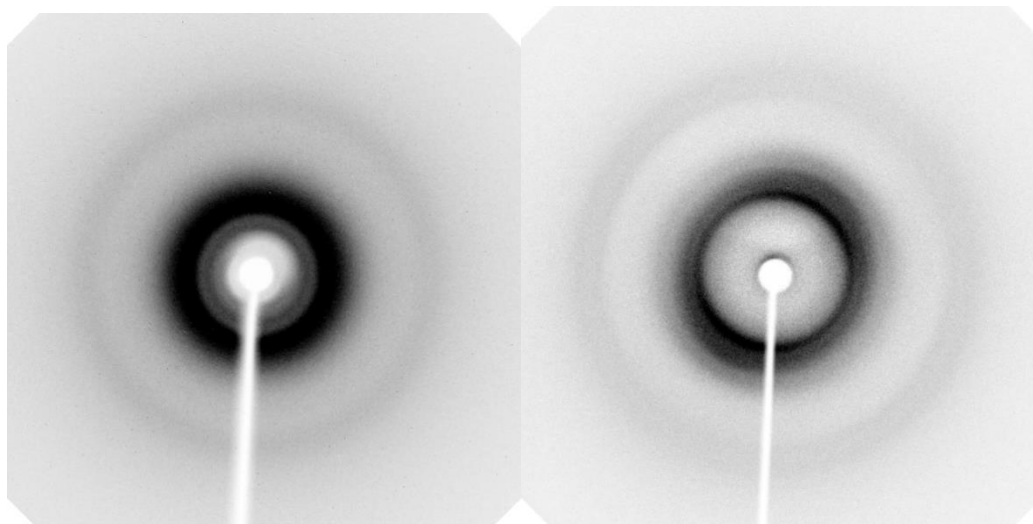
Figure 43. Powder X-ray diffraction patterns of a pressed film of **42** before shaving (left) and **6** after shaving (right). Distance between sample and detector: 130 mm, wavelength: 0.71 Å, inversed greyscale.

A clear assignment of the signals is not trivial. The most intense reflections have their maximum at 1.15 Å^{-1} (**42**) and 1.26 Å^{-1} (**6**) respectively. This corresponds to interplanar distances of 5.40 Å (**42**) and 4.96 Å (**6**). Common π-π stacking distances in related polymers are commonly 3.3-3.8 Å but in some cases can go up to 4.2 Å.[110],[111] A report on oligomeric paraphenylenes shows that direct π-π interactions between two phenylene segments are not the main feature of order in these compounds.[112] The unit cell dimensions observed for these compounds vary between 5.63-5.55 Å in their shortest dimension. This indicates that a similar type of orientation between the chains is present. In addition, what can be noted is that the main structural feature of the two compounds indicates a denser packing in the target material **6** compared with the precursor **42**. Minor reflections are summarized in Table 7.

Table 7. Summary of the observed reflections for interplanar distances for polymer **42** and **6**.

d-spacing of 42 [Å]	d-spacing of 6 [Å]
7.68	4.96 (main reflection)
5.40 (main reflection)	4.29 (shoulder)
2.28	3.41 (shoulder)
	2.20
	2.02
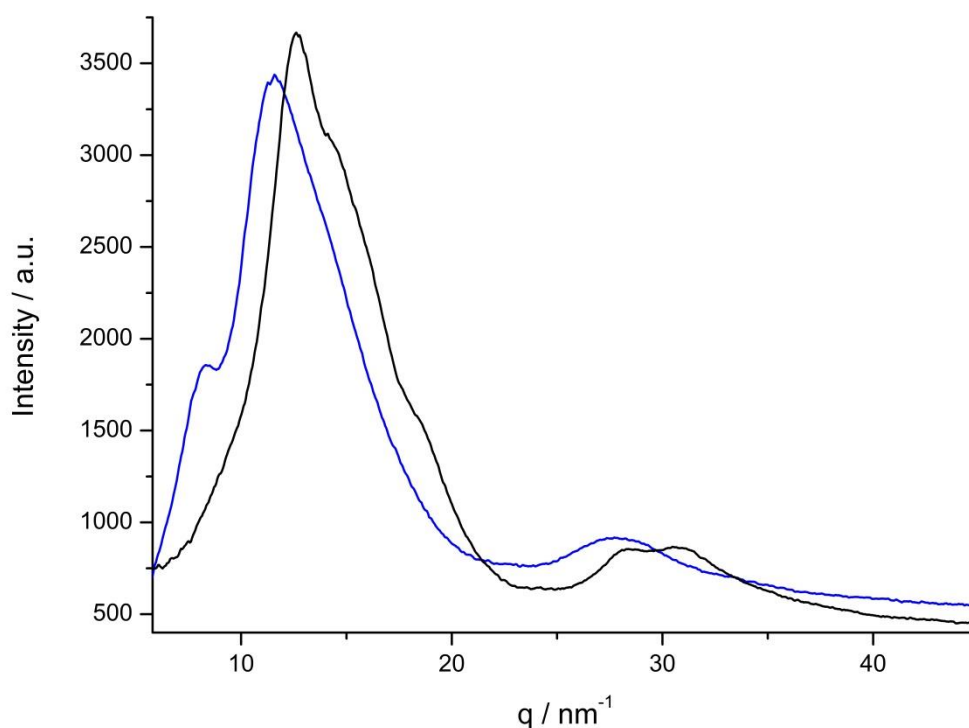
Figure 44. Superposition of the integration of the two diffraction patterns of a film based of **42** (blue) and the acid treated **6** (black). Signal intensity is given versus reciprocal distance.

7.2. Shaving of polymer 78

Whereas the work focused on polymer **42**, which was employing a chemical reaction in order to remove the undesired side-chains, a whole different approach

was taken for polymer **78**. Using thermal treatment to remove the side-chains is intriguing. If a clean process can be developed there are significant advantages for the thermal process compared to a removal by chemical reaction. The main advantage being that for a thermal process the sample is treated in a homogeneous fashion.

As a first test reaction like experiment the monomer carrying the side-chain (**56**) was analyzed by electron impact high resolution mass spectrometry (EI-HRMS, Figure 45). The two most interesting fragmentations observed are the signals at 171.14 amu and 260.85 amu respectively. The former corresponds to the mass of the complete side-chain. The latter could be associated with a fragmentation of the side-chain. A C=O group remains on the aromatic ring while the remainder of the side-chain is cleaved off.
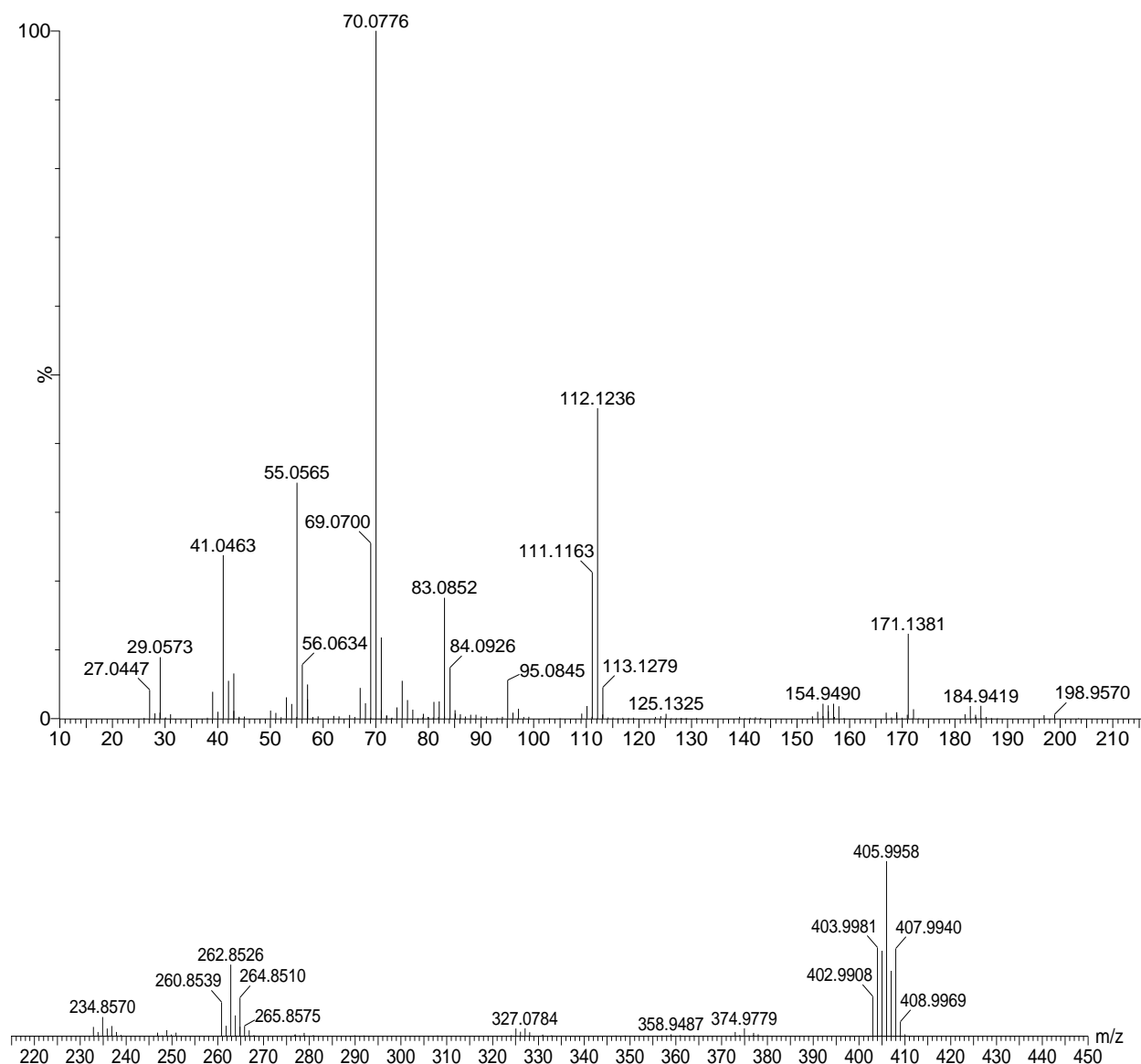
Figure 45. EI-HRMS spectrum of **56**. Top: Mass range 0-215 m/z, bottom: mass range 215-450 m/z.

7.2.1. Thermal properties of polymer 78

To gain some insights into the thermal properties of polymer **78** a temperature ramped thermo-gravimetric analysis (TGA) Figure 46 a) and differential scanning calorimetry (Figure 46 b) was carried out. Slow degradation starts to set in at 300 °C, at 395 °C maximum degradation speed is observed. Ideal degradation conditions are expected for temperatures between 300 °C and 375 °C. Higher temperatures could lead to unwanted degradation. Figure 46 c shows that for temperatures below 200 °C no major degradation takes place. The degradation process starts between 200-

250 °C, making these temperatures the lower limit where side-chain cleavage is still possible.
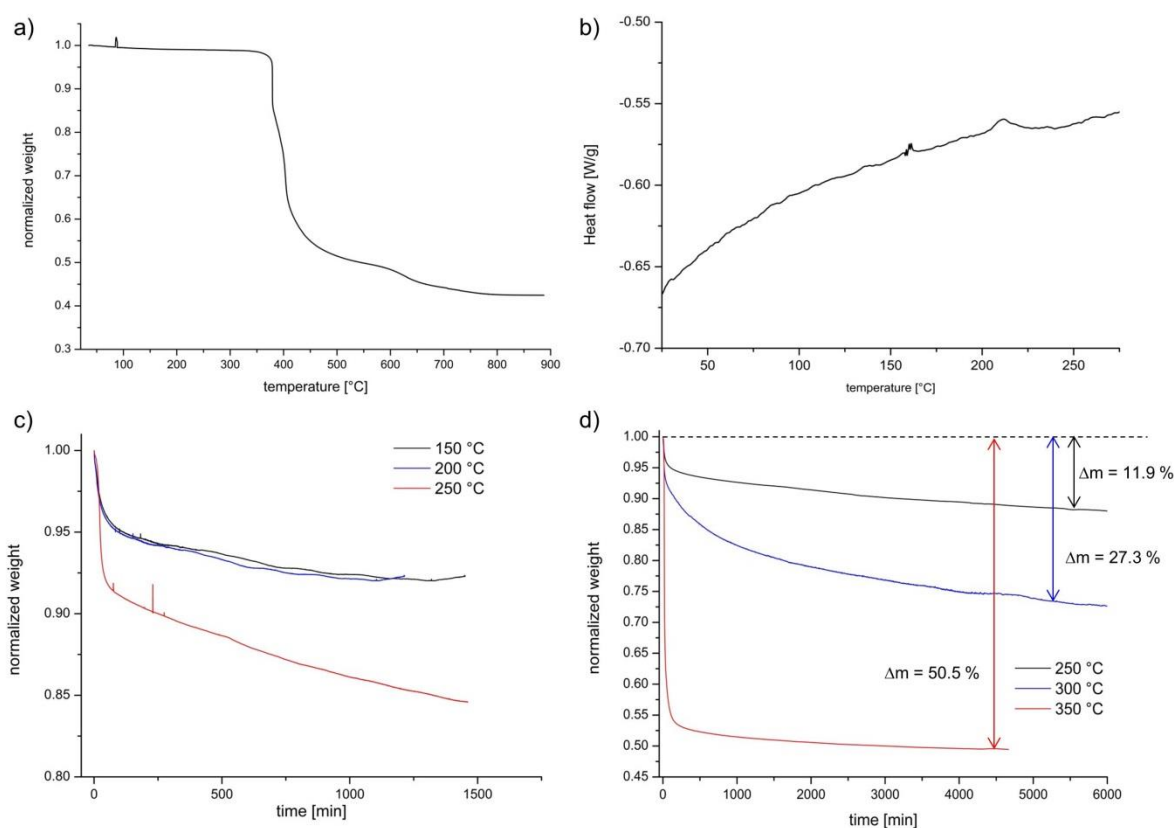
Figure 46. a) TGA trace of polymer **78** recorded with 5°C /min heating rate. b) DSC-curve of polymer **78**, showing a T$_g$ at 200-225 °C. Curve of second heating, cooling traces are omitted. c) TGA curves of polymer **78**, all curves are recorded isothermal after ramping with a rate of 20 °C/min to the given temperature. d) TGA traces of long time isothermal measurements of polymer **78** for three chosen temperatures. Black 250 °C, blue 300 °C and red 350 °C.

Using 375 °C as cleaving temperature, a weight loss of 57.8 % was observed (see Figure 47). As the side-chain accounts for 53.1 % of the mass in each r.u. this value indicates that 375 °C is too high for a long-term degradation process and the reaction would have to be stopped preemptively.
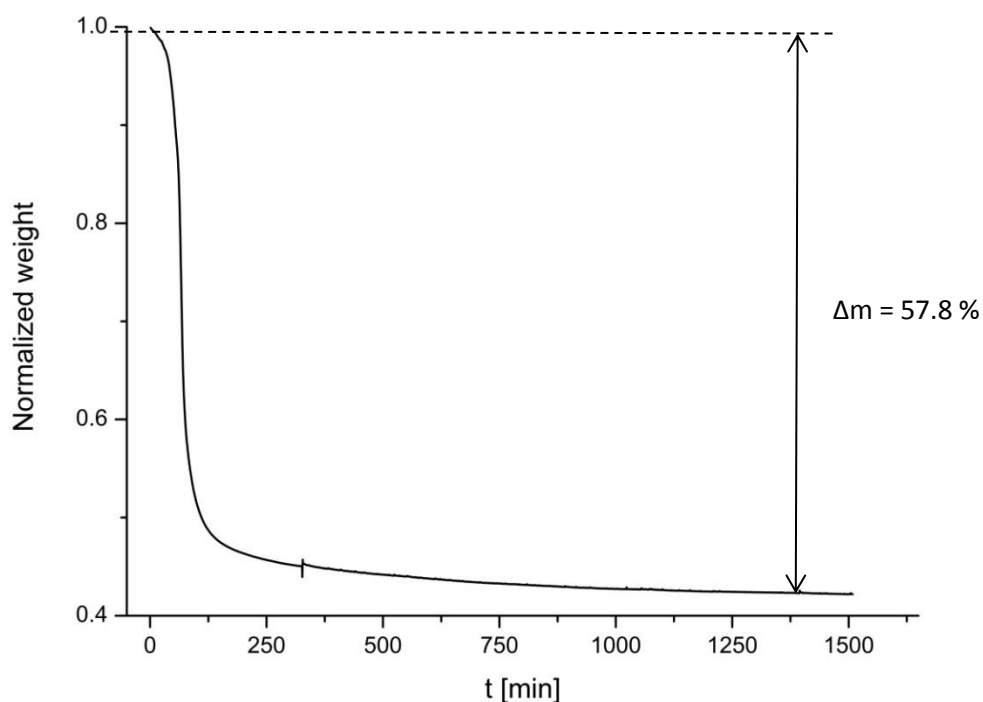
Figure 47. TGA curve of polymer **78**. Recorded isothermal after heating to 375 °C with 20 °C/min.

In a series of long term measurements a relatively clear picture of the kinetics of the partial degradation process was obtained (Figure 46 d). Degradation is sluggish at 250°C. Even excessive reaction times (> 5 days) resulted in a mass loss of less than 10 % and after 5 days degradation came close to a halt. A steady but still slow degradation was observed for a reaction temperature of 300 °C. Extrapolated a degradation time of three weeks was expected for complete degradation of mass corresponding to the side-chains. If degradation temperature was increased to 350°C relatively rapid degradation was observed at first which decelerated after approximately 45 % mass loss and leveled at 50.5 % mass lost. Therefore even for 350°C no complete degradation of the side-chains can be assumed. Consequently 375 °C reaction temperature and a pre-emptive reaction stop was chosen for the side-chain degradation reaction.

7.2.2. Structural analysis of shaving product

The shaving was carried out in a tube furnace, polymer **78** was placed in a ceramic bowl. In parallel a comparative sample was treated with the same temperature profile in the thermo-gravimetric analyzer (Figure 48).
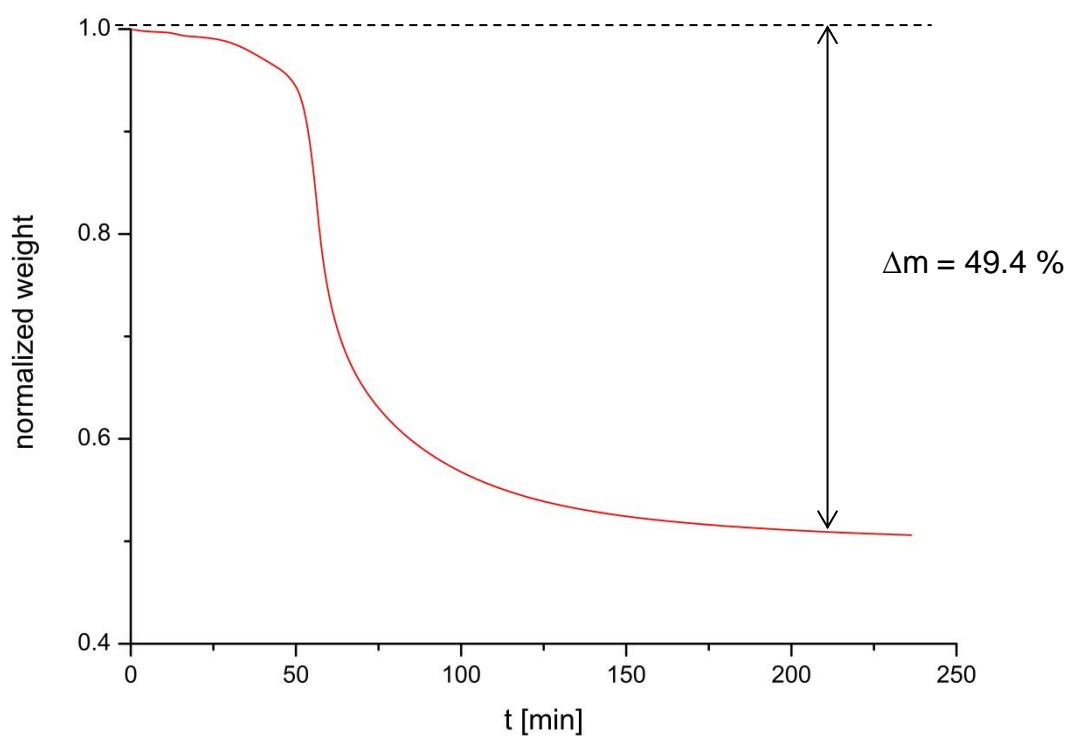
Figure 48. TGA trace of a comparative sample for the thermal decomposition reaction of **78**. Heating with 6 °C/min to 375 °C, isothermal for 180 min, cooling with 10 °C/min.
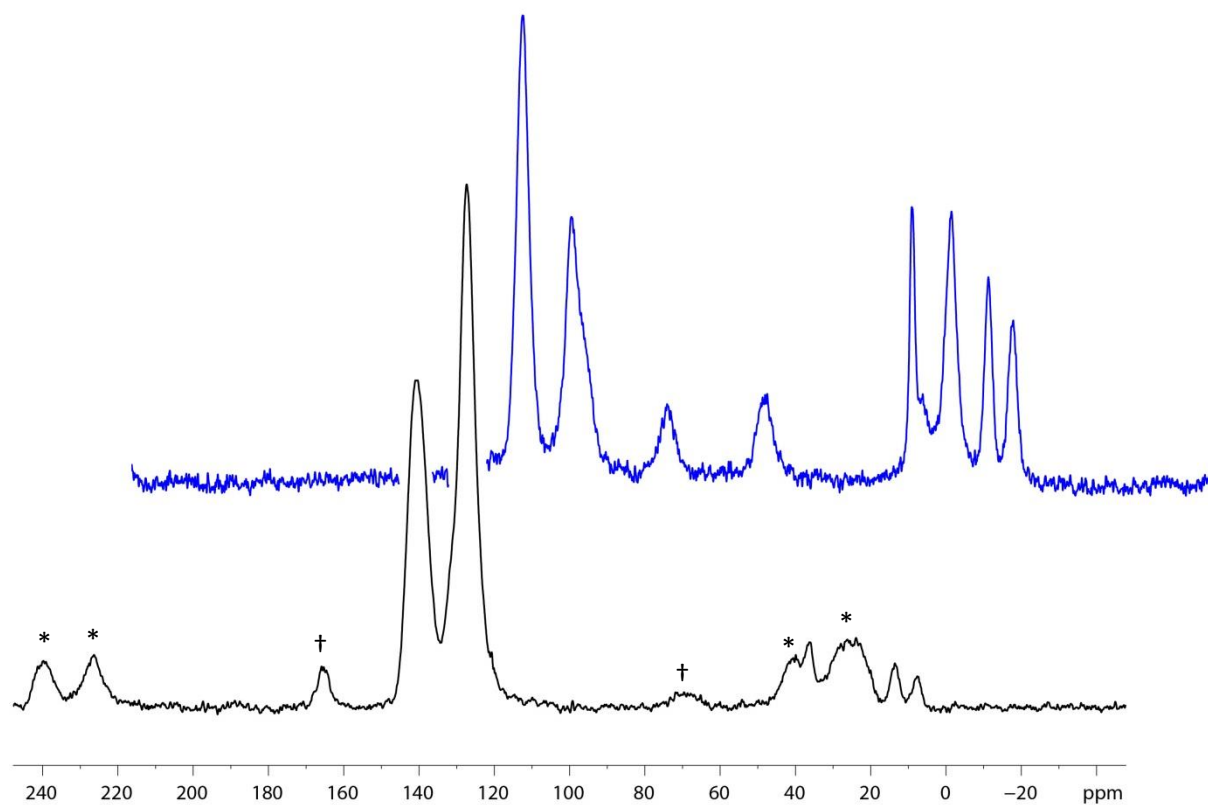
Figure 49. CP MAS ^{13}C-NMR of polymer **78** (top, blue) and the product of its controlled thermal degradation (bottom, black). The blue spectrum was measured at a spinning frequency of 20 k Hz, while the black spectrum could only be measured at 10 kHz spinning frequency, hence the spinning side-bands marked with asterisk. The signals marked with a dagger are consistent with the expected signals for an ester functionality.

The ^{13}C-CP MAS NMR shows that the shaving process is not complete (Figure 49). Some signals in the aliphatic regions are remaining. In addition the signals origination from carbon atoms located next to oxygen atoms are shifted. The signal pattern in the product can be assigned to an ester functionality. It is reasonable to expect a certain amount of rearrangement reactions to take place at these high temperatures. The observation of an ester functionality is consistent with findings in ATR-IR spectroscopy (see Figure 50). The band at 1732 cm^{-1} is consistent with the stretching vibration of an aromatic ester.
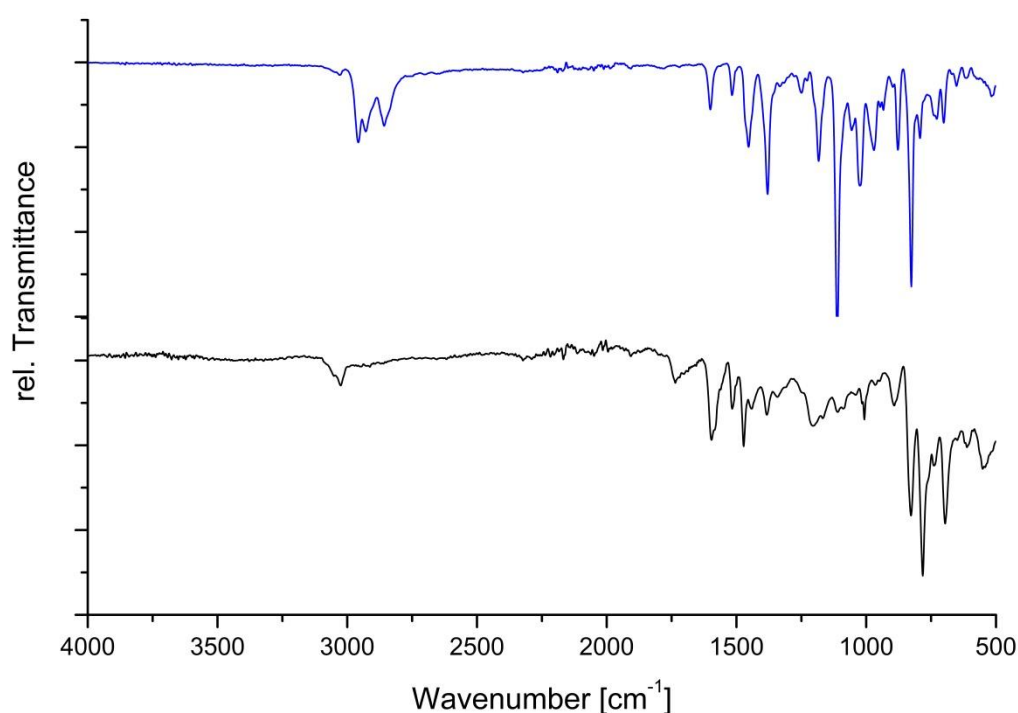
Figure 50. ATR-IR spectra of **78** before (top, blue) and after (bottom, black) thermal treatment.

Table 8. Elemental analysis of polymer **78** after heat treatment and two calculated compositions of precursor **78** and target polymer **78**.

Element	Composition found [%]	Composition starting material [%]	Composition target material [%]
C	89.00	81.95	94.70
H	5.13	8.13	5.30
N	0.17	0.00	0.00
O	3.55	9.92	0.00

Elemental analysis confirms the presence of oxygen in the sample (see Table 8). In a rough comparison from expected elemental composition and observed composition can give some information regarding how many chains are still present. From these basic calculations one can expect a rearranged side-group on every third repeat unit. This, however, is only estimation, since no clear prediction on the exact structure of these side-groups can be made. In a report by Krebs *et al.* for a polythiophene system a temperature dependent leftover was reported.[77, 113] If thermal decomposition was carried out at 200 °C a carboxyl group was remaining on the polymer main chain, while for decomposition at 300 °C complete removal of the side-group was observed.

A major obstacle for this cleaving method, however, is the fact that the required temperature for conversion on a reasonable timeframe is above T_g of polymer **78** (see 7.2.1). As a consequence any orientation which would be induced during processing would be lost and self-standing objects would be affected in their macroscopic shape. This makes thermal shaving in this specific case a major obstacle towards a macroscopic object based on bare polyphenylene.

8.   Processing of Polymer 42

8.1.   Film formation

By the documented fractionation techniques (see 6.1.2) polymer **42** could be obtained in a molecular weight range which made first attempts at processing **42** into a macroscopic object like a film or a fiber possible. Besides the desire to investigate

such an object with regards to its materials properties, a crucial aspect to the shaving protocol had to be investigated. During fiber spinning processes usually a molecular orientation is induced, which contributes significantly to the mechanical properties of the fiber. If the investigated shaving protocol should be successfully applied, the induced order has to be retained during the shaving process. At first, however, attempts were made to cast films of polymer **42** from a chloroform solution. An example for such a film is shown in Figure 51. The haze and the light microscopy image reveal the semi-crystalline nature of **42** obtained under these conditions.
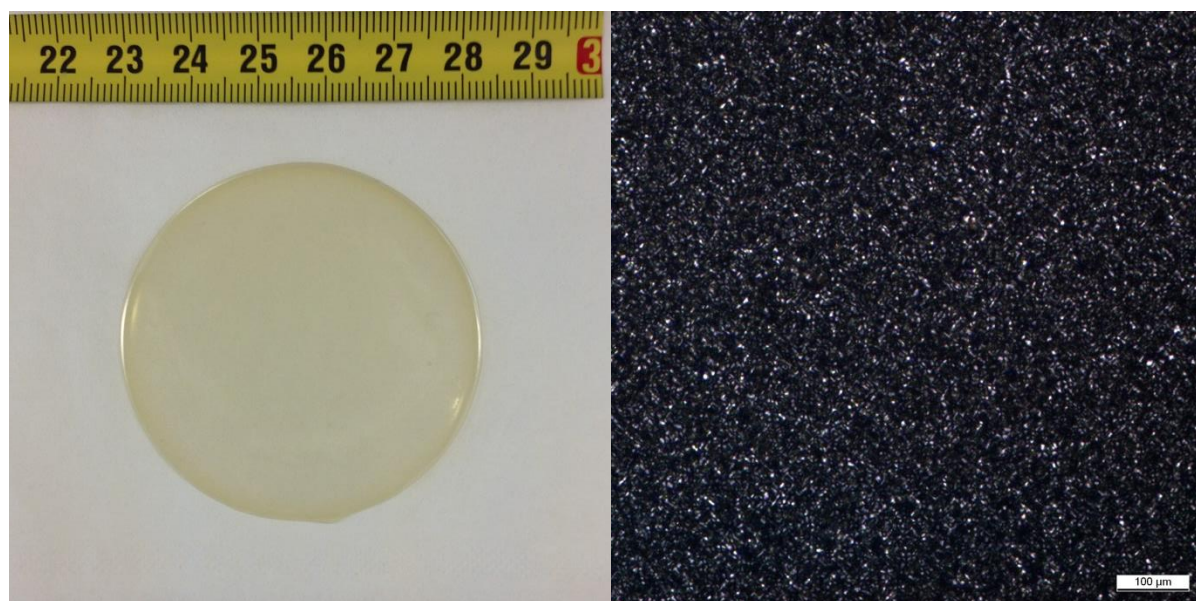
Figure 51. Picture of a film of **42** cast by slow evaporation from $CHCl_3$ (left), cross polarized light microscopy image of the film (right).

The DSC spectrum (Figure 52) of **42** showed an exceptionally high melting temperature domain of 330-385°C during the first cycle and a glass transition at 200-230 °C in the second cycle. For processing reasons a rejuvenation of the film would be needed as processing temperatures above 385 °C are not feasible. However, examination of the DSC sample after measurement revealed that the piece of film could not be dissolved in $CHCl_3$ anymore, hence a cross-linking has taken place, despite the addition of anti-oxidants such as Irgaphos^{TM} and Irganox^{TM} (0.5 % each). This is consistent with observations from TGA (Figure 53) which indicates the start of decomposition at 350 °C. These properties required alternative ways of processing.
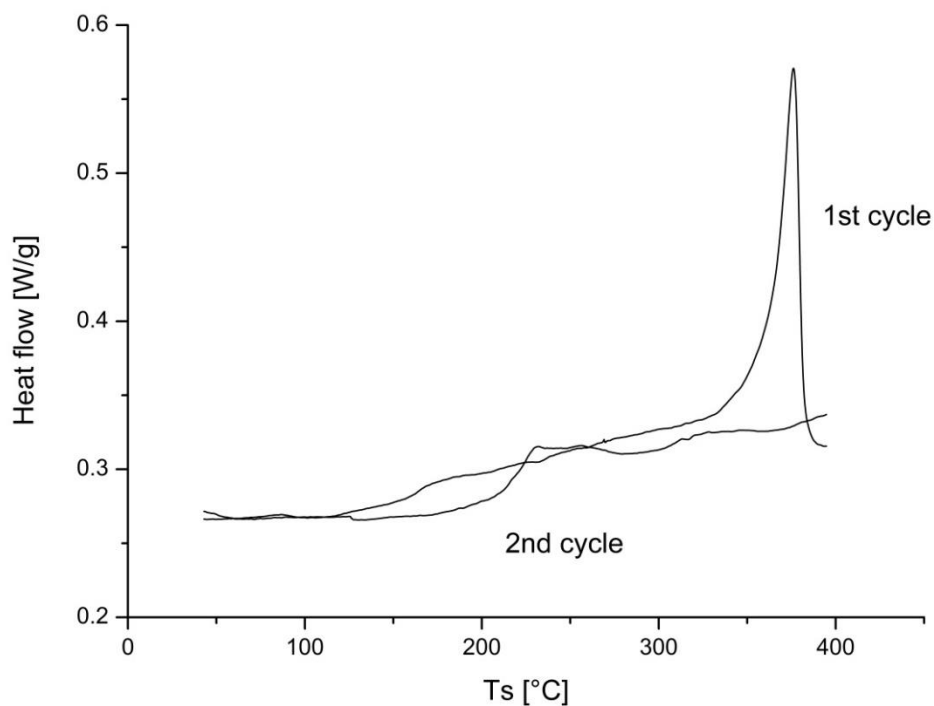
Figure 52. DSC trace of a film of **42** cast from CHCl$_3$ with a total of 1 % of antioxidants added, measured under N$_2$.
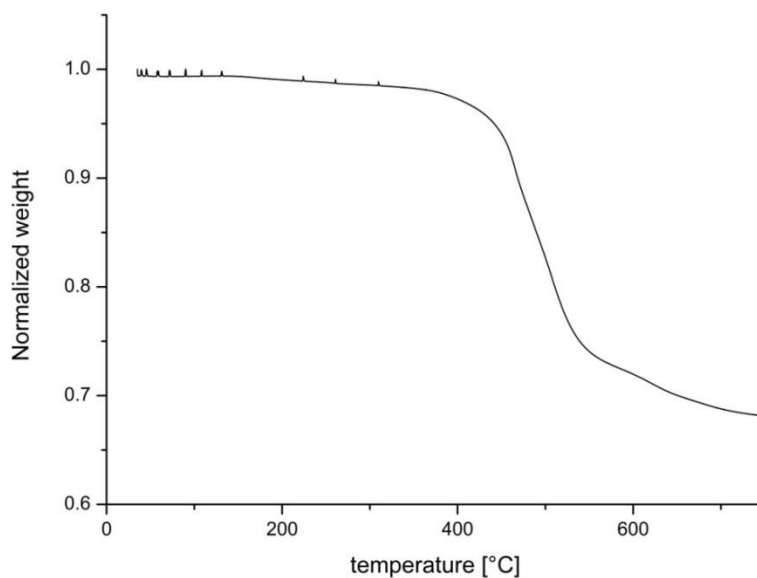
Figure 53. TGA curve of polymer **42**. Heating rate 10 °C/min under N$_2$.

Rapid precipitation of **42** in liquid N$_2$ cooled MeOH and subsequent hot pressing of the resulting white powder led to an inhomogeneous film. Despite the expected random orientation of chains, the resulting film showed strong birefringence in some domains(Figure 54). During hot-pressing, polymer **42** shows poor flow behavior. This

leads to the many small void domains within the film stemming from inhomogeneous sample distribution.
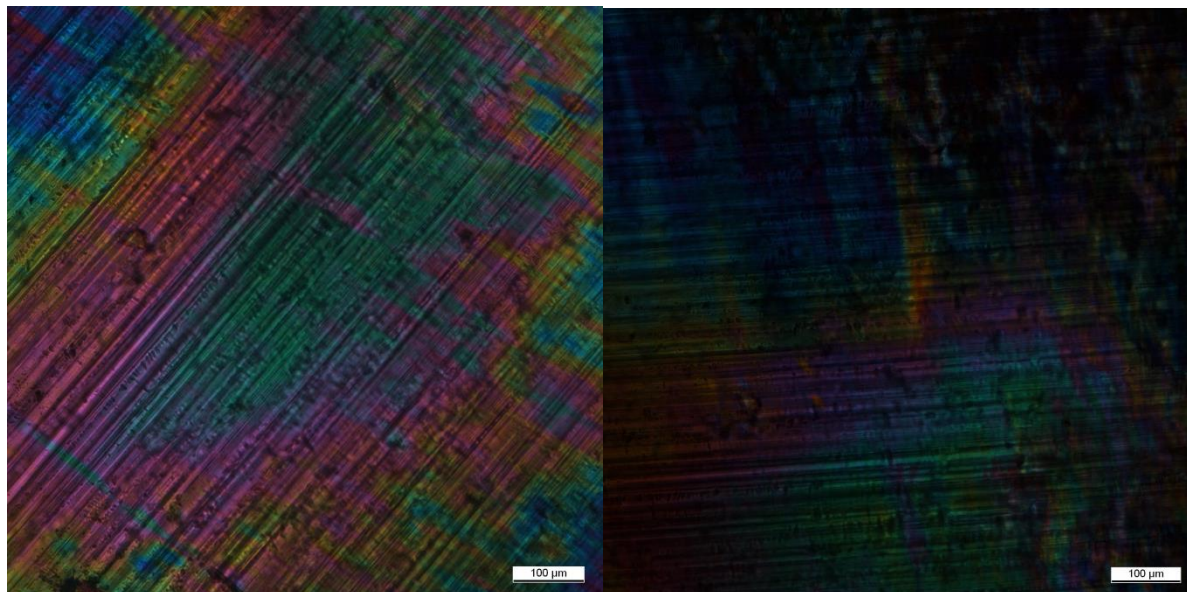
Figure 54. Cross polarized light microscopy images of a film obtained by hot-pressing a powder of **42**. From left to right the sample was rotated by 45 ° in the viewing plane.

8.2. Fiber formation

The thermal properties of **42** proved to be a major obstacle in melt processing **42** into films. Consequently for processing **42** into fibers solution processes were chosen. The relatively low molecular weight of **42** made wet and dry-spinning undesirable as the viscosity of even highly concentrated polymer solutions was still low. The good solubility of **42** in CHCl$_3$ made electrospinning an obvious choice. One of the big advantages of the method is its applicability to a broad variety of polymers. A 20 wt-% solution of **42** in CHCl$_3$ was spun at 7 kV, the flow rate of polymer solution was 2 ml/hr. The spinning distances between nozzle and target were 10, 15 and 20 cm. The target cylinder was rotated 2000 and 3000 rpm. Scanning electron microscopy images of the obtained fibers are shown in Figure 55 a,b and c. Fiber shape, thickness and orientation were of particular interest. The mentioned figures are composed of two SEM pictures each; the relevant spinning parameters are given in the respective figure captions. The fiber morphology was typical for fibers obtained by electrospinning, rather than a circular cross section, the fibers are relatively flat. In addition, the fibers show a large number of fine pores. Both features are a result of

solvent evaporation being the main driving force for fiber formation during the electrospinning process. It is important to note that no fiber welding was observed. The observed fiber diameter for fibers lying flat on the support was in the order of 13 µm. These are rather thick fibers as fibers of thicknesses in the tens of nanometer range are obtainable by electrospinning.[90] A small decrease in fiber thickness with increasing spinning distance from 10 cm to 15 cm could be observed. However, the change was within the general polydispersity observed for the fibers within a single set of spinning parameters. Fiber orientation is mainly important for technical reasons. If the mechanical properties of the obtained fibers should be investigated nicely aligned fibers facilitate the isolation of single fibers. In order to minimize fibers intercrossing each other the collecting cylinder should be rotated at 3000 rpm or higher (see Figure 55 c).
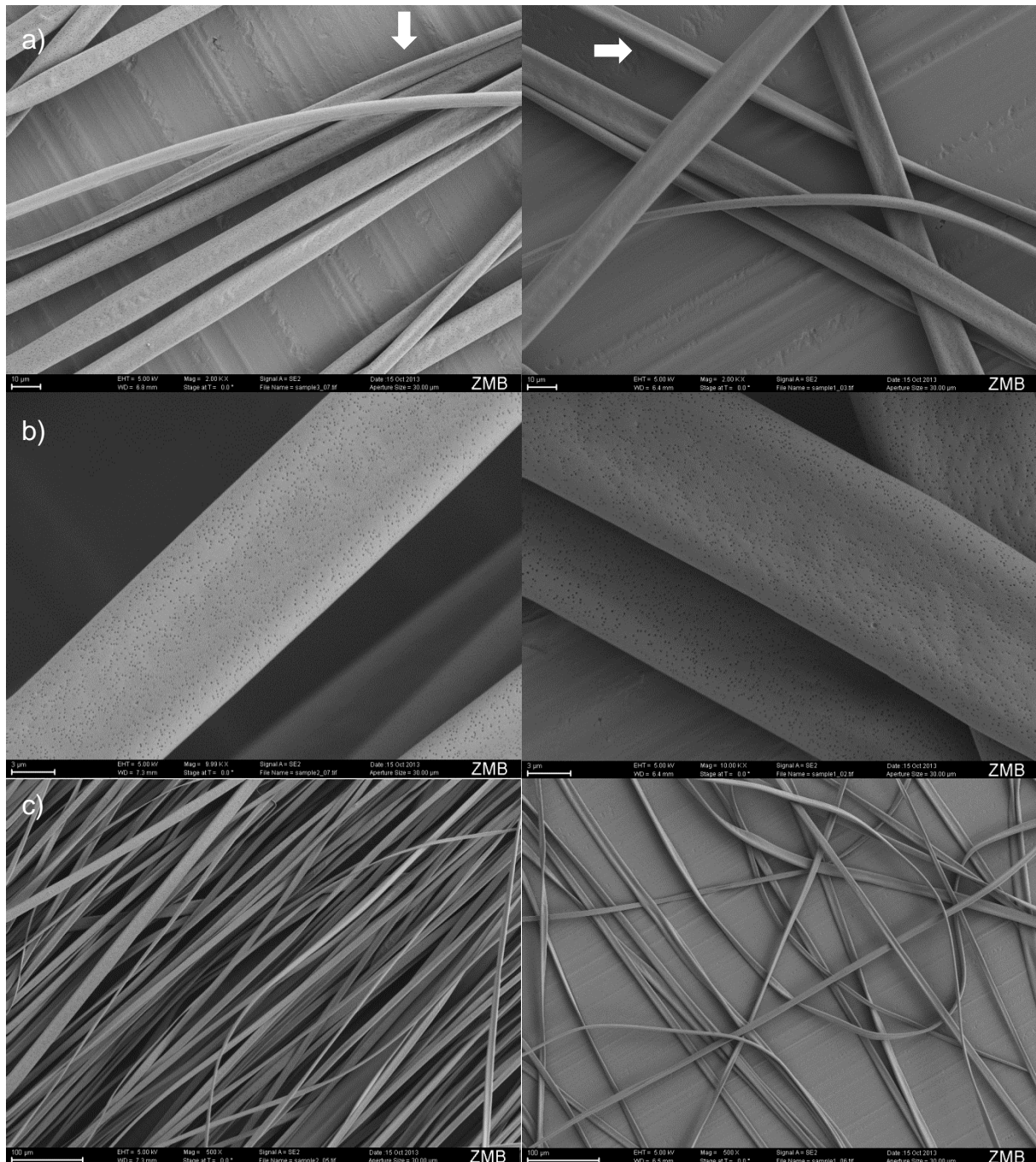
Figure 55. SEM images showing fibers of polymer **42** with 15 cm (left) and 10 cm (right) spinning distance. a) The flat shape is most visible for the twisted fibers marked with arrows. b) Illustrates the fiber thickness is in the order of 13 μm and the fibers have a large number of small pores. c) Shows the effect of fiber orientation as a result of rapid rotation of the collector, which was rotated at 3000 rpm (left) and 2000 rpm (right), respectively.

Light microscopy revealed strong birefringence for the obtained fibers. Indicating that a certain degree of order is induced during the electrospinning process. This is not the case for all polymers. There are differing reports with regard to the presence of birefringence in electrospun polymer fibers.[90] In some cases strong birefringence is

observed[114] and even quantified.[115] While other investigations report low degrees of molecular orientation.[116],[117] In a report a lower degree of crystallinity in electrospun fibers than in the un-spun parent material is observed. [118] This is accounted to the fast evaporation rate of solvent. Srinivasan and Reneker observed strong birefringence for poly(*p*-phenylene terephthalamid) (Kevlar®) fibers.[91] The induced order in the electrospinning process is crucial for the mechanical properties. Any induced order needs to be retained during the shaving process.
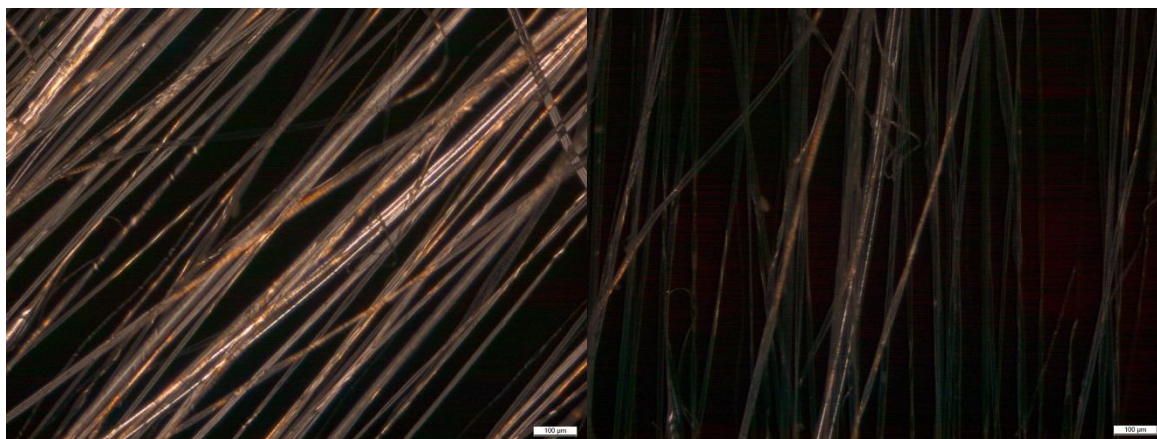
Figure 56. Cross polarized light microscopy images of polymer fibers of **42**. Spun by electrospinning from a CHCl$_3$ solution. Spinning distance 15 cm, rotation speed of collector 3000 rpm.

When electrospun fibers were subjected to the shaving conditions described in 7.1.3, the fibers could not be converted as desired. The reason for this was immediate dissolution of the fibers upon addition of the swelling agent *p*-xylene. To avoid preemptive dissolution the neat fibers were doused with triflic acid for 30 seconds, then the acid was diluted with MeOH and quenched with triethylamine. The fibers were washed multiple times with MeOH. In a solid state ^{13}C-NMR measurement of the treated fibers no aliphatic Carbon signals could be observed (Figure 57).
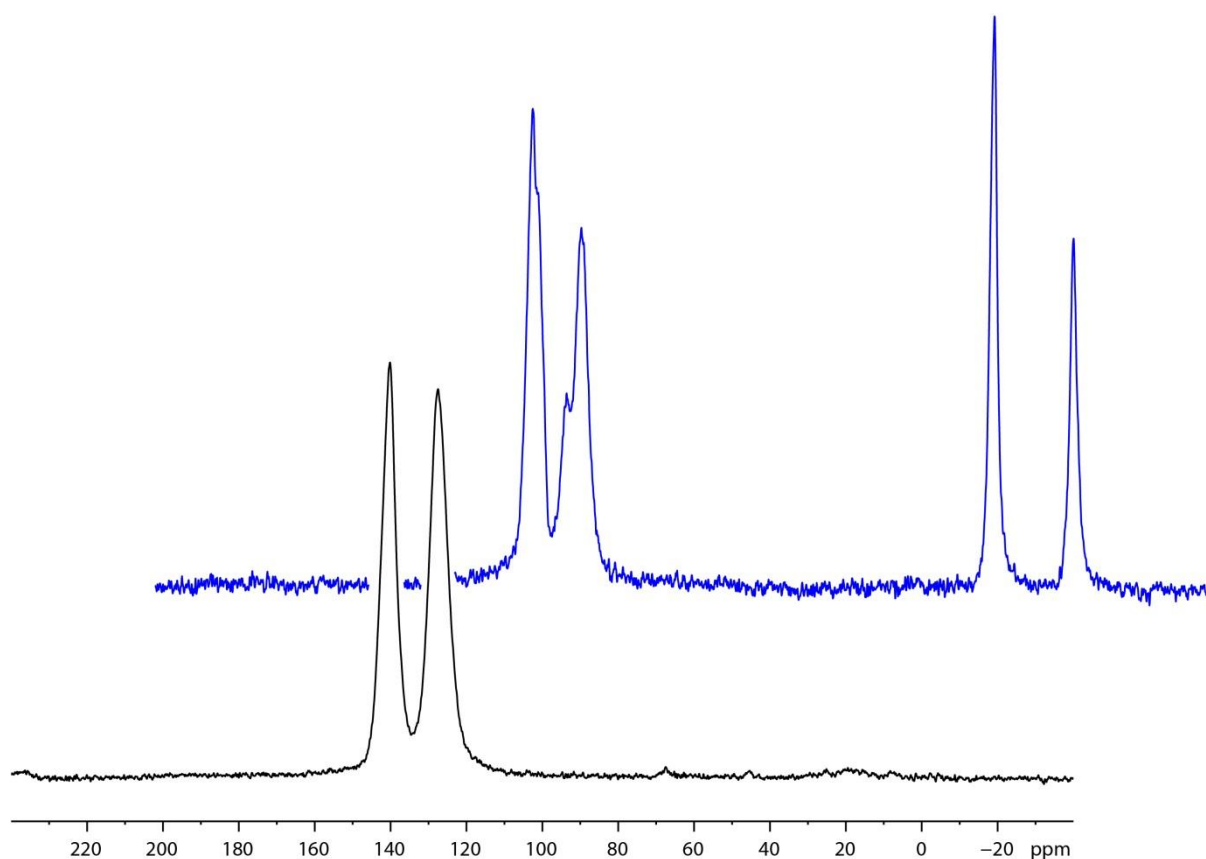
Figure 57. ^{13}C CP MAS-NMR spectrum of the precursor **42** (top, blue) and acid treated fibers (bottom, black). Spinning frequency 20 kHz.

This indicates complete removal of the side-chains to pure fibers made up of polyphenylene **6**. When investigated under cross polarized light the fibers still show birefringence (see Figure 58). It is therefore reasonable to assume that the previously induced order has not been majorly affected by the shaving process. Interesting to note is the color of the fibers. Contrary to the film shaved by preemptive swelling in a poor solvent, the color change was minor. Only a slight yellow stain could be observed on some of the fibers while others remained white. Attempts to get more insight into the crystalline structure by XRD-analysis failed due to insufficient contrast obtained at maximal acceptable exposure time. Attempts to increase the contrast by bundling the fibers more densely were unsuccessful.
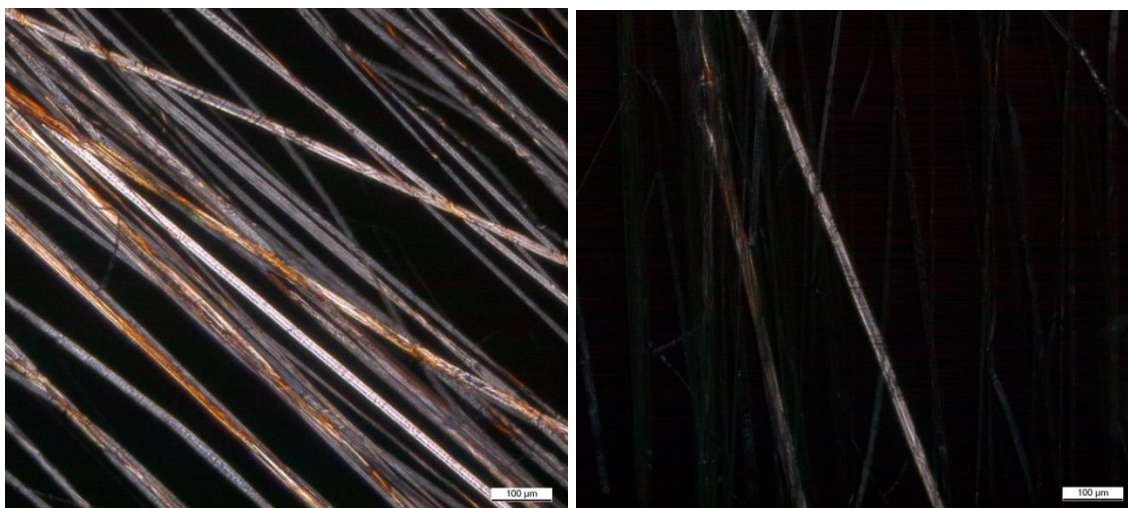
Figure 58. Cross polarized light microscopy images of the acid treated fibers, recorded at angle 0° and 45° respectively.

Fiber topology and thickness after the relatively harsh shaving process were of particular interest. SEM analysis revealed that the number of larger pores increased although not to a significant degree otherwise fiber topology seems to be unaffected (see Figure 59). A slight decrease in average fiber diameter was observed. However, the polydispersity of the diameters of treated and untreated fibers overlap to a certain degree. 20 artificially chosen fibers were gauged for non-treated and treated fibers, respectively. The non-treated fibers showed an average diameter of 13 ± 4 µm, whereas for the treated fibers the average diameter was 10 ± 3 µm. Given these findings it was not possible to exclude the presence of degraded side-chains within the fiber structure. To exclude this, fibers were investigated by solid state ^{29}Si- MAS NMR (Figure 60).
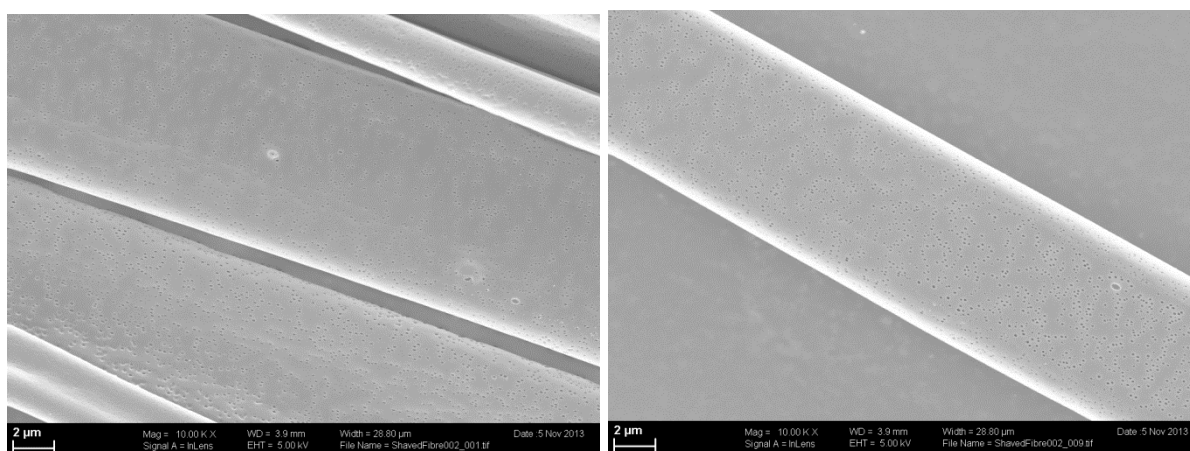
Figure 59. SEM images of two artificially chosen fibers of **6**. Only minor defects are observed which are not exclusive to acid treated fibers but are also observed on fibers of **42**. A slight increase in average pore size compared to untreated fibers can be observed.
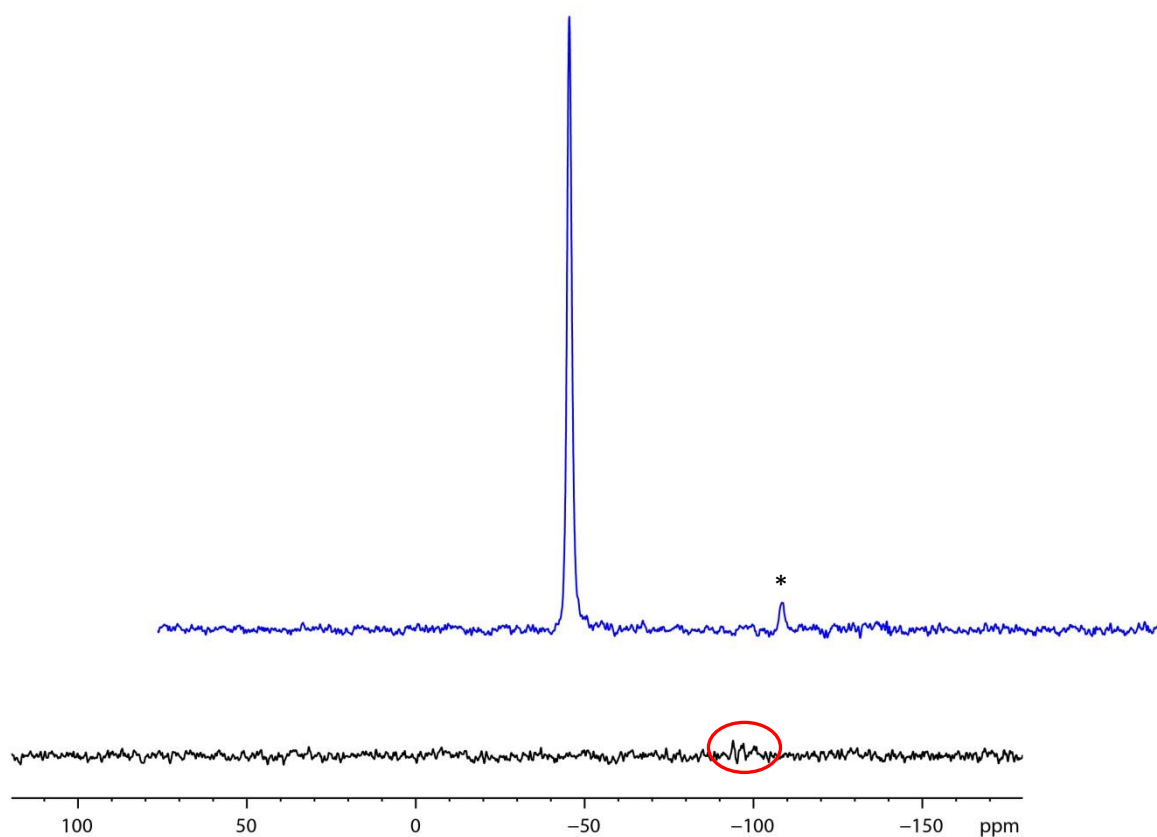
Figure 60. ^{29}Si-MAS NMR spectra of the precursor polymer 42 (top, blue) and the shaved fibers (black, bottom) recorded at 5 kHz spinning frequency. The signal marked with an asterisk is a spinning side-band. The signals origination from the side-chain degradation product is encircled.

The spectra of starting material and processed fibers were recorded with approximately 10 mg of material. Only a very small amount of Si-O based impurities, visible at – 100 ppm, are present within the fibers. This strongly suggests that the shaving process using neat triflic acid was indeed successful and intact, shaved fibers with a significant degree of molecular orientation could be obtained.

9.   Conclusion and Outlook

9.1.   Conclusion

On route to obtaining an all polyphenylene based material, various monomers were targeted in synthesis. Of these, five different monomers could be synthesized on a multigram scale with a high degree of purity. Application of these monomers to AA/BB-type SPC conditions lead to three different polymer structures.

One of these structures (**77**) showed poor solubility, but could be thoroughly investigated with regard to end-groups present and side-reactions impeding polymer growth.

Polymers **42** and **78** could be obtained with M_w of 50 kDa and 49 kDa, respectively. These molecular weights were obtained in yields >90 % directly from polymerization. If the sample was fractionated during work-up the molecular weights for **42** a M_w of 94 kDa could be obtained. In addition to GPC analysis the polymers were characterized by MALDI-TOF mass spectrometry, ATR-IR spectroscopy and solution NMR spectroscopy. Employing a microwave reactor for polymer synthesis allowed to significantly reduce reaction times, but the molecular weights obtained were comparable or slightly lower than the ones observed for conventional heating techniques.

The synthesized polymers carried specifically designed side-groups which were investigated towards their removal from the main chain. Test reactions showed that side-chain removal should be possible for both structures. The found conditions were employed for the polymer material. In the case of **42** this was done by acid treatment, whereas **78** was convertible by heat treatment at 375°C.

Structural analysis for the obtained products by MALDI-TOF mass spectrometry, ATR-IR spectroscopy, solid-state NMR spectroscopy and elemental analysis revealed that the target structure **6** could be obtained from precursor **42**. Precursor **78** led to an intermediate polymer, which was still decorated with side-chains to a certain degree. The side-chains, however, were structurally modified with respect to the ones present in **78**. It is reasonable to assume that the acetal moiety rearranges to form a carboxylic ester.

The side-chain removal in solution of **42** was further expanded. It could be shown that by swelling a large object (large, that is, in comparison with molecules) almost complete removal of all side-chains is possible and core-shell anisotropy could be avoided. Acid treated films were slightly deformed (bent) and shrunk in size, both effects are believed to result from the significant loss in sample mass during the 'shaving' process. XRD analysis revealed a change in the crystal structure between precursor and target material.

Thermal processing of **42** proofed to be a major obstacle. High T_g 200-230 °C and high mp. 350-385 °C lead to the inability to thermally process the material. This was due to degradation of the material at likewise temperatures as the melting temperature.

By electrospinning from a $CHCl_3$-solution stable fibers of **42** could be obtained. SEM analysis revealed that the fibers are relatively flat and when lying flat on the substrate have a thickness of 13 ± 4 nm. They show a homogeneous topology which is dominated by a multitude of small but homogeneous pores. The fibers showed strong birefringence under cross polarized light.

Attempts to swell these fibers lead to immediate disintegration. Treating the fibers with neat triflic acid for 30 seconds, led to almost quantitative removal of the side-chains, while leaving the fibers intact. This was confirmed by solid state ^{13}C-NMR spectroscopy. Moreover, solid state ^{29}Si-NMR spectroscopy confirmed that only negligible amounts of degraded side-chains are entrapped within the fibers. Only minor reduction in fiber dimension to 10 ± 3 nm was observable using SEM. XRD measurements of the obtained fibers before and after acid treatment, was not possible due to the poor scattering properties and the small amounts of polymer mass present in the beam.

9.2. Outlook

An important feature of the AA/BB-type Suzuki polycondensation, the flexibility in monomer design, was only exploited to a small degree in the present project. An important part of any future work would be to exploit this feature to a much higher degree.

Already the synthesized polymer **42** showed strong tendencies to form crystalline phases in solution. This may be one of the reasons for the relatively poor solubility during synthesis. It is, however, emphasized in the fibers obtained by electrospinning. The strong birefringence observed in these fibers is a phenomenon which is generally observed for polymers known to form liquid crystalline phases in their given spinning solvent.[91] Predictions on the stability of the liquid crystalline phases for rigid rod polymers have been made. It is assumed that the stability of the liquid crystalline phases is increased with increasing aspect ratio between the length of the stiff segments and the diameter of the molecular cross-section.[119]

Bearing in mind this theoretical prediction in combination with the synthetical flexibility offered by AA/BB-type SPC. It would be fascinating to synthesize a series of polymers with slightly increasing aspect ratio and observe effect of slight alterations in chemical structure on the properties of liquid crystalline phases and the mechanical properties of fibers from the respective polymers. Employing the presently developed shaving procedures the precursor polymers shown in Figure 61 could be crucial stepping stones on route to this ambitious goal.

Crucial elements for success, however, would be access to polymeric material of higher molecular weight than the one achieved in the present work. In addition to the previously employed analysis methods, selected area electron diffraction (SAED) could be an important tool to gain insight into the crystalline structure present in produced fibers.
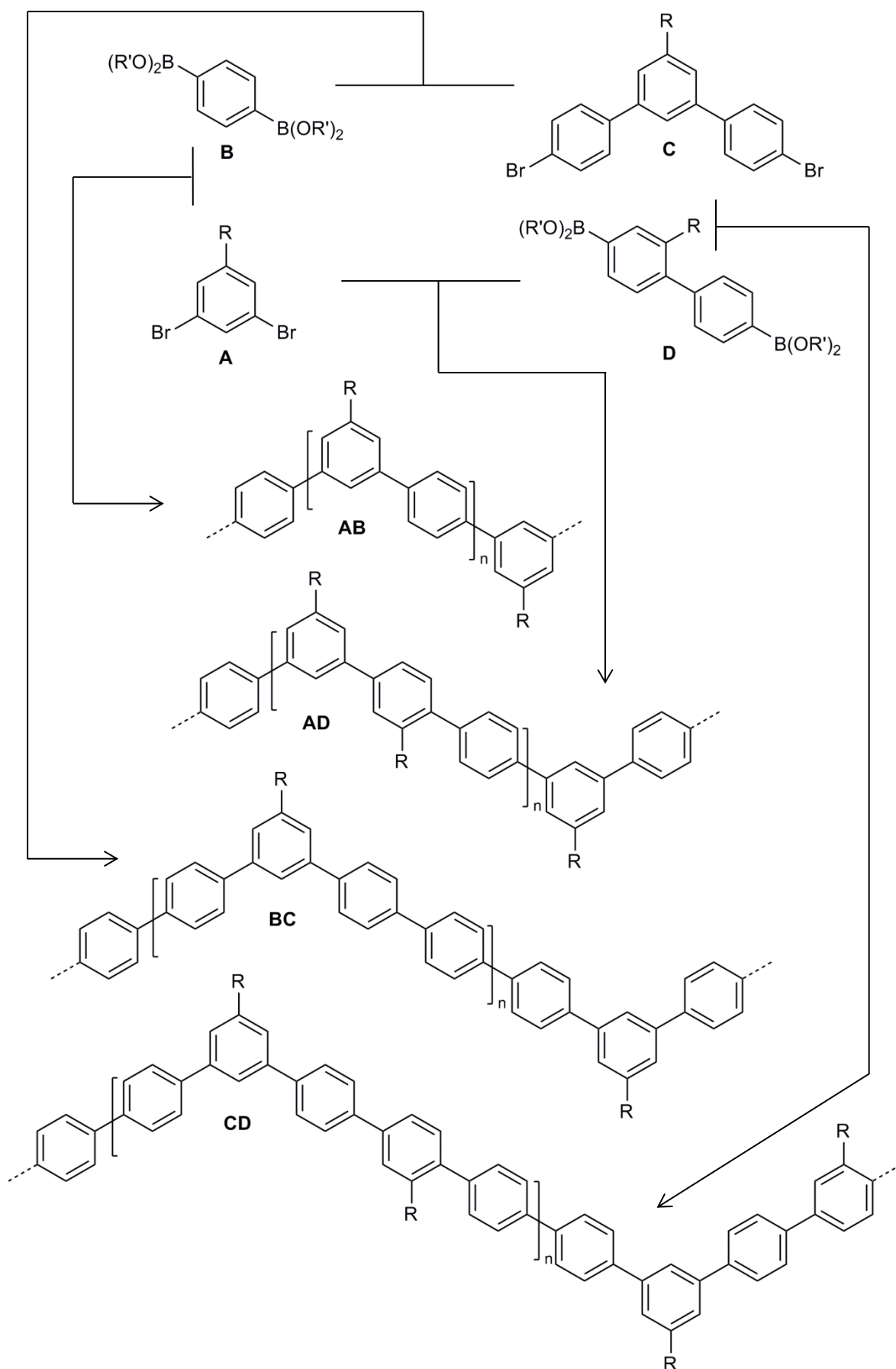
Figure 61. Envisioned route to four precursor polymers AB, AD, BC and CD using only 4 monomeric building blocks.

10. Experimental

10.1. Materials and methods

All the reactions were carried out under nitrogen by using standard Schlenk techniques. All the reagents were purchased from commercial sources and used without further purification unless noted. n-BuLi was used as a 1.6 M solution in hexane. 1,3,5-Tribromobenzen was recrystallized before use. The catalyst used for SPC was prepared according to literature procedure.[120] Column chromatography was performed by using Fluka silica gel Si60 (particle size 40-63 μm) and Bio-Beads S-X1.

Solution NMR spectroscopy was performed with Bruker AM at room temperature using chloroform-d and DMSO-d_6 as solvents. The signal from the solvent was used as internal standard for chemical shift (CDCl$_3$: 1H: δ = 7.26 ppm, 13C: δ = 77.00 ppm; DMSO-d_6: 1H: δ = 2.50, 13C: δ = 39.52). 1H and 19F solid-state NMR spectra were recorded on a Bruker Avance 700 spectrometer operating at 700 and 658.8 MHz for 1H and 19F, respectively, under magic angle spinning (MAS) conditions with single-pulse excitation and a repetition delay of 10 s. The sample rotation frequency was 15 kHz using 2.5 mm rotors. 13C CP/MAS spectra were recorded on a Bruker DRX 500 and a Bruker AMX 400 spectrometer operating at 125.8 MHz for 13C under MAS conditions with 4 mm and 2.5mm rotors using a sample rotation frequency of 8 and 20 kHz respectively, cross-polarization (CP) employing a contact time of 1 ms and 1H high-power decoupling. 29Si solid state NMR spectra were recorded on a Bruker AMX 400 spectrometer under MAS conditions with single-pulse excitation and 1H high-power decoupling. A repetition delay of 30 s was employed and the sample rotation frequency was 5 kHz using 7 mm and 4 mm rotors. Chemical shifts are expressed relative to tetramethylsilane and CCl3F for the 1H, 13C, 29Si and 19F isotopes, respectively.

High-resolution mass spectrosmetory (HRMS) analyses were performed by the MS-service in the laboratory of organic chemistry at ETH Zurich using an electron-ionization (EI) MS spectrometer (Micromass AutoSpec-Ultima) and en electron spray ionization (ESI) MS spectrometer (Bruker maXis) with a quadrupol-time-of-flight tandem analyzer (Q-Tof). MALDI-TOF mass spectra were recorded using a Bruker

UltraFlex II MALDI-TOF mass spectrometer (Bremen, Germany) equipped with a N2 smartbeam laser (λ = 337 nm, 150 µJ, 3 ns) operating at a pulse rate of 100 Hz. For MALDI-TOF MS analyses, the ions were accelerated with pulsed ion extraction (PIE) by a voltage of 25 kV. The analyzer was operated in reflection mode unless otherwise stated, and the ions were detected using a microchannel plate detector. A total of 500-1000 shots were accumulated for each mass spectrum. Samples were prepared with a solvent-free method[121] in which an analyte, matrix and AgOTf/NaOTf were mixed by milling at room temperature to be in the molar ratio of 1/10/1 for all samples except for **6** which was milled in a ratio of 1/500/50. The matrix used for all samples was trans-2-[3-(4-tert-butylphenyl)-2-methyl-2-propenylidene]malononitrile (DCTB) except for **6** where tetracyanoquinodimethane (TCNQ) was used. Calibration was carried out during each measurement on surrounding spots using peptide calibration standard II (Bruker) dissolved in 0.1% trifluoroacetic acid (TFA) with α-cyano-4-hydroxicinnamic acid (HCCA) in a mixed solvent of CH3CN/0.1% TFA 1:2.

Elemental analyses were performed by the Micro-Laboratory in the laboratory of organic chemistry at ETH Zurich using LECO CHN-900 (infrared detection for C and H), combustion carried out at 1000 ºC.

Analytical GPC measurements were performed using a Viscotek GPC-System with chloroform eluent, equipped with a pump and a degasser (GPCmax VE2001, flow rate 1.0 ml/min), a detector module (Viscotek 302 TDA) and two columns (1 $\times$ PLGel Mix-C and 1 $\times$ PLGel Mix-B, 7.5 $\times$ 300 mm for each). Calibration was performed with polystyrene standards (Polymer laboratories) in the range of Mp 1480 to 4340000. Prior to injection, the sample solution was filtered through a sintered stainless steel filter (pore size 2 µm and 0.45 µm).

Infrared spectroscopic analyses were carried out using attenuated total reflection (ATR) - Fourier transform infrared (FTIR) spectrometer (Bruker Optics Alpha system with a built-in diamond ATR). OPUS 6 from Bruker was used as software. The data represent the average of 24 scans in the wavenumber range between 4000 – 500 cm-1 at a resolution of 1.42 cm-1.

TGA was measured on a TGA Q500 (TA Instruments, USA) under N_2 atmosphere in a platinum pan. Thermal stress tests were carried out isothermally

with a heating ramp of 20 °C/min. Overview measurements were done at a heating rate of 10 °C/min. The sample mass was between 2-10 mg.

DSC was measured on a DSC Q1000 (TA Instrument, USA) and a DSC 822^e (Mettler Toledo, Switzerland) using aluminum pans. Heating and cooling rate were 10 °C/min.

Films were casted from a chloroform solution using 10-15 wt % of polymer. All solutions were heated to 50 °C while stirring for 6 hours prior to film casting. Films were cast into petri-dishes, after filtration through a 0.45 µm mesh size PTFE filter. The closed petri-dishes were left to stand until solvent evaporation was complete.

Pressed films were cast in a Rondol Technology hot press at 210 °C between two thin aluminum plates. To the samples 0.5 % of Irgaphos and 0.5 % of Irganox were added as stabilizers to prevent oxidation.

Fiber spinning was done on an in house assembled electrospinning device. An AL-1000 syringe pump was used to pump the solution to a flat tipped steel cannula. A DC high voltage supply (Glassmann high voltage Inc., USA) was operated at 7kV and 5 mA. A hollow aluminum cylinder (diameter: 80 mm, wall thickness: 5 mm) served as collector, which was rotated at 2000-3000 rpm.

Light microscopy images were measured on a Leica DMRX instrument using a Leica DFC480 camera in transmission mode.

SEM images were recorded on a Zeiss SUPRA 50 VP and a Zeiss LEO Gemini 1560 (Zeiss, Germany) using secondary electron detection. Accelerating voltage was 5 kV, aperture width was 30.00 µm and 28.80 µm respectively. A SCD500 and SCD050 sputter coater (Bal-Tec, Liechtenstein) was used to deposit a 10 nm platinum layer (50 mA, 60 s) on the samples.

Powder XRD measurements were carried out on a XCalibur single-crystal X-ray diffractometer (Oxford Diffraction, UK) using an Onyx CCD detector. The wavelength used was Mo-K$_\alpha$ (λ = 0.71073 Å) using a graphite monochromator. Data evaluation was done with FIT2D.[122]

10.2. 1,4-di(1,3,2-dioxaborinan-2-yl)benzene[123] (32)
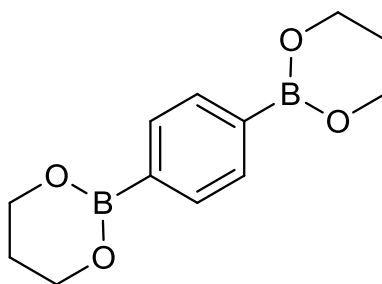
A 2 L round bottom flask was charged with 27.22 g (164.2 mmol) of 1,4 - phenylenediboronic acid (**15**) and 25.62 g (336.7 mmol, 2.05 eq) of propan-1,3-diol. The starting materials were dissolved in 1000 ml toluene and the reaction was heated at a Dean-Stark apparatus overnight. The solvent was removed in vacuum and the resulting solid was redissolved in Diethylether. Hot filtration and subsequent crystallization (2x) yielded the desired product as colorless crystals (29.42 g, 72.9 %).

^{1}H-NMR(CDCl$_3$, 300.23 MHz): δ = 7.77 (s, 4 H, arom. H), 4.19 (t, J = 5.48 Hz, 8 H, O-CH$_2$), 2.08 (quin, J = 5.48 Hz, 4 H, CH$_2$) ppm.

10.3. 1,4-bis(4,4,5,5-tetramethyl-1,3,2-dioxaborolan-2-yl)benzene (52)
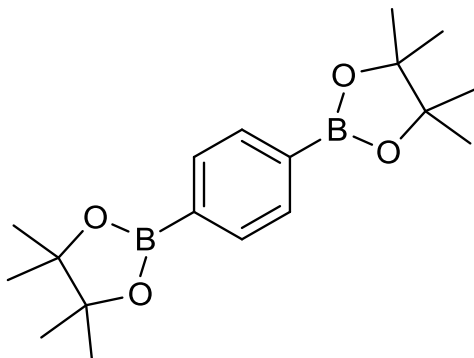
A 2 L round bottom flask was filled with 31.73 g (191.4 mmol) of 1,4 - phenylenediboronic acid (**15**) and 46.37 g (392.4 mmol, 2.05 eq) of pinacol. The starting materials were dissolved in 1000 ml toluene and the reaction was heated at a Dean-Stark apparatus overnight. The solvent was removed in vacuum and the resulting solid was redissolved in Diethylether. Hot filtration and subsequent crystallization (2x) yielded the desired product as colorless crystals (54.56 g, 86.4 %).

^{1}H-NMR(CDCl$_3$, 300.23 MHz): δ = 7.80 (s, 4 H, arom. H), 1.35 (s, 24 H, CH$_3$) ppm.[124]

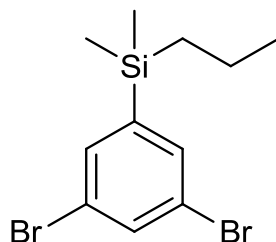## 10.4. (3,5-dibromophenyl)dimethyl(propyl)silane (53)

In a 2 L Schlenk-flask 50.00 g (158.8 mmol) of 1,3,5 – Tribromobenzene (**54**) were dissolved in 1.2 L dry Diethylether. The solution was cooled to − 78 °C upon which it turned into a slurry. Under constant stirring 10 mL (160.0 mmol,1.01 eq.) *n*-BuLi-solution (1.6 M in hexane) was added drop wise over 45 min to the reaction mixture. Stirring was continued for another 60 min. Thereafter 29.95 ml Dimethyl(propyl)silylchloride (190.6 mmol, 1.20 eq) were added slowly to the reaction mixture. The mixture was allowed to slowly reach room temperature. Excess electrophile was quenched by the addition of water, the organic and the aqueous phase were separated and the organic phase was washed with water (2x). After drying over $MgSO_4$ and filtration the solvent was evaporated. The crude product (dark-brown oil) was subjected to column chromatography (silica gel, hexane). The resulting colourless oil still contained small amounts of starting material which were removed by sublimation. After subsequent vacuum distillation the product was obtained as colourless oil, 33.40 g (63 %).

^{1}H-NMR(CDCl$_3$, 300.23 MHz): δ = 7.64 (t, *J* = 1.7 Hz, 1 H, arom.), 7.49 (d, *J* = 1.7 Hz, 2 H, arom.), 1.34 (m, 2 H, CH$_2$), 0.96 (t, *J* = 7.2 Hz, 3 H, CH$_3$), 0.73 (m, 2 H, CH$_2$), 0.25 (s, 6 H, CH$_3$) ppm. ^{13}C-NMR(CDCl$_3$, 50 MHz): δ = 145.5, 134.8, 134.3, 123.3, 18.3, 18.1, 17.4, -3.0. HRMS (EI): calculated for C$_{11}$H$_{13}$Br$_2$Si [M$^+$]: 335.9363, found: 335.9363 (molecular ion), 320.9128 (loss of CH$_3$, calc. 320.9133), 292.8823 (100 %-peak, loss of propyl group, calc. 292.8820).

10.5. ethyl 4-amino-3,5-dibromobenzoate[98] (58)
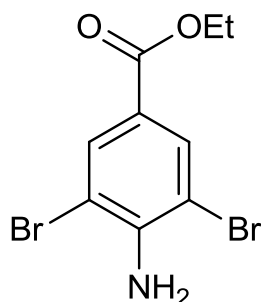
To a 2 l round bottom flask 93.0g (563 mmol) of 4-amino-ethylbenzoate (**57**) was dissolved in 1.25 l of AcOH. The flask was fitted with a dropping funnel through which, under constant stirring, 60 ml (1.17 mol, 2.07 eq) of Br_2 in 150 ml AcOH was added over 2.5 h. The reaction was heated to 85 °C and the temperature was maintained for 1.5 h. After the reaction was cooled to room temperature, it was poured on ice and left to stand overnight. The resulting suspension was filtered and washed with water. The resulting light yellow solid was recrystallized from MeOH. Affording 156 g (86 %) of the pure product. ^{1}H-NMR (300.23 MHz, CDCl$_3$) δ/ppm: 8.07 (s, 2 H, arom. H), 4.98 (s broad, 2 H, NH$_2$), 4.33 (q, J = 7.1 Hz, 2 H, CH$_2$), 1.37 (t, J = 7.0 Hz, 3 H, CH$_3$) ppm.

10.6. ethyl 3,5-dibromobenzoate[98] (59)

$$O = \overset{OEt}{\underset{Br \quad\quad Br}{\bigcirc}}$$
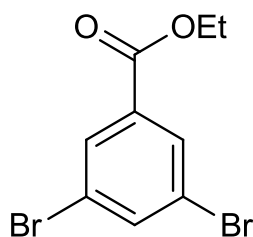
156 g (0.483 mol) of ethyl 4-amino-3,5-dibromobenzoate (**58**) was dissolved in a 3-l round bottom flask with 1.3 l of EtOH. After heating to 50 °C 200 ml of concentrated H_2SO_4 (3.62 mol, 7.5 eq) was added dropwise. The reaction was heated to 70°C and 101 g (1.46 mol, 3 eq) of $NaNO_2$ in 210 ml water was added dropwise. During the addition the solution turned brown. After 16 h heating was stopped and the reaction was allowed to cool to room temperature. The reaction was poured on ice and filtered. The residue was washed with water and recrystallized from Isopropanol (2x). Affording 49.5 g (33 %) of the product as colorless crystals. ^{1}H-NMR (300.23 MHz, $CDCl_3$) δ = 8.10 (d, J = 1.77 Hz, 2 H, arom. H), 7.84 (t, J = 1.74 Hz, 1 H, arom. H), 4.39 (q, J = 7.12 Hz, 2 H, CH_2), 1.40 (t, J = 7.09 Hz, 3 H, CH_3) ppm.

10.7. (3,5-dibromophenyl)methanol[98] (60)
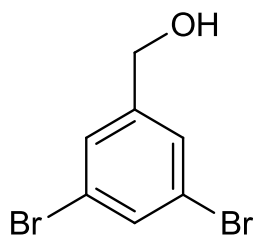
A 1 l schlenk-flask was charged with 350 ml Et_2O and cooled to 0° C under inert atmosphere. 10 g of LAH (0.236 mol, 1.6 eq) were added. 49.5 g (0.160 mol) of ethyl 3,5-dibromobenzoate (**59**) were dissolved in 250 ml of Et_2O. This solution was added dropwise over 75 min. The reaction mixture was allowed to slowly reach room temperature. For quenching the reaction mixture was cooled to 0 °C. After sequential addition of 10 ml H_2O and 40 ml of 15 % NaOH-sol. the mixture was allowed to reach room temperature and stirring was continued for 15 min. $MgSO_4$ was added and the suspension was filtered. The residue was washed with Et_2O. Removal of solvent yielded 38 g of the crude product, which was recrystallized from Hex:EtOAc (4:1) to yield 32.6 g (76.4 %) of the product as colorless crystals. ^{1}H-NMR (300.23 MHz, $CDCl_3$) δ = 7.58 (m, 1 H, arom. H), 7.45 (m, 2 H, arom. H), 4.67 (s, 2 H, CH_2), 1.77 (s, 1 H, OH) ppm.

10.8. 2-((3,5-dibromobenzyl)oxy)tetrahydro-2H-pyran[27] (61)
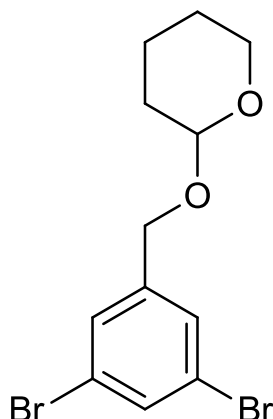
A 500 ml schlenk-flask was charged with 24.3 g (91.4 mmol) (3,5-dibromophenyl)methanol (**60**) in 300 ml dry DCM and cooled to 0°C. 12.5 ml of Dihydropyrane (137 mmol, 1.5 eq) were added in addition to 175 mg of *p*-TsOH·H_2O (0.9 mmol, 1 mol %). The reaction was allowed to reach room temperature overnight. The reaction was quenched by addition of 1 ml NEt_3. The solvent was removed under reduced pressure. Column chromatography (Silica gel, Hex:DCM 3:1, Hex:DCM 1:1, DCM (+0.5 % of NEt_3 for all elution mixtures)) afforded 25.8 g (80.6 %) of the product as a colorless oil. ^{1}H-NMR (300.23 MHz, $CDCl_3$) δ = 7.57 (m, 1 H, arom. H), 7.44 (m, 2 H, arom. H), 4.67 (d, *J*= 12.7 Hz, 1 H, CH_2) and 4.46 (d, *J*= 12.7 Hz, 1 H, arom.-CH_2-O), 4.68-4.70 (m, 1 H, CH), 3.83-3.90 (m, 1 H, O-CH_2) and 3.52-3.59 (m, 1 H, O-CH_2), 1.50-1.93 (m, 6 H, CH_2) ppm.

10.9. 3,5 – Dibromobenzaldehyde[96] (55)
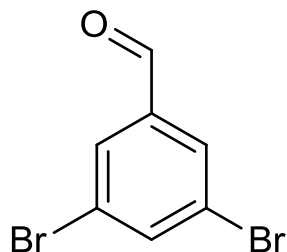
In a 1 L Schlenk-flask 20 g (63.5 mmol) of 1,3,5 – Tribromobenzene (**54**) were dissolved in 500 ml dry Diethylether. The solution was cooled to – 78°C upon which it turned into a slurry. Under constant stirring 42 mL (66.7 mmol,1.05 eq.) *n*-BuLi-solution (1.6 M in hexane) was added drop wise over 35 min to the reaction mixture. Stirring was continued for another 45 min. Thereafter 15 ml dry DMF (194 mmol, 3.1 eq) were added slowly to the reaction mixture. After 1 h stirring the reaction was quenched with 160 ml of 10 % HCl-solution. After reaching room temperature, the organic and the aqueous phase were separated and the organic phase was washed with water (2x). After drying over $MgSO_4$ and filtration the solvent was evaporated. The crude product (dark-brown solid) was recrystallized from Et_2O/hex which afforded 12.21 g (73 %) of the pure product as dark brown needles.

^{1}H-NMR($CDCl_3$, 300.23 MHz): δ = 9.93 (s, 1 H, aldehyde H), 7.95 (m, 3 H, arom.) ppm. ^{13}C-NMR($CDCl_3$, 50 MHz): δ = 189.3, 139.7, 139.0, 131.4, 124.1 ppm.

10.10.　　5-Butyl-2-(3,5-dibromophenyl)-5-ethyl-1,3-dioxane (56)
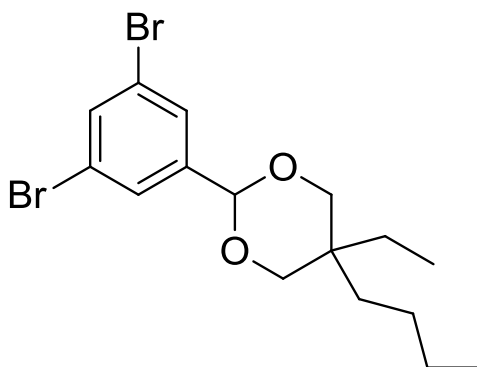
In a 250 ml Schlenk flask, charged with 120 ml of toluene, 8.00 g (30.31 mmol) of 3,5 – dibromobenzaldehyde (**55**) and 5.10 g (31.83 mmol, 1.05 eq) of 2-Butyl-2-ethylpropane-1,3-diol were brought into solution. After the addition of 560 mg (2.94 mmol, 0.097 eq) 4-Methylbenzenesulfonic acid monohydrate the vessel was fitted with a Dean-Stark-apparatus and the reaction was heated to reflux over night. The reaction was quenched by the addition of 2 ml NEt$_3$. After removal of solvent under reduced pressure the residue was purified by silica gel chromatography (10:1 hexane/ethylacetate + 1 % NEt$_3$). The resulting yellow oil was further purified by vacuum distillation (0.02 mbar, 185 °C) which afforded 9.45 g (77 %) of the pure product as colourless oil.

^{1}H – NMR (CDCl$_3$, 30.23 MHz): δ = 7.63 (s, 1H, arom.), 7.58 (s, 2 H, arom.), 5.31 (s, 1 H, -CH (- O-)$_2$), 3.94 (d, J = 11.1 Hz, O-CH_2-), 3.62 (dd, J = 11.7, 4.5 Hz, O-CH_2-), 1.85 - 1.65 (m, 2 H, alkyl), 1.45 – 1.00 (m, 6 H, alkyl), 1.00 – 0.75 (m, 6 H, alkyl) ppm. ^{13}C-NMR(CDCl$_3$, 75.5 MHz): δ = 142.3, 134.2, 128.3, 122.8, 99.8, 75.3 and 75.1, 34.9 and 34.8, 31.7 and 30.1, 25.4 and 25.0, 24.3 and 23.6, 23.5 and 23.3, 14.3 and 14.0, 7.7 and 6.8 ppm. HRMS(EI): [M$^+$] calc: 403.9981 amu, found: 403.9981 amu. other signals (amu): 83.0852, 70.0776 (100 %), 55.0565, 41.0463 (alkyl fragmentation series); 171.1381 (acetal moiety, calc. 171.1385).

10.11.   1,3-dibromo-5-nitrobenzene (64)
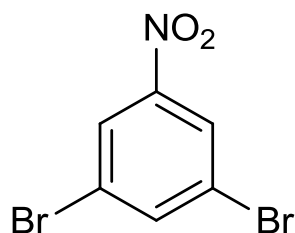
19.23 g (65.0 mmol) of 2,6-dibromo-4-nitroaniline (**63**) were dissolved in 220 ml EtOH in a two-neck flask. After slow addition of 22 ml concentrated H_2SO_4 the solution was heated to reflux. 14.46 g (209 mmol, 3.22 eq) of $NaNO_2$ was added portion wise. After the addition was complete stirring was continued for 2 hours. The reaction was allowed to cool to room temperature and poured on ice. The resulting mixture was filtered and the residue was washed with water and dispersed in hot EtOH. After hot filtration crystals formed from solution, 14.2 g (77.5 % yield). ^{1}H-NMR (300.23 MHz, $CDCl_3$) δ = 8.32 (d, J = 1.8 Hz, 2 H, arom. H), 8.00 (t, J = 1.5 Hz, 1 H, arom. H) ppm.[125]

10.12.   3,5-dibromoaniline (65)
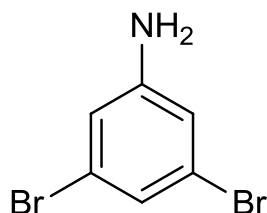
In a 100 ml round bottom flask 2.41 g (8.58 mmol) of 1,3-dibromo-5-nitrobenzene (**64**) was dissolved in 40 ml THF/EtOH (1:1). While stirring 10.0 g (44.3 mmol, 5.17 eq) of $SnCl_2 \cdot 2\,H_2O$ was added slowly and the reaction was stirred at room temperature for 20 hours. The solvent was evaporated and the residue was dispersed in in dilute NaOH (aq.). Extraction with Et_2O, subsequent drying over Na_2SO_4 and removal of solvent yielded 1.82 g (84.7 %) of the pure product. ^{1}H-NMR (300.23 MHz, $CDCl_3$) δ = 7.02 (m, 1 H, arom. H), 6.74 (d, J = 1.5 Hz, 2 H, arom. H), 3.76 (s, 2 H, NH_2) ppm.[126]

10.13.   tert-butyl (3,5-dibromophenyl)carbamate (62)
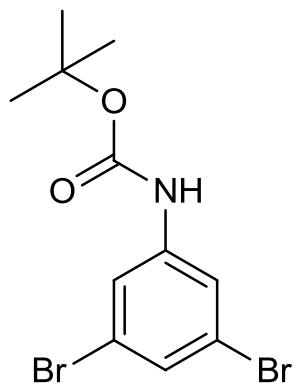
In a 250 ml round bottom flask 4.2 g (16.7 mmol) of 3,5 –Dibromoaniline (**65**) were dissolved in 80 ml of toluene. After addition of 20 ml (87.0 mmol, 5.2 eq) Boc_2O and 10 ml (57.8 mmol, 3.5 eq) of DIEA the solution was heated to reflux for 24 h. Removal of solvent and recrystallization from Et_2O afforded 1.44 g (24.4 %) of the pure product as white needles. ^{1}H-NMR ($CDCl_3$, 300.23 MHz) δ = 7.61 (t, J = 1.60 Hz, 1 H, arom. H), 7.27 (d, J = 1.67 Hz, 2 H, arom. H), 1.45 (s, 9 H, CH_3) ppm. ^{13}C-NMR ($CDCl_3$, 75.5 MHz) δ = 151.2, 141.3, 133.3, 130.4, 122.3, 83.8, 28.1 ppm. HRMS (ESI): [M+Na]$^+$ calculated: 373.9185 amu, found: 373.9189 amu.

10.14.   4,4'-dibromo-2,2'-dinitro-1,1'-biphenyl (67)
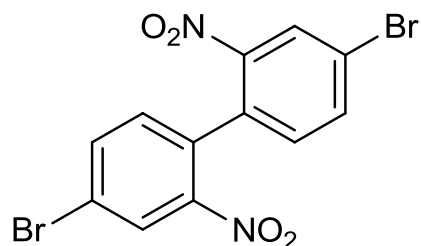
In a 250 ml round bottom flask 24 g (85.4 mmol) of 1,4-Dibromo-2-nitrobenzene (**66**) was dissolved in 110 ml Dimethylformamide. 12 g (188.9 mmol, 2.2 eq) copper powder was added portion wise while stirring. After the addition the suspension was heated to 125 °C for 3 h. After removal of solvent the resulting solid was dispersed in 600 ml benzene, the suspension was filtered through celite. Removal of solvent at reduced pressure yielded the crude product. After recrystallization from isopropanol the product was obtained as yellow crystals, 12.08 g (70 % yield). ^{1}H-NMR (300.23 MHz, CDCl$_3$) δ = 8.38 (d, J = 1.9 Hz, 2 H), 7.83 (dd, J_1= 8.2 Hz, J_2 = 1.9 Hz, 2 H), 7.16 (d, J = 8.2 Hz, 2 H) ppm.[102]

10.15. 4,4'-dibromo-[1,1'-biphenyl]-2,2'-diamine (68)
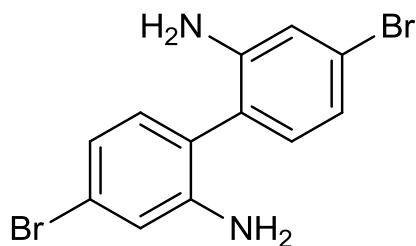
In a 250 ml Schlenk flask 7.27 g (18.1 mmol) of 4,4'-dibromo-2,2'-dinitro-1,1'-biphenyl (**67**) was dissolved in 90 ml ethanol. While continuously stirring, 9.67 g (81.5 mmol, 4.5 eq) Sn powder was added portion wise. After Sn-addition was completed 52 ml of fuming HCl (32 % w/w) were added. Another 9.69 g (81.7 mmol, 4.5 eq) of Sn powder was added over 10 min, thereafter the reaction was heated to reflux for 2 hours. The reaction was allowed to reach room temperature and poured on ice. The mixtures pH was brought to 9 with the addition of 20 % (w/w) of NaOH (aq.) solution and extracted with diethylether. The organic phase was washed with brine and dried over magnesium sulfate, after filtration and removal of solvent yielded 5.90 g (95 %) of the product as light brown solid. ^{1}H-NMR (300.23 MHz, d-DMSO) δ = 7.78 (s, 4 H, NH$_2$), 7.46 (d, J = 1.7 Hz, 2 H, arom. H), 7.25 (dd, J_1 = 8.2 Hz, J_2 = 1.7 Hz, 2 H, arom. H), 7.17 (d, J = 8.2 Hz, 2 H, arom. H) ppm.[102]

10.16.   4,4'-dibromo-2,2'-diiodo-1,1'-biphenyl (69)
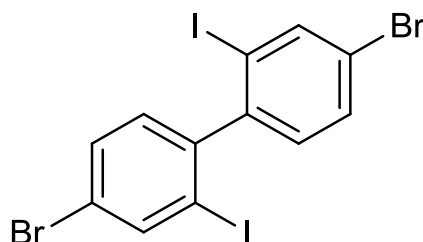
In a 1 l schlenk flask 10 g (29.2 mmol) of 4,4'-dibromo-[1,1'-biphenyl]-2,2'-diamine (**68**) were dissolved in 150 ml of 9 % H_2SO_4. The mixture was cooled to 0 °C and 10.08 g (146 mmol, 5 eq.) in 50 ml of water were added slowly under vigorous stirring. After 45 min, 53.82 g (324 mmol, 11 eq) of KI in 100 ml of water was added and the reaction was allowed to reach room temperature within 4 h. An excess of $Na_2S_2O_3$ solution was added to quench the reaction. The mixture was extracted with hexane:DCM (9:1), the organic phase was dried with $MgSO_4$ and solvent was removed. The residue was dissolved in $CHCl_3$ and the solution was concentrated. Crystals formed which were removed by filtration (side-product, mono-transformation), the mother liquor was concentrated completely. Column chromatography (silica gel, hexane) gave 3.70 g (22.5 %) of the product as light yellow solid. 1H-NMR (CDCl$_3$, 300.23 MHz) δ = 8.10 (d, J = 1.70 Hz, 2 H, arom. H), 7.56 (dd, J_1 = 1.76 Hz, J_2 = 8.16 Hz, 2 H, arom. H), 7.03 (d, J = 8.16 Hz, 2 H, arom. H) ppm. ^{13}C-NMR (CDCl$_3$, 75.5 MHz) δ = 146.9, 141.1, 131.5, 130.9, 122.6, 100.0 ppm. HRMS (EI): [M]$^+$ calculated: 561.6926 amu found: 561.6948 amu, [M - I]$^+$ calc: 434.7881 amu, found: 434.7867 amu, [M – I -Br]$^+$.calc: 355.8698 amu, found: 355.8683 amu, [M - 2 I]$^+$ calc: 307.8836 amu, found: 307.8842 amu, [M - 2 I - Br]$^+$ calc: 228.9653 amu, found: 228.9651 amu, [M - 2 I – 2 Br]$^+$ calc: 150.0470 amu, found: 150.0465 amu.

10.17.   di-tert-butyl (4,4'-dibromo-[1,1'-biphenyl]-2,2'-diyl)dicarbamate
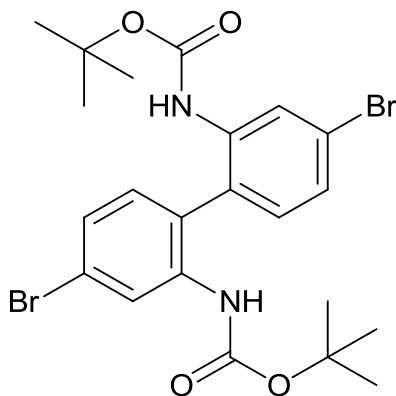
In a 100 ml round bottom flask 1.50 g (4.39 mmol) of 4,4'-dibromo-[1,1'-biphenyl]-2,2'-diamine (**68**) was dissolved in 20 ml of THF and 3.4 ml (18.86 mmol, 4.3 eq) of DIEA was added and the solution was stirred for 15 min. After addition of 2.3 ml (9.65 mmol, 2.2 eq) of Boc-anhydride the solution was heated to reflux. The reaction course was followed by TLC after 24 and 48 hours respectively an additional 2 ml (8.4 mmol, 2 eq) anhydride was added. After 72 hours TLC indicated complete consumption of starting material. Water was added and the mixture was extracted with ethylacetate, drying over magnesium sulfate and removal of solvent under reduced pressure afforded the crude product. Purification by column chromatography (silica gel, hexane/CH_2Cl_2) yielded 1.14 g (48 %) of the pure product. ^{1}H-NMR (300.23 MHz, CDCl$_3$) δ = 8.50 (d, J = 1.6 Hz, 2 H, arom. H), 7.27 (dd, J_1 = 1.8 Hz, J_2 = 8.1 Hz, 2 H, arom. H), 6.70 (d, J = 8.0 Hz, 2 H, arom. H), 6.14 (s, 2 H, NH), 1.46 (s, 9 H, CH$_3$) ppm. ^{13}C-NMR (75.5 MHz, CDCl$_3$) δ = 152.24, 137.71, 131.50, 126.39, 123.82, 123.54, 122.60, 81.58, 28.20 ppm. ESI-MS: calc. 543.03 amu, found: 543.03 amu.

10.18.　　4,4'-dibromo-2-nitro-1,1'-biphenyl (73)
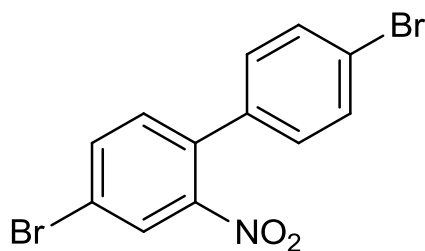
In a 500 ml 3-neck flask a solution of 20 g (64.1mmol) 4,4'-Dibromo-1,1'-biphenyl (**72**) in AcOH was heated to 100 °C. A solution of 92.5 ml (2.22 mol, 34.7 eq) fuming HNO_3 and 7 ml water was added drop-wise to the reaction mixture upon which a precipitate formed. Heating for 30 min resulted in the precipitate dissolving again. Upon complete dissolution, heating was stopped. After the reaction mixture cooled down, it was poured into 1.5 l of 0.6 M NaOH-solution. Filtration and washing with water afforded the crude product as a yellow solid, which could be recrystallized from EtOH. 15.18 g (42.5 mmol, 66 %) of the pure product was obtained as yellow crystals. ^{1}H-NMR (CDCl$_3$, 300.23 MHz) δ = 8.00 (d, J = 1.80 Hz, 1 H, arom.), 7.73 (dd, J_1 = 1.91 Hz, J_2 = 8.24 Hz, 1 H, arom.), 7.53 (d, J = 8.37 Hz, 1 H, arom.), 7.26 (d, J = 8.20 Hz, 2 H, arom.), 7.13 (d, J = 8.35 Hz, 2 H, arom.) ppm.[103] melting-point: 117-121 °C. Lit: 124 °C.[127]

10.19. 4,4'-dibromo-[1,1'-biphenyl]-2-amine (74)
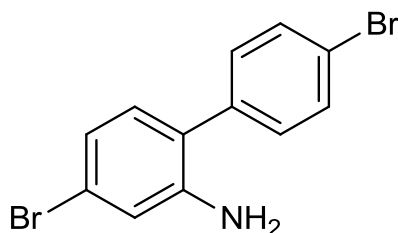
In a 50 ml round bottom flask 0.50 g (1.4 mmol) of 4,4'-dibromo-2-nitro-1,1'-biphenyl (**73**) were suspended in10 ml of EtOH. 2.6 ml (86 mmol, 61 eq) of concentrated HCl (aq.) was added slowly. After portion-wise addition of 0.33 g (2.8 mmol, 2 eq) of Sn(s) the reaction was heated to 85 °C upon which complete dissolution occurred, heating was continued overnight. The reaction was quenched by the addition of NaOH (aq.) to a pH ~ 8. The mixture was extracted with DCM, dried over $NaSO_4$ and filtered. Removal of solvent under reduced pressure yielded a light brown solid, 0.44 g (96 %). ^{1}H-NMR (CDCl$_3$, 300.23 MHz) δ = 7.55-7.57 (m, 2 H, arom. H), 7.28 – 7.31 (m, 2 H, arom. H), 6.94 – 7.02 (m, 3 H, arom. H), 4.61 (s (broad), 2 H, NH$_2$) ppm.[104]

10.20.   4,4'-dibromo-2-iodo-1,1'-biphenyl (75)
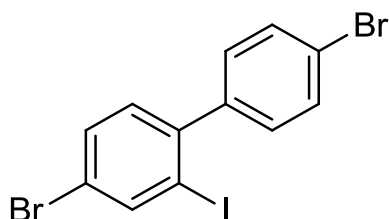
In a 2 l flask 19.0 g (58.1 mmol) of 4,4'-dibromo-[1,1'-biphenyl]-2-amine (**74**) was suspended in 500 ml of water and 100 ml of concentrated H_2SO_4. The mixture was cooled bellow 5 °C and slowly 5 g (72.6 mmol, 1.25 eq) of $NaNO_2$ in 50 ml of water was added. Stirring was continued for 1 h. 20 g (120 mmol, 2.1 eq) of KI in 100 ml of water was added. The reaction was allowed to slowly reach room temperature. The mixture was extracted with DCM. The organic phase was washed with $Na_2S_2O_3$ (aq.), NaOH (aq.) and dried over $MgSO_4$. Removal of solvent gave the crude product as dark brown oil. Column chromatography (silica gel, hexane) and subsequent recrystallization from hexane yielded the product as light yellow solid (7.01 g, 27.5 %). 1H-NMR (CDCl$_3$, 300.23 MHz) δ = 8.10 (d, J = 1.73 Hz, 1 H, arom. H (2)), 7.50-7.58 (m, 3 H, arom. H (5, 2', 6')), 7.16-7.20 (m, 2 H, arom. H (3', 5')), 7.13 (d, J = 8.21 Hz, arom. H (6)) ppm. ^{13}C-NMR (CDCl$_3$, 75.5 MHz) δ = 144.5, 142.0, 141.6, 131.5, 131.4, 130.9, 130.8, 122.4, 122.1, 98.9 ppm. HRMS (EI): [M]$^+$ calculated: 435.7954 amu, found: 435.7949 amu; other signals: [M]$^+$ - Br – I calculated: 229.9731 amu, found: 229.9725 amu; [M]$^+$ - halogens calculated: 151.0548 amu, found: 141.0543 amu.

10.21.   Suzuki-Polycondensation procedures

Standart SPC procedure for the synthesis of polymer 42

To a 1 l schlenk-flask 7.01642 g (20.8736 mmol) of monomer **53** and 6.88901 g (20.8736 mmol, 1.00000 eq) of monomer **52** were added. All weighing-vessels were carefully rinsed repeatedly with THF to ensure complete transfer. The total amount of THF used was 500 ml, which was complemented with 100 ml of water. To this solution 16.8 g (0.2 mol, 10 eq) of $NaHCO_3$ was added. Subsequently the mixture was degased. To the degased reaction mixture 120 mg (0.18 mmol, 0.58 mol-%) of catalyst were added in a solution of degased THF. The reaction mixture was heated to 72 °C for 96 h. After cooling toluene was added to the mixture and the layers were separated. The organic phase was washed with water (2x). Thereafter the suspension was heated to 150°C in a pressure vessel for at least 6 h. After cooling insoluble parts were filtered off and collected separately. To the resulting solution a NaCN solution (basic pH by $NaHCO_3$) was added and the mixture was stirred vigorously for a minimum of 6 h. The inorganic phase was separated and the organic phase was washed with dilute $NaHCO_3$ solution (2x) and water (2x), concentrated and precipitated from cold MeOH to afford 4.99 g (94.5 %) of polymer **42** as a white powder.

Microwave assisted SPC procedure for the synthesis of polymer 42

25 ml of a 0.028 M stock solution (0.7 mmol), containing monomer **52** and monomer **53** in equimolar amounts, was added with 10 ml of H2O to a degasing vessel. The reaction solution was subsequently degased by repeated freeze-pump-thaw cycles (3x). The microwave reaction vessel was charged with 0.375 g (4.5 mmol, 6.4 eq.) of $NaHCO_3$ and put under N_2. The reaction solution was transferred to the microwave vessel and by bubbling Ar (g) through the reaction mixture a gas exchange from nitrogen to argon was performed. Thereafter 4 mg (0.56 mol %) of catalyst dissolved in THF was added. The reaction vessel was transferred to the microwave oven, 3 pump-purge with N_2 cycles were performed and the reaction was started. The microwave was operated in temperature-control mode. After the reaction was finished toluene was added, the phases were separated and the organic phase was washed with water (2x). The organic phase was subsequently heated in the pressure vessel to 150°C for at least 6 h. The mixture was filtered; insoluble gel and polymer solution were collected separately. The polymer solution was stirred vigorously with a basic NaCN-solution for 6 h. After phase separation the organic phase was washed with dilute NaHCO3- solution (2x) and water (2x), concentrated and precipitated in cold MeOH yielding the polymer as a white powder.

10.22. Poly(1,1'-4',5-3-(dimethyl(propyl)silyl)phenylene) (42)
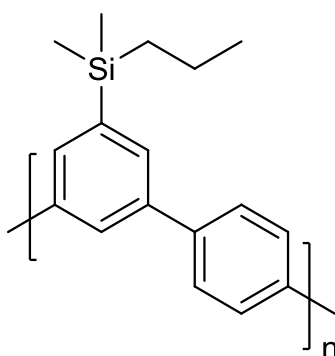
^{1}H-NMR (CDCl$_3$, 300.23 MHz) δ = 7.91 (s, 1 H, arom. H), 7.83-7.73 (m (broad), 6 H, arom. H), 1.58-1.36 (m, 2 H, CH$_2$), 1.02 (t, J = 7.03 Hz, CH$_3$), 0.93-0.81 (m, 2 H, Si-CH$_2$), 0.39 (s, 6 H, Si-CH$_3$) ppm. ^{13}C-NMR (CDCl$_3$, 75.5 MHz) δ = 141.37, 140.82, 140.78, 131.64, 128.00, 126.80, 18.60, 18.53, 17.67, -2.65 ppm.

10.23.   Poly(1,1'-4',5-3-((tetrahydropyranyloxy)methyl)phenylene) (77)
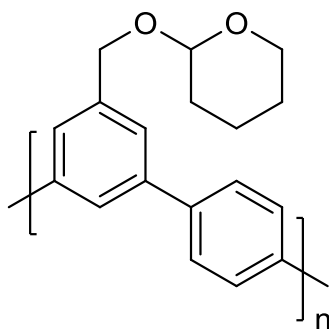
^{1}H-NMR (CDCl$_3$, 300.23 MHz) δ = 7.88 (s, 1 H, arom. H), 7.81 (s, 4 H, arom. H), 7.69 (s, 2 H, arom. H), 4.85 (m, 1 H, O-CH-O), 4.98 and 4.69 (d, J_1 = 12.3 Hz, 2H, Ar-CH_2-O), 4.01 and 3.63 (m, 2 H, O-CH$_2$), 1.99-1.55 (m, 6 H, CH$_2$) ppm. ^{13}C-NMR (CDCl$_3$, 75.5 MHz) δ = 141.6, 140.3, 139.7, 127.9, 125.8, 125.3, 98.1, 69.0, 62.4, 30.8, 25.6, 19.5 ppm.

10.24.   Poly(1,1'-4',5-3-(5-butyl-5-ethyl-1,3-dioxan-2-yl)phenylene) (78)
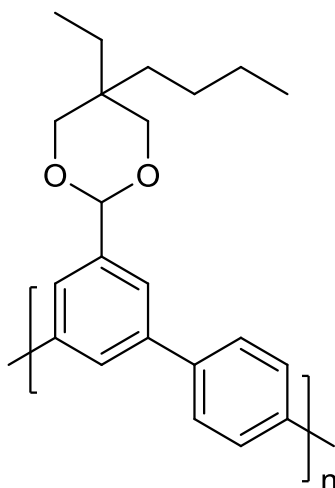
^{1}H-NMR (CDCl$_3$, 300.23 MHz) δ = 7.91 (s, 1 H, arom. H), 7.80 (s, 6 H, arom. H), 5.57 (s, 1 H, Ar-CH), 4.04 (d, J = 11.1 Hz, 2 H, O-CH$_2$), 3.73-3.64 (m, 2 H, O-CH$_2$), 1.97-1.79 (m, 2 H, aliphatic C-H), 1.47-0.81 (m, 12 H, aliphatic C-H) ppm. ^{13}C-NMR(CDCl$_3$, 75.5 MHz): δ = 141.6, 140.3, 139.9, 127.9, 126.6, 124.2, 102.0 (2 signals), 75.6 and 75.4, 35.1 and 35.0, 32.0 and 30.3, 25.6 and 25.2, 25.0 and 24.5, 23.7 and 23.6, 23.5, 14.4 and 14.1, 7.8 and 6.9 ppm.

11. Appendix

11.1. Abbreviations and symbols

Ar	aryl
ATR-IR	Attenuated transmission reflection infrared
ATRP	atom transfer radical polymerization
BnzOTHP	Benzyloxytetrahydropyranyl
Boc	*tert*-butoxycarbonyl
CP	cross polarisation
CRP	controlled radical polymerization
d	doublet
Da	dalton
Dba	dibenzylideneacetone
DCM	dichloromethane
DFT	density functional theory
DIBAL-H	Diisobutylaluminumhydride
DIEA	Diisopropylethylamine
DMSO	dimethylsulfoxide
Dppf	1,1'-Bis(diphenylphosphino)ferrocene
DSC	differential scanning calorimetry
EI	electron ionization
ESI	electron spray ionization
EtOH	ethanol
FRP	free radical polymerization
GPC	gel permeation chromatography
HRMS	high resolution mass spectrometry

m	multiplet
MALDI	matrix assisted laser desorption ionization
MAS	magic angle spinning
MeOH	methanol
NMP	Nitroxide mediated polymerization
RAFT	reversible addition-fragmentation chain transfer polymerization
ROP	ring opening polymerization
rpm	revolutions per minute
s	singlet
SEM	scanning electron microscopy
SMC	Suzuki Miyaura cross-coupling
OAc	acetate
OLEDs	organic light emitting diodes
OTf	Triflate
PA	Polyamide
PE	Polyethylene
PET	Polytheneterephtalate
PDI	polydispersity index
PMMA	Polymethylmethacrylate
PB*m*P	Poly((butoxylyl)*meta-para*phenylene)
PMP	Poly*meta*phenylene
P*mp*P	Poly(*meta-para*phenylene)
PPP	Poly*para*phenylene
PTFE	Polytetrafluoroethane
quin	quintet
RUs	repeat units
SPC	Suzuki polycondensation
SPhos	2-Dicyclohexylphosphino-2',6'-dimethoxybiphenyl

t	triplet
TGA	thermo-gravimetric analysis
THF	Tetrahydrofurane
TOF	time of flight
Tol	tolyl
TLC	thin layer chromatography
UV/Vis	Ultraviolet-visible
XRD	X-ray diffraction

t	triplet

12. References

[1] Plastics Europe, **2012**.
[2] H. Staudinger, *Ber. Dtsch. Chem. Ges.* **1920**, *53*, 1073-1085.
[3] H. Staudinger, *Ber. Dtsch. Chem. Ges.* **1924**, *57*, 1203-1208.
[4] R. Freudenberger, W. Claussen, A. D. Schlüter, H. Wallmeier, *Polymer* **1994**, *35*, 4496-4501.
[5] I. K. Spiliopoulos, J. A. Mikroyannidis, *Macromolecules* **1996**, *29*, 5313-5319.
[6] R. Kandre, K. Feldman, H. E. H. Meijer, P. Smith, A. D. Schlüter, *Angew. Chem. Int. Ed.* **2007**, *46*, 4956-4959.
[7] A. R. Postema, K. Liou, F. Wudl, P. Smith, *Macromolecules* **1990**, *23*, 1842-1845.
[8] P.-O. Johansson, J. Lindberg, M. J. Blackman, I. Kvarnström, L. Vrang, E. Hamelink, A. Hallberg, Å. Rosenquist, B. Samuelsson, *J. Med. Chem.* **2005**, *48*, 4400-4409.
[9] S. Caron, A. Ghosh, S. Gut Ruggeri, N. D. Ide, J. D. Nelson, J. A. Ragan, in *Practical Synthetic Organic Chemistry*, John Wiley & Sons, Inc., **2011**, pp. 279-340.
[10] N. Miyaura, K. Yamada, A. Suzuki, *Tetrahedron Lett.* **1979**, *20*, 3437-3440.
[11] N. Miyaura, A. Suzuki, *J. Chem. Soc., Chem. Commun.* **1979**, 866-867.
[12] S. Baba, E. Negishi, *J. Am. Chem. Soc.* **1976**, *98*, 6729-6731.
[13] R. C. Larock, *The Journal of Organic Chemistry* **1976**, *41*, 2241-2246.
[14] D. Milstein, J. K. Stille, *J. Am. Chem. Soc.* **1978**, *100*, 3636-3638.
[15] H. A. Dieck, R. F. Heck, *J. Am. Chem. Soc.* **1974**, *96*, 1133-1136.
[16] J. K. Stille, *Angewandte Chemie International Edition in English* **1986**, *25*, 508-524.
[17] A. O. Aliprantis, J. W. Canary, *J. Am. Chem. Soc.* **1994**, *116*, 6985-6986.
[18] N. Miyaura, K. Yamada, H. Suginome, A. Suzuki, *J. Am. Chem. Soc.* **1985**, *107*, 972-980.
[19] H. Nakai, S. Ogo, Y. Watanabe, *Organometallics* **2002**, *21*, 1674-1678.
[20] V. V. Grushin, H. Alper, *Chem. Rev.* **1994**, *94*, 1047-1062.
[21] J.-P. Corbet, G. Mignani, *Chem. Rev.* **2006**, *106*, 2651-2710.
[22] A. L. Casado, P. Espinet, *Organometallics* **1998**, *17*, 954-959.
[23] N. Miyaura, A. Suzuki, *Chem. Rev.* **1995**, *95*, 2457-2483.
[24] M. Rehahn, A.-D. Schlüter, G. Wegner, W. J. Feast, *Polymer* **1989**, *30*, 1060-1062.
[25] J. Sakamoto, M. Rehahn, G. Wegner, A. D. Schlüter, *Macromol. Rapid Commun.* **2009**, *30*, 653-687.
[26] G. Brodowski, A. Horvath, M. Ballauff, M. Rehahn, *Macromolecules* **1996**, *29*, 6962-6965.
[27] B. Hohl, L. Bertschi, X. Zhang, A. D. Schlüter, J. Sakamoto, *Macromolecules* **2012**, *45*, 5418-5426.
[28] W. H. Carothers, *Transactions of the Faraday Society* **1936**, *32*, 39-49.
[29] Z. Bo, A. D. Schlüter, *Chemistry – A European Journal* **2000**, *6*, 3235-3241.
[30] J. Murage, J. W. Eddy, J. R. Zimbalist, T. B. McIntyre, Z. R. Wagner, F. E. Goodson, *Macromolecules* **2008**, *41*, 7330-7338.
[31] W. Zhang, P. Lu, Z. Wang, Y. Ma, *J. Polym. Sci., Part A: Polym. Chem.* **2013**, *51*, 1950-1955.
[32] Z. Xue, A. D. Finke, J. S. Moore, *Macromolecules* **2010**, *43*, 9277-9282.

[33]   Z. Z. Song, H. N. C. Wong, *The Journal of Organic Chemistry* **1994**, *59*, 33-41.

[34]   C. M. So, Z. Zhou, C. P. Lau, F. Y. Kwong, *Angew. Chem. Int. Ed.* **2008**, *47*, 6402-6406.

[35]   D. Zim, S. L. Buchwald, *Org. Lett.* **2003**, *5*, 2413-2415.

[36]   S. D. Walker, T. E. Barder, J. R. Martinelli, S. L. Buchwald, *Angew. Chem. Int. Ed.* **2004**, *43*, 1871-1876.

[37]   N. E. Leadbeater, M. Marco, *The Journal of Organic Chemistry* **2003**, *68*, 5660-5667.

[38]   H. Yan, P. Lee, N. R. Armstrong, A. Graham, G. A. Evmenenko, P. Dutta, T. J. Marks, *J. Am. Chem. Soc.* **2005**, *127*, 3172-3183.

[39]   W. W. Inbasekaran; Michael, Woo; Edmund P., in *U.S. Patent*, 5.777.070, **1997**.

[40]   B. Liu, W.-L. Yu, Y.-H. Lai, W. Huang, *Macromolecules* **2000**, *33*, 8945-8952.

[41]   F. Galbrecht, T. W. Bünnagel, U. Scherf, T. Farrell, *Macromol. Rapid Commun.* **2007**, *28*, 387-394.

[42]   S. Jakob, A. Moreno, X. Zhang, L. Bertschi, P. Smith, A. D. Schlüter, J. Sakamoto, *Macromolecules* **2010**, *43*, 7916-7918.

[43]   K. T. Nielsen, K. Bechgaard, F. C. Krebs, *Macromolecules* **2005**, *38*, 658-659.

[44]   A. Schätz, O. Reiser, W. J. Stark, *Chemistry – A European Journal* **2010**, *16*, 8950-8967.

[45]   G. M. Scheuermann, L. Rumi, P. Steurer, W. Bannwarth, R. Mülhaupt, *J. Am. Chem. Soc.* **2009**, *131*, 8262-8270.

[46]   K. C. Kong, C. H. Cheng, *J. Am. Chem. Soc.* **1991**, *113*, 6313-6315.

[47]   W. A. Herrmann, C. Broßmer, T. Priermeier, K. Öfele, *J. Organomet. Chem.* **1994**, *481*, 97-108.

[48]   D. Agrawal, E.-L. Zins, D. Schröder, *Chemistry – An Asian Journal* **2010**, *5*, 1667-1676.

[49]   F. E. Goodson, T. I. Wallow, B. M. Novak, *Macromolecules* **1998**, *31*, 2047-2056.

[50]   J. Frahn, B. Karakaya, A. Schäfer, A. D. Schlüter, *Tetrahedron* **1997**, *53*, 15459-15467.

[51]   H. G. Kuivila, J. F. Reuwer Jr, J. A. Mangravite, *Can. J. Chem.* **1963**, *41*, 3081-3090.

[52]   T. Bauer, A. D. Schlüter, J. Sakamoto, *Synlett* **2010**, *2010*, 877-880.

[53]   H. G. Kuivila, J. F. Reuwer, J. A. Mangravite, *J. Am. Chem. Soc.* **1964**, *86*, 2666-2670.

[54]   M.-S. Schiedel, C. A. Briehn, P. Bäuerle, *J. Organomet. Chem.* **2002**, *653*, 200-208.

[55]   A. J. J. Lennox, G. C. Lloyd-Jones, *J. Am. Chem. Soc.* **2012**, *134*, 7431-7441.

[56]   M. Moreno-Mañas, M. Pérez, R. Pleixats, *The Journal of Organic Chemistry* **1996**, *61*, 2346-2351.

[57]   H. Sibtain, A. B. Stephen, in *Synthetics, Mineral Oils, and Bio-Based Lubricants*, CRC Press, **2005**.

[58]   D. G. H. Ballard, A. Courtis, I. M. Shirley, S. C. Taylor, *Macromolecules* **1988**, *21*, 294-304.

[59]   P. Kovacic, C. Wu, *Journal of Polymer Science* **1960**, *47*, 45-54.

[60]   A. A. Berlin, *Journal of Polymer Science* **1961**, *55*, 621-641.

[61]   G. Goldschimiedt, *Monatshefte für Chemie und verwandte Teile anderer Wissenschaften* **1886**, *7*, 40-47.

[62]   T. Yamamoto, Y. Hayashi, A. Yamamoto, *Bull. Chem. Soc. Jpn.* **1978**, *51*, 2091-2097.

[63] J. L. Musfeldt, J. R. Reynolds, D. B. Tanner, J. P. Ruiz, J. Wang, M. Pomerantz, *J. Polym. Sci., Part B: Polym. Phys.* **1994**, *32*, 2395-2404.
[64] J. L. Reddinger, J. R. Reynolds, *Macromolecules* **1997**, *30*, 479-481.
[65] V. S. Claesson, R. Gehm, W. Kern, *Die Makromolekulare Chemie* **1951**, *7*, 46-61.
[66] J. Majnusz, J. M. Catala, R. W. Lenz, *Eur. Polym. J.* **1983**, *19*, 1043-1046.
[67] M. Ballauff, G. F. Schmidt, *Molecular Crystals and Liquid Crystals* **1987**, *147*, 163-177.
[68] M. B. Jones, P. Kovacic, D. Lanska, *Journal of Polymer Science: Polymer Chemistry Edition* **1981**, *19*, 89-101.
[69] M. Rehahn, A.-D. Schlüter, G. Wegner, *Die Makromolekulare Chemie* **1990**, *191*, 1991-2003.
[70] C. Ambrosch-Draxl, J. A. Majewski, P. Vogl, G. Leising, *Physical Review B* **1995**, *51*, 9668-9676.
[71] M. P. Stevens, 3rd ed., Oxford University Press, **1999**, p. 485.
[72] J. H. Edwards, W. J. Feast, *Polymer* **1980**, *21*, 595-596.
[73] D. A. Halliday, P. L. Burn, R. H. Friend, A. B. Holmes, *J. Chem. Soc., Chem. Commun.* **1992**, *0*, 1685-1687.
[74] J. M. Batson, T. M. Swager, *ACS Macro Letters* **2012**, *1*, 1121-1123.
[75] D. R. McKean, J. K. Stille, *Macromolecules* **1987**, *20*, 1787-1792.
[76] Z. He, F. J. Davis, G. R. Mitchell, *Polymer* **1994**, *35*, 2218-2221.
[77] E. Bundgaard, O. Hagemann, M. Bjerring, N. C. Nielsen, J. W. Andreasen, B. Andreasen, F. C. Krebs, *Macromolecules* **2012**, *45*, 3644-3646.
[78] J. Liu, E. N. Kadnikova, Y. Liu, M. D. McGehee, J. M. J. Fréchet, *J. Am. Chem. Soc.* **2004**, *126*, 9486-9487.
[79] R. Gedye, F. Smith, K. Westaway, H. Ali, L. Baldisera, L. Laberge, J. Rousell, *Tetrahedron Lett.* **1986**, *27*, 279-282.
[80] R. J. Giguere, T. L. Bray, S. M. Duncan, G. Majetich, *Tetrahedron Lett.* **1986**, *27*, 4945-4948.
[81] M. Larhed, A. Hallberg, *The Journal of Organic Chemistry* **1996**, *61*, 9582-9584.
[82] C. Ebner, T. Bodner, F. Stelzer, F. Wiesbrock, *Macromol. Rapid Commun.* **2011**, *32*, 254-288.
[83] K. Kempe, C. R. Becer, U. S. Schubert, *Macromolecules* **2011**, *44*, 5825-5842.
[84] R. M. Paulus, C. R. Becer, R. Hoogenboom, U. S. Schubert, *Aust. J. Chem.* **2009**, *62*, 254-259.
[85] D. Roy, A. Ullah, B. S. Sumerlin, *Macromolecules* **2009**, *42*, 7701-7708.
[86] Y. Kwak, R. T. Mathers, K. Matyjaszewski, *Macromol. Rapid Commun.* **2012**, *33*, 80-86.
[87] B. S. Nehls, U. Asawapirom, S. Füldner, E. Preis, T. Farrell, U. Scherf, *Adv. Funct. Mater.* **2004**, *14*, 352-356.
[88] B. S. Nehls, S. Füldner, E. Preis, T. Farrell, U. Scherf, *Macromolecules* **2005**, *38*, 687-694.
[89] W. Zhang, P. Lu, Z. Wang, Y. Ma, *Sci. China Chem.* **2012**, *55*, 844-849.
[90] A. Greiner, J. H. Wendorff, *Angew. Chem. Int. Ed.* **2007**, *46*, 5670-5703.
[91] G. Srinivasan, D. H. Reneker, *Polym. Int.* **1995**, *36*, 195-201.
[92] R. Kessick, J. Fenn, G. Tepper, *Polymer* **2004**, *45*, 2981-2984.
[93] H. Fong, I. Chun, D. H. Reneker, *Polymer* **1999**, *40*, 4585-4592.
[94] S. Agarwal, A. Greiner, J. H. Wendorff, *Prog. Polym. Sci.* **2013**, *38*, 963-991.
[95] S. Ramakrishna, K. Fujihara, W.-E. Teo, T.-C. Lim, Z. Ma, *An Introduction To Electrospinning And Nanofibers*, World Scientific Publishing, **2005**.

[96]   J. Xia, S. Yuan, Z. Wang, S. Kirklin, B. Dorney, D.-J. Liu, L. Yu, *Macromolecules* **2010**, *43*, 3325-3330.

[97]   P. Li, J. Li, F. Arikan, W. Ahlbrecht, M. Dieckmann, D. Menche, *The Journal of Organic Chemistry* **2010**, *75*, 2429-2444.

[98]   P. Kissel, S. Breitler, V. Reinmüller, P. Lanz, L. Federer, A. D. Schlüter, J. Sakamoto, *Eur. J. Org. Chem.* **2009**, *2009*, 2953-2955.

[99]   L. I. Zakharkin, I. M. Khorlina, *Tetrahedron Lett.* **1962**, *3*, 619-620.

[100] M. Alami, C. Amatore, S. Bensalem, A. Choukchou-Brahim, A. Jutand, *Eur. J. Inorg. Chem.* **2001**, *2001*, 2675-2681.

[101] T. S. Khaibulova, I. A. Boyarskaya, V. P. Boyarskii, *Russ. J. Org. Chem.* **2013**, *49*, 360-365.

[102] G. Lu, H. Usta, C. Risko, L. Wang, A. Facchetti, M. A. Ratner, T. J. Marks, *J. Am. Chem. Soc.* **2008**, *130*, 7670-7685.

[103] F. Dierschke, A. C. Grimsdale, K. Müllen, *Synthesis* **2003**, *2003*, 2470-2472.

[104] Y. Chen, F. Li, Z. Bo, *Macromolecules* **2010**, *43*, 1349-1355.

[105] C.-C. Chi, C.-L. Chiang, S.-W. Liu, H. Yueh, C.-T. Chen, C.-T. Chen, *J. Mater. Chem.* **2009**, *19*, 5561-5571.

[106] F. Francuskiewicz, *Polymer Fractionation*, Springer Berlin Heidelberg, **1994**.

[107] M. Sun, Y. Fu, J. Li, Z. Bo, *Macromol. Rapid Commun.* **2005**, *26*, 1064-1069.

[108] J. Clayden, S. Warren, N. Greeves, P. Wothers, *Organic Chemistry, Vol. 5*, Oxford University Press, **2001**.

[109] E. Pretsch, P. Bühlmann, C. Affolter, M. Badertscher, *Spektroskopische Daten zur Strukturaufklärung organischer Verbindungen, Vol. 4*, Springer Verlag, **2001**.

[110] D. A. M. Egbe, S. Türk, S. Rathgeber, F. Kühnlenz, R. Jadhav, A. Wild, E. Birckner, G. Adam, A. Pivrikas, V. Cimrova, G. n. Knör, N. S. Sariciftci, H. Hoppe, *Macromolecules* **2010**, *43*, 1261-1269.

[111] H. Jun Song, D. Hun Kim, M. Hee Choi, S. Won Heo, J. Young Lee, J. Yong Lee, D. Kyung Moon, *Sol. Energy Mater. Sol. Cells* **2013**, *117*, 285-292.

[112] K. N. Baker, A. V. Fratini, T. Resch, H. C. Knachel, W. W. Adams, E. P. Socci, B. L. Farmer, *Polymer* **1993**, *34*, 1571-1587.

[113] F. C. Krebs, H. Spanggaard, *Chem. Mater.* **2005**, *17*, 5235-5237.

[114] H. Fong, D. H. Reneker, *J. Polym. Sci., Part B: Polym. Phys.* **1999**, *37*, 3488-3493.

[115] D. Kołbuk, P. Sajkiewicz, T. A. Kowalewski, *Eur. Polym. J.* **2012**, *48*, 275-283.

[116] J. M. Deitzel, J. D. Kleinmeyer, J. K. Hirvonen, N. C. Beck Tan, *Polymer* **2001**, *42*, 8163-8170.

[117] L. Larrondo, R. St. John Manley, *Journal of Polymer Science: Polymer Physics Edition* **1981**, *19*, 909-920.

[118] X. Zong, K. Kim, D. Fang, S. Ran, B. S. Hsiao, B. Chu, *Polymer* **2002**, *43*, 4403-4412.

[119] U. W. Gedde, *Polymer Physics, Vol. 1*, Kluwer Academic Publishers, **1995**.

[120] C. A. Tolman, W. C. Seidel, D. H. Gerlach, *J. Am. Chem. Soc.* **1972**, *94*, 2669-2676.

[121] S. Trimpin, A. Rouhanipour, R. Az, H. J. Räder, K. Müllen, *Rapid Commun. Mass Spectrom.* **2001**, *15*, 1364-1373.

[122] A. P. Hammersley, S. O. Svensson, M. Hanfland, A. N. Fitch, D. Hausermann, *High Pressure Research* **1996**, *14*, 235-248.

[123] U. Lauter, W. H. Meyer, G. Wegner, *Macromolecules* **1997**, *30*, 2092-2101.

[124] A. Balamurugan, M. L. P. Reddy, M. Jayakannan, *The Journal of Physical Chemistry B* **2011**, *115*, 10789-10800.

[125] A. V. Malkov, K. Vranková, R. C. Sigerson, S. Stončius, P. Kočovský, *Tetrahedron* **2009**, *65*, 9481-9486.

[126] S. H. Chanteau, J. M. Tour, *The Journal of Organic Chemistry* **2003**, *68*, 8750-8766.

[127] J. I. G. Cadogan, M. Cameron-Wood, R. K. Mackie, R. J. G. Searle, *Journal of the Chemical Society (Resumed)* **1965**, 4831-4837.

Acknowledgments

While my name is written on the cover of this booklet, I couldn't have done so without the major or minor help of the following people.

First and foremost I would like to thank Prof. A. Dieter Schlüter for his help and guidance throughout my PhD. Feeling his support especially during difficult times was vital during my doctoral studies.

I would also like to thank Prof. Junji Sakamoto for supervising me during the first part of my PhD and providing important ideas to the project.

I am thankfull to Prof. Paul Smith and Prof. Holger Frauenrath for taking the time need for co-refereeing my thesis.

I would, especially, like to thank Dr. Thomas Schweizer for his instructions and insight into GPC, DSC, TGA, Rheology and other daily problems in the lab.

Many thanks to Prof. Theo Tervoort and Dr. Kirill Feldman for their help and discussions, regarding polymer processing and ligh-microscopy.

Thanks to Dr. René Verel for help with NMR spectroscopy, particularly setting up the machine for a multitude of solid-state NMR measurements.

Thanks to the ETH Zurich mass service headed by Dr. Xiangyang Zhang for mass spectroscopy analysis. Most noteworthy Dr. Louis Bertschi for measuring many MALDI-TOF mass-spectra for me.

The help of Dr. Julia Dschemuchadse with measuring XRD, Olivera Evrova with electrospinning and Jingyi Rao with SEM measurements is gratefully acknowledged.

I would like to thank my students Gian Cadisch and Andreas Bielmann for their help in the lab and John E. Philips for proofreading.

I would like to thank all the former and current member of the Schlüter-group for the nice working atmosphere. Most notably: Dr. Benjamin Hohl for constant exchange of ideas, doubts and hopes surrounding Suzuki-Polycondensation, my lab mates Jingyi, Simon, Andri and Wenjang for the extraordinary working atmosphere, the "drü" people for good laughs and fruitful discussion over a cup of coffee.

Acknowledgements

I would like to thank my friends for helping me refresh my mind, gain new energy, funny and sad moments which they shared with me during my time at ETH: Anna, Esther, Marco, Raphael, Matthias, Nicola, Christian, Philip, Beat, Martin, Dave H., Sara, Vincent, Thomas, Christian O., Lars M., Lars N., Hannes, Peter, Dave M., Christina and Sandra. Without you live would just be so much less fun.

At last but not least I would like to thank my family. Most of all my parents Christina and Andreas, but also my siblings Ruth, Lee, Benjamin and Annina. Thank you for just loving me the way I am, you are awesome!

Curriculum Vitae

Personal

Name: Samuel Paul Jakob

                   Citizen of Hombrechtikon (ZH)

Date of birth: 09.09.1983

Education

1996-2002   **Mature (Old languages)**, Kantonsschule zürcher Oberland
                   Wetzikon, Switzerland

2003-2008   **Bachelor of Science in Chemistry**, ETH Zurich, Switzerland

2008-2010   **Master of Science in Chemistry**, ETH Zurich, Switzerland

2010-2014   **Doctor of Sciences**, ETH Zurich, Switzerland

Work experiences

07.2005 – 09.2005 **Tecan Group Ltd.** (Männedorf, Switzerland), Liquid Handling
                   Engenieer, *Development of a laboratory robot for clinical
                   diagnostics*

02.2010 - 01.2014 **ETH Zurich** (Zurich, Switzerland), PhD Program
                   *Synthesis of Polyphenylenes with removable side chains -
                   towards an all Polyphenylene material*

Miscellaneous

09.2002-11.2002   **Wimbledon School of English** (Wimbledon, England),
                   Language Studies

List of publications

Papers

N- Arylated 3,5-dihydro-4H-dinaphtho[2,1-c:1',2'-e]azepines: Axially chiral donors with high helical twisting powers for nonplanar push-pull chromophores, Frank, Brian B.; Camafort Blanco, Berta; Jakob, Samuel; Ferroni, Fiammetta; Pieraccini, Silvia; Ferrarini, Alberta; Boudon, Corinne; Gisselbrecht, Jean-Paul; Seiler, Paul; Spada, Gian Piero; Diederich, Francois, *Chemistry - A European Journal*, 2009, 15, 9005-9016.

Synthesis of Polyphenylenes from a Soluble Precursor: The "Shaving" Approach, Jakob, Samuel; Moreno, Aitor; Zhang, Xyanjang; Bertschi, Louis; Smith, Paul; Schlüter, A. Dieter; Sakamoto, Junji, *Macromolecules*, 2010, 43, 7916-7918.

Synthesis of poly(m,p-phenylene)s by Suzuki polycondensation using AA/BB monomers, Jakob, Samuel; Schlüter, A. Dieter; Sakamoto, Junji, *Polymer Preprints (American Chemical Society, Division of Polymer Chemistry)*, 2011, 52, 368-369.

Posters

"Shaving" of polymer: A route to bare polyphenylenes, Jakob, Samuel; Moreno, Aitor; Zhang, Xyanjang; Bertschi, Louis; Smith, Paul; Schlüter, A. Dieter; Sakamoto, Junji, **2010***, EuChems Nürnberg.*

Synthesis of Poly(*m*-phenylene)s and Poly(*m,p*-phenylene)s by Suzuki polycondensation, Hohl, Benjamin; Jakob, Samuel; Sakamoto, Junji; Schlüter, A. Dieter, **2010**, *SCS Fall meeting Zürich.*

Synthesis of poly(m,p-phenylene)s by Suzuki polycondensation using AA/BB monomers, Jakob, Samuel; Schlüter, A. Dieter; Sakamoto, Junji, **2011**, *ACS Fall meeting Denver.*

Towards new polymeric materials based on poly(*m,p*-phenylene) by Suzuki polycondensation, Jakob, Samuel; Schlüter, A. Dieter; Sakamoto, Junji, **2012**, *SCS Fall meeting Zürich*.